Deltares

Enabling Delta Life

Literature study Dutch lower shoreface

Deltares

Literature study Dutch lower shoreface

Jebbe van der Werf
Bart Grasmeijer
Erik Hendriks
Ad van der Spek
Tommer Vermaas

1220339-004

Deltares

Title
Literature study Dutch lower shoreface

Client	Project	Reference	Pages
Rijkswaterstaat WVL	1220339-004	1220339-004-ZKS-0001	97

Keywords
Coastal foundation, Dutch lower shoreface morphodynamics, field measurements, numerical modelling

Summary
This report describes an inventory of existing knowledge, field data and models of the Dutch lower shoreface. The Dutch lower shoreface is defined as the area between the upper shoreface (regular and dominant wave action) and the continental shelf (only wave action during storm events). This is roughly the zone between the outer breaker bar (about NAP -8 m) and the NAP -20 m depth contour. This literature review is the first phase of the Coastal Genesis 2.0, Lower Shoreface project in support of Dutch coastal policy, in which the definition of the offshore boundary of the coastal foundation plays an important role. This report gives a system description of the Dutch lower shoreface morphodynamics, defines the state-of-the-art knowledge and outlines further research activities, new field measurements and numerical modelling in particular.

Version	Date	Author	Initials	Review	Initials	Approval	Initials
1	7 July 2017	Jebbe van der Werf		Bert van der Valk		Frank Hoozemans	
2	19 Oct 2017	Jebbe van der Werf		Bert van der Valk		Frank Hoozemans	
		Bart Grasmeijer					
		Erik Hendriks					
		Ad van der Spek					
		Tommer Vermaas					

State
final

Samenvatting

Inleiding
Het Nederlandse kustbeleid streeft naar een structureel veilige, economisch sterke en aantrekkelijke kust. Dit wordt bereikt door het onderhouden van het gedeelte van de kust dat deze functies mogelijk maakt; het Kustfundament. Dit gebeurt door middel van zandsuppleties; het suppletievolume is ongeveer 12 miljoen m^3/jaar sinds 2000.

In 2020 neemt het Ministerie van Infrastructuur en Milieu een beslissing over een eventuele aanpassing van het suppletievolume. Het Kustgenese-2 (KG-2) programma heeft als doel hiervoor de kennis en onderbouwing te leveren. Deltares richt zich in opdracht van Rijkswaterstaat binnen KG-2 op twee hoofdvragen:

1 Is er een andere zeewaartse begrenzing mogelijk voor het kustfundament?
2 Wat is het benodigde suppletievolume om het kustfundament te laten meegroeien met zeespiegelstijging?

Het KG-2 deelproject “Diepere Vooroever” (DV) draagt aan beide vragen bij. De diepere vooroever is het gedeelte van de kust met waterdieptes tussen de 8 en 20 m, waar golven een belangrijke, maar geen dominante rol spelen. Het kustdwarse zandtransport staat centraal in het KG2-DV project, met name in relatie tot de zeewaartse grens van het Kustfundament die momenteel op de NAP -20 m dieptecontour ligt.

Dit rapport geeft een overzicht van de huidige kennis van de Nederlandse diepere vooroever, alsook van de beschikbare veldgegevens en numerieke modellen. Op basis hiervan wordt richting gegeven aan het vervolgonderzoek van het KG-2 DV project.

Bestaande kennis, data en modellen
De Nederlandse vooroever is een complex gebied dat gedeeltelijk bepaald is door historische ontwikkelingen, maar dat ook beïnvloed wordt door processen die op dit moment plaatsvinden. De toekomstige ontwikkeling zal mede bepaald worden door de grootschalige, kunstmatige zandaanvoer door suppleties, ook al is er tot op heden geen toename van het sedimentvolume van de diepere vooroever waargenomen.

De Nederlandse vooroever is niet-uniform, wat blijkt uit bodemhelling en de aanwezigheid van buitendelta’s in de zuidwestelijke Delta en het Waddengebied en van vooroever-aangehechte-zandbanken in het centraal deel van de Hollandse kust. De zeewaartse flanken van deze zandbanken bouwen uit in noordwestelijke richting, terwijl ze in het zuidelijk gedeelte erosief van aard zijn. De ontwikkeling van de meeste buitendelta’s is sterk beïnvloed door menselijke ingrepen in de zeegaten en de achterliggende getijdebekkens.

De diepere vooroever is gevormd door getijdebekken- en rivierafzettingen gedurende de landwaartse verschuiving van de kustlijn in de periode voor 5000 BP (*Before Present*, vóór heden). Bovenop deze afzettingen ligt een zandlaag die reageert op veranderingen in getij-, wind- en golfcondities.

Afzettingen op de vooroever door uitbouwende strandwallen langs de Hollandse kust wijzen op de dominantie van golfprocessen die afneemt met diepte. Bovendien suggereren deze afzettingen dat re-suspensie onder stormgolven plaatsvindt, en dat de kans hierop afneemt met de diepte.

Op basis van studies langs met name de Hollands kust, blijkt dat het diepwater transport episodisch van aard is, bodemtransport de meest voorkomende transportwijze is en dat hoge (storm) golven het netto jaarlijkse transport bepalen. Potentiele transportmechanismen zijn:

- kustwaarts: dichtheidsgedreven stroming, asymmetrie orbitaalsnelheden (golfscheefheid), Longuet-Higgins grenslaagstroming en upwelling.
- zeewaarts: retourstroming, (gebonden) lange golven, zeewaartse grensslaagstroming door turbulentie-asymmetrie en downwelling.

Het effect van de zeewaartse grensslaagstroming door turbulentie-asymmetrie en up- en downwelling is niet onderzocht voor de Nederlandse vooroever. De bijdrage van de kustdwarse getij-gedreven stromingscomponenten, met name mogelijk relevant voor de Delta en Wadden diepere vooroever, is onbekend. De dichtheidsgedreven stroming is vooral van belang voor de Hollandse kust die onder directe invloed staat van de Rijn.

Het geschatte kustwaartse netto zandtransport over de NAP -20 m lijn langs de Hollandse kust is 0-20 m^3/m/jaar, oftewel een import van 0-2 miljoen m^3/jaar naar dit kustvak. Huidige berekeningen laten zien dat kust- en zeewaartse transportbijdrages elkaar min of meer opheffen op de NAP -8 m contour langs de Hollandse kust. We hebben geen schatting kunnen vinden van netto kustdwars zandtransport op de diepere Delta en Wadden vooroever.

Bestaande metingen zijn vooral uitgevoerd op de diepere vooroever van de Hollandse kust. Tijdens drie meetcampagnes (SANDPIT, STRAINS/MegaPex, Kustgenese) zijn zandtransportprocessen op de diepe vooroever gemeten. Er is een relatief grote hoeveelheid data van de morfologie en de ondergrond beschikbaar, met een sterk wisselende kwaliteit.

Sinds de jaren ‘80 is een aantal diepere vooroever modelstudies uitgevoerd. Deze studies hebben veel kennis opgeleverd, maar de gehanteerde modellen zijn beperkt gevalideerd. Bovendien richtten deze studies zich vooral op de Hollandse kust, en zijn effecten van de verticale stromingsstructuur en kustlangse variatie niet of schematisch meegenomen.

In de berekening van het jaarlijkse suppletievolume wordt aangenomen dat er geen netto zandtransport plaatsvindt over de zeewaartse grens van het kustfundament. Deze grens wordt gevormd door de NAP -20 m dieptecontour en is sterk gekoppeld aan de landwaartse grens van het gebied waar zandwinning is toegestaan. Deze grens is niet eenduidig onderbouwd. Het is vooral gebaseerd op de hellingsovergang van ~1:100 naar ~1:1000, waarbij de vooroever-aangehecht-zandbanken langs het centrale van de Hollandse kust worden meegenomen vanwege het vermeende positieve effect op de kuststabiliteit. Andere manieren om de zeewaartse grens van het kustfundament te definiëren, wijzen erop dat die keuze voor de NAP -20 m dieptecontour mogelijk aan de veilige kant is.

Vervolgonderzoek binnen KG-2 DV

De kennis van de Nederlandse diepere vooroever is beperkt, wat het moeilijk maakt om te adviseren over de zeewaartse grens van het kustfundament en het bijbehorende suppletievolume. Deze kennislacune wordt voornamelijk veroorzaakt door een gebrek aan goede veldmetingen en gedetailleerde numerieke modellering. Daarom stellen we voor om op de vooroevers van Terschelling, Ameland en Noordwijk multibeamopnamen te doen, boxcores en vibrocores te nemen en zandtransportprocessen te meten. Deze data kunnen gebruikt voor het valideren van numerieke modellen. Het modelonderzoek is complementair aan de metingen, omdat deze beperkt in de plaats en tijd zijn. De gevalideerde modellen kunnen gebruikt worden voor scenario-onderzoek om de systeemkennis van de Nederlandse diepere vooroever te vergroten en bestaande ideeën over de kustdwarse zanduitwisseling op de diepere vooroever, in het bijzonder de rol van golfwerking, nader te onderzoeken.

Contents

1 Introduction

1.1 Background

The Dutch coastal policy aims for a safe, economically strong and attractive coast (Deltaprogramma, 2015). This is achieved by maintaining the part of the coast that supports these functions; the coastal foundation. The coastal foundation is maintained by means of sand nourishments; the total nourishment volume is approximately 12 million m^3/year since 2000.

In 2020 the Dutch Ministry of Infrastructure and Environment will make a new decision about the nourishment volume. The Kustgenese-2 (KG2) programme is aimed to deliver knowledge to enable this decision making. The scope of the KG2 project, commissioned by Rijkswaterstaat to Deltares, is determined by two main questions:

1 What are possibilities for an alternative offshore boundary of the coastal foundation?
2 How much sediment is required for the coastal foundation to grow with sea level rise?

The Deltares KG2 subproject “Diepere Vooroever” (DV, lower shoreface) contributes to both questions. The KG2-DV project studies the morphodynamics of the Dutch lower shoreface, in particular the net cross-shore sand transport as function of depth on the basis of field measurements, numerical modelling and system knowledge.

1.2 Objective and scope

This literature study is an inventory of existing knowledge, field data and numerical models of the Dutch lower shoreface in order to 1) define the state-of-the-art, ii) make a system description, and iii) to detail the upcoming DV project activities, in particular the field measurements and numerical modelling. It builds on the lower shoreface knowledge inventory by Cleveringa (2016).

The study focusses on the Dutch lower shoreface which is defined as the area between the upper shoreface (with regular and dominant wave action) and the shelf (wave action limited to storms). This is roughly the zone between the outer breaker bar (around NAP -8 m) and the NAP -20 m depth contour. The report mainly discusses sand instead of sediment (sand + mud) transport processes, as the interaction between fine sediment transport and lower shoreface dynamics is assumed to be limited (see also Section 2.3).

1.3 Outline of the report

This report is organised as follows. Chapter 2 defines the Dutch shoreface and coastal foundation, in particular the seaward boundary and the related depth-of-closure concept. Chapter 3 discusses the large-scale Dutch lower shoreface morphology, sedimentology and geology, as well as the prevailing physical processes. The available Dutch lower shoreface field measurements and models are presented in Chapters 4 and 5, respectively. Chapter 6 presents the conclusions and outline of the further research within the KG2-DV project.

2 Introduction to Dutch shoreface, coastal foundation and depth of closure concept

2.1 The Dutch shoreface

The shoreface is the active littoral zone off the low water line between the shore and the continental shelf. There exist different shoreface subzone classifications, see e.g. Van Rijn (1998). We define the upper shoreface as the beach and surf zone with breaking waves and breaker bars between the waterline and approximately the NAP -8 m depth contour with mean bed slopes varying between 1:50 to 1:200 (Figure 2.1). We define the lower shoreface as the zone between approx. the NAP -8 m and NAP -20 m depth contours with typical bed slopes between 1:200 and 1:1000, and where sand ridges may be present[1]. Offshore the shoreface merges with the continental shelf where the slope is generally less than 1:1000; tidal sand waves and sand banks may be present here.

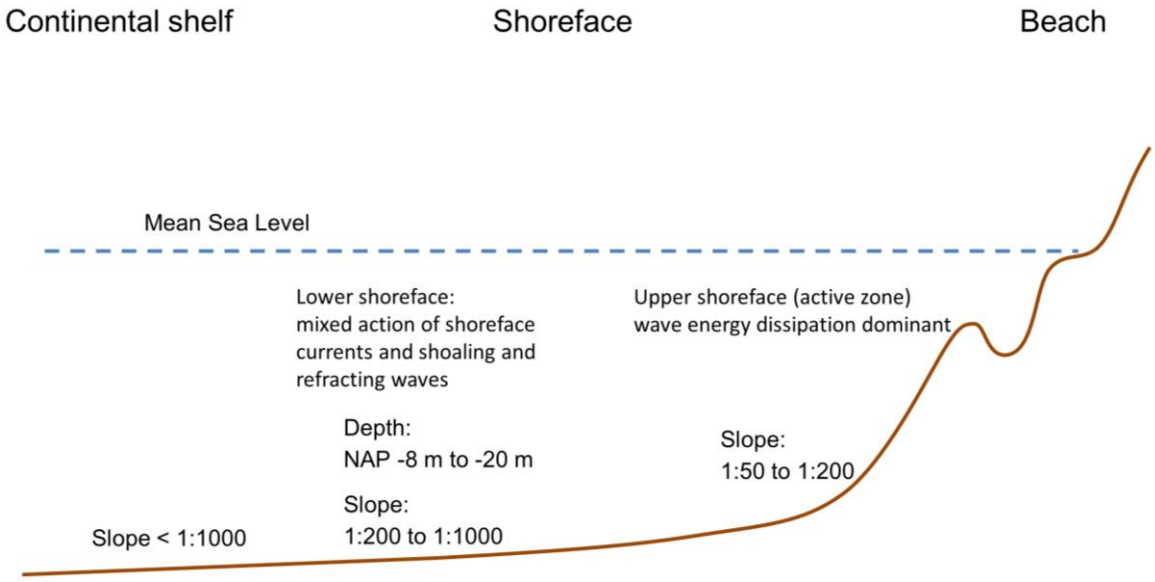

Figure 2.1 Typical Dutch cross-shore coastal profile (not to vertical scale).

The effects due to wave energy dissipation are dominant in the upper shoreface. The upper shoreface is denoted as “active zone” as transport rates are relatively large and the morphological response time is fast, almost on the scale of events. The lower shoreface is the zone where the mixed action of shoreface currents (incl. tide) and shoaling and refracting waves is predominant. Transport rates are relatively small and hence the lower shoreface undergoes relatively slow adaptations.

The shape of the shoreface profile differs along the entire Dutch coast. For instance, the shoreface profile along tidal deltas has a convex shape, while the shoreface profile along the Holland coast has a concave shape.

[1] *Van Rijn (1998) calls this the middle shoreface.*

The Dutch shoreface morphology and underlying physical processes are further discussed in Chapter 3.

2.2 The coastal foundation

Dutch coastal policy aims for a safe, economically strong and attractive coast. This is achieved by maintaining the part of the coast that supports these functions; the coastal foundation. The offshore boundary of the coastal foundation is taken at the NAP -20 m depth contour, the onshore limit is formed by the landward edge of the dune area (closed coast) and by the tidal inlets (open coast). The borders with Belgium and Germany are the lateral boundaries (Figure 2.2).

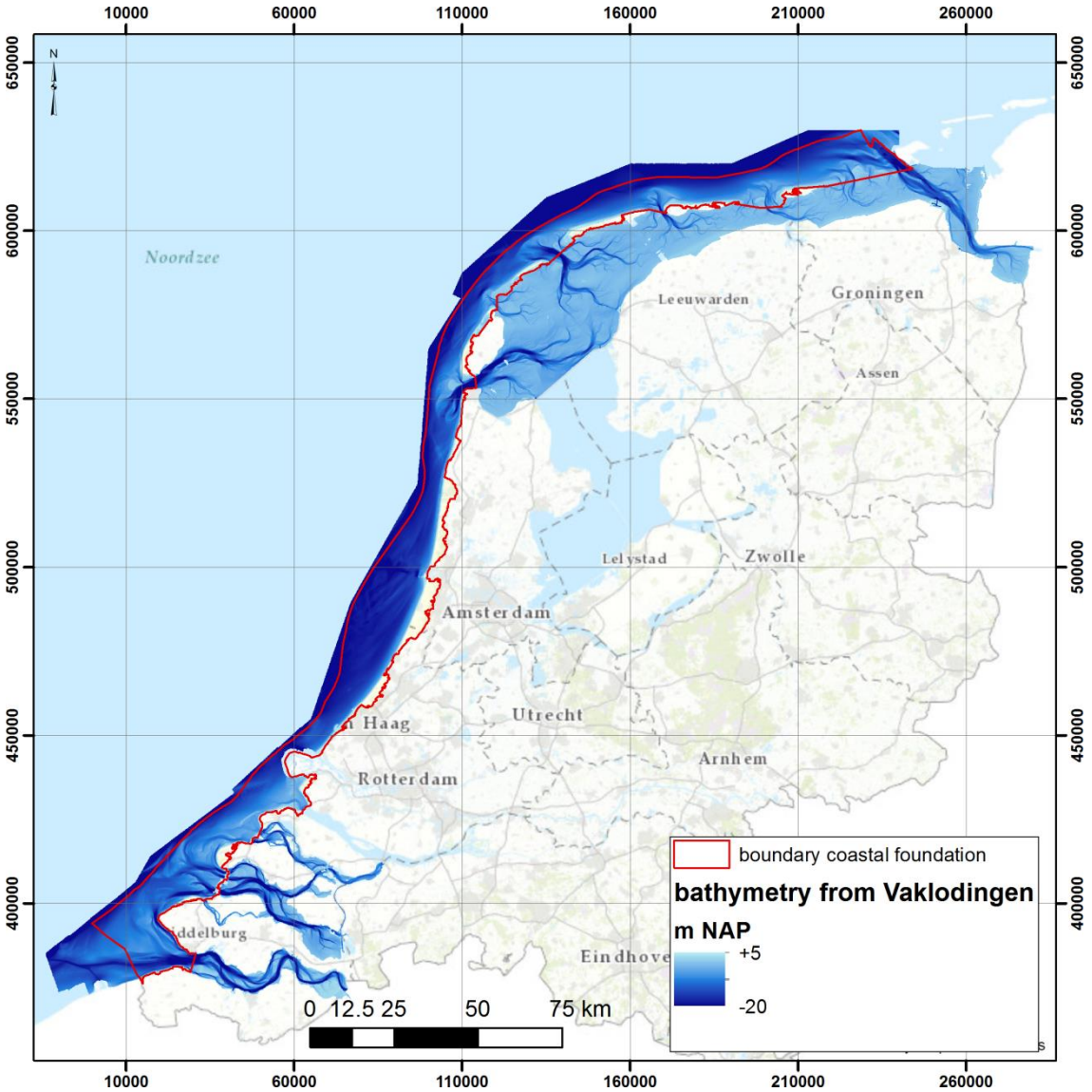

Figure 2.2 Coastal foundation on top of bathymetry from Vaklodingen measurements between 2009 and 2014.

The coastal foundation is maintained by means of sand nourishments. Currently, the total yearly nourishment volume follows from (Lodder, 2016):

$$Q_{nour} = A_{KF} * \mathrm{SLR} + \mathrm{losses} = \left(A_{KF} + A_{WS} + A_{WZ} \right) * \mathrm{SLR} \quad (2.1)$$

where $A_{KF,}$ A_{WS}, A_{WZ} are the areas of the coastal foundation, Western Scheldt and Wadden Sea basins, respectively, and SLR the actual sea level rise. This equation assumes negligible onshore, offshore and lateral losses, does not account for land subsidence and computes the import into the Western Scheldt and Wadden Sea by multiplying the basin area with the sea level rise. With A_{KF} = 4181 km^2, A_{WS} = 253 km^2 (Dutch part only), A_{WZ} = 2497 km^2 (Nederbragt, 2005) and SLR = 0.18 cm/year the nourishment volume is 12.5 million m^3/year, which is actually nourished every year since 2000.

Recent studies showed that some assumptions behind Eq. (2.1) might not be valid. Especially, the sediment loss to the Wadden Sea is likely to be higher than the area of the Wadden Sea basin multiplied with sea level rise, because of morphological adaptations to the closure of the Zuiderzee (1932) and Lauwerszee (1969) and subsidence due to gas and salt mining. Therefore, Lodder (2016) proposed the following expression to compute the yearly nourishment volume:

$$Q_{nour} = A_{\mathrm{KF,new}} * \mathrm{SLR} + Q_{\mathrm{loss,basins}} + Q_{\mathrm{loss,ming}} + Q_{\mathrm{loss,borders}} \quad (2.2)$$

with terms accounting for the net sediment loss into the Western Scheldt and Wadden Sea, sediment loss within the KF due to subsidence related to gas and other extractions, and net sediment loss to Belgium and Germany. This expression still assumes no net sediment transport across the offshore and onshore boundaries of the coastal foundation. The on- and offshore boundaries and hence the size of the coastal foundation can be different than before (Eq. 2.1). ENW (2017) gave a positive advice about this new formulation to determine the nourishment volume, and to serve as a basis for the KG-2 research programme.

2.3 Seaward boundary coastal foundation

The *seaward* boundary of the coastal foundation (coastal policy) is strongly linked to the *landward* boundary of the sand extraction zone (spatial planning policy). The influence of sand extraction on the coastal zone (functions) should be limited. This resulted in the continuous (“doorgaande”) NAP -20 m depth contour as landward boundary for sand extraction (Ministerie van Verkeer en Waterstaat, 1991).

This boundary was chosen based on the coastal profile shape. In front of the Delta and Wadden coasts, the bed slope flattens in offshore direction from ~1:100 to ~1:1000 at water depths of about 20 m. In front of the Holland coast the transition occurs closer to the coast at a water depth of about 16 m. This change in bed slope was assumed to mark the area in which wave action becomes important for sediment transport processes (Wiersma & Van Alphen, 1988).

We could not find a more clear explanation why a change in coastal slope is a good indicator of wave influence, and why waves should become important at the bed slope transition from 1:100 to 1:1000. Furthermore, there is no such clear coastal profile discontinuity. The water depth, given an offshore wave climate, seems a more physics-based definition of the onset of wave influence on the lower shoreface sediment bed (see also Section 2.4). The thought of using the bed slope as proxy for wave influence possibly originated from the equilibrium cross-shore profile concept. No bed level change implies a zero cross-shore sand transport gradient. There is generally a net onshore-directed wave-related transport, which is balanced by an offshore, bed slope-related component due to gravity. This means that a very small

cross-shore bed slope corresponds to a very small net cross-shore sand transport rate. This is a simplistic view, particularly because of neglecting alongshore effects and current-related sand transport processes (see also Section 3.4).

Later, this landward boundary of the sand extraction zone was adjusted to have a simpler definition at the *Zeeland banken*. At the same time, the distance from this landward boundary and the coastline was limited to 20 km in order to avoid large shipping distances offshore South- and North-Holland. Sand extraction takes place between the landward boundary of the sand extraction zone and the 12-miles zone (approx. 22 km off the coast).

Boers & Jacobse (2000) studied the influence of sand banks along the Zeeland and South-Hollands islands (offshore from the defined NAP-20 m depth contour) on the nearshore wave conditions based on SWAN (2D) and ENDEC (1D) wave calculations, in relation to possible sand extraction. It was shown that lowering these sand banks to NAP-20 m only leads to a small increase of nearshore wave heights, even for a 1:4000 storm condition. This is because most wave energy is dissipated in the relatively shallow ebb tidal deltas in front of the coast. Therefore, Boers & Jacobse stated that these results do not necessary apply for other parts of the Dutch coast.

Van der Werf & Giardino (2009) studied effects of extreme deepening (up to 12 m) of the sand extraction zone in relation to the required sediment supply to compensate for sea level rise (up to 1.3 m in 2100), based on morphostatic Delft3D simulations. They found a maximum of 10% wave height increase in the coastal zone. The model predicted a net sediment import into the Dutch coastal foundation which decreased with 10% (realistic scenario) to 40% (most extreme scenario), because the tidal current is deflected offshore related to the lower friction in the deep sand extraction zone. This model study will be discussed more elaborately in Section 5.2.3.

These two studies support the idea that (realistic) sand extraction offshore the NAP -20 m contour has a limited effect on the coastal foundation.

The landward boundary of the sand extraction zone has become the seaward boundary of the coastal foundation (4e Nota Waterhuishounding, Ministerie van Verkeer en Waterstaat, 1998; Nota Ruimte, Ministerie van Ruimtelijke Ordening en Milieu, 2004). Mulder (2000) states that the coastal foundation corresponds to the area with a “free” and “significant” sand exchange within a certain time scale, i.e. of the order of decades. Mulder (2000) constructed a sand balance of the coastal foundation for which he (implicitly) assumed that the coastal foundation at the Wadden Sea and south-western Delta only contains sand and that transport of fine sediments does not contribute to the sediment balance. Indeed the amount of mud on the Dutch shoreface is limited (see Section 3.2.1). This is different from the *coastal system* which includes the Western Scheldt and Wadden Sea, with import of mud from the coastal foundation into these basins. In line with this, De Ronde (2008) estimated the net *sand* transport across the offshore boundary of the coastal foundation (NAP -20m depth contour) on the basis of the study of Van Rijn (1997) to check whether the *sediment* balance was closed.

The assumption is thus that there is no significant net sand transport across the seaward boundary of the coastal foundation. The associated depths depend on the time scale of consideration, because sand transport at the lower shoreface occurs mainly during large storms with a low probability of occurrence. In line with the reasoning behind the landward boundary of the sand extraction zone, Mulder (2000) links the lower boundary of the active

coastal system (coastal foundation) to the morphological change from the mildly sloping shoreface (between 1:100 and 1:1000) to the (almost) flat offshore seabed. At the Delta and Wadden Coast, this slope transition occurs close to the NAP -20 m depth contour, whereas in front of the central Holland Coast this transition is at round the NAP -16 m depth contour. There are shoreface connected ridges between the 16 and 20 m depth contour in front of this stable part of the Holland Coast. For this reason the NAP -20 m depth contour is taken as seaward boundary of the coastal foundation here as well, although the interaction between these shoreface connected ridges and nearshore morphology is not clear.

This seaward definition is in line with the cross-shore classification of Stive *et al.* (1990). They distinguish the following morphological units:

- Active zone or upper shoreface from the first dune row to 8 m water depth.
- Middle and lower shoreface from 8 m to 20 m water depth.
- Inner shelf below 20 m water depth.

They define the transition of the active zone to the middle shoreface as “the level above which profile changes occur as observable from profile measurements over one average year”. We interpret this as where yearly bed level changes are significant, i.e. larger than measurement errors, ~0.1 m. The middle and lower shoreface is a morphodynamically weakly varying zone, where the decadal changes can be derived from initial sediment transport calculations (Roelvink & Stive, 1990). According to Stive *et al.* (1990) the transport rates at the seaward boundary of the middle and lower shoreface are tide-dominated and wave-dominated at the shoreward boundary. The inner shelf is “morphodynamically negligible” for the scales under consideration (decades), i.e. a steady average level with undulations. This definition of the seaward boundary of the middle and lower shoreface on the basis of morphodynamic activity and the relative importance of waves is closely related to the depth of closure concept that is being described in the next section.

2.4 Depth of closure concept

The depth of closure for a given or characteristic time interval is the most landward depth seaward of which there is no significant change in bottom elevation and no significant net sediment transport between the nearshore and the offshore.

There are different ways to estimate the closure depth. Hallermeier (1981) defines a littoral zone with “extreme near-breaking waves and breaker-related currents” and a shoal zone that extends from the seaward edge of the littoral zone to a water depth where expected surface waves are likely to cause little sand transport. Seaward of the shoal zone lies the offshore zone, of relatively deep water with respect to surface wave effects on the bed (Figure 2.3).

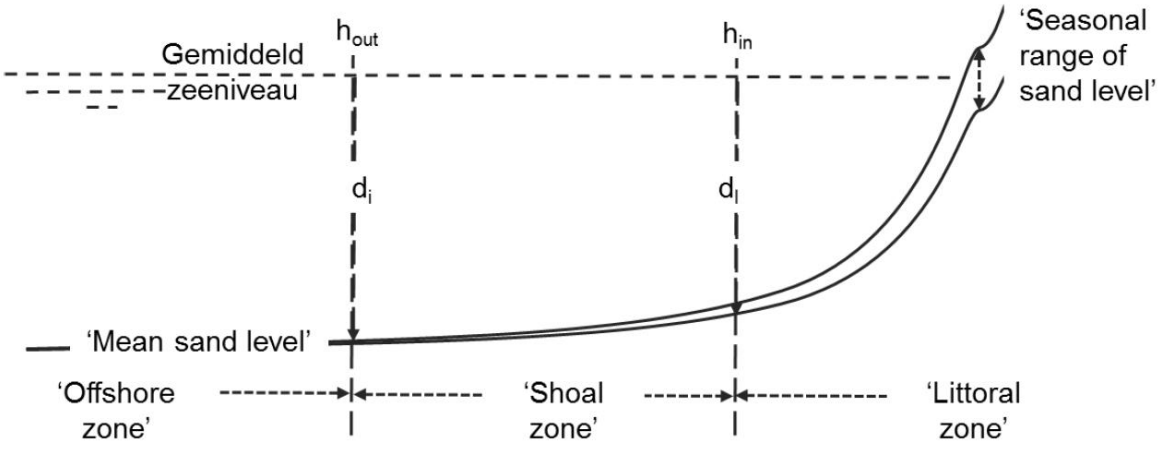

Figure 2.3 Schematic cross-shore profile with the zones and depths of closure as defined by Hallermeier (1981). Figure taken from Cleveringa (2016).

The (approximation of the) expression for the seaward boundary of the shoal zone reads as follows:

$$h_{out} = 0.018 H_m T_m \sqrt{\frac{g}{D_{50}(s-1)}} \tag{2.3}$$

with H_m the yearly median wave height, T_m the median wave period, g the acceleration due to gravity, D_{50} the median grain-size and s the ratio of the sediment and water density. This expression originated from the required orbital velocity to mobilise sand grains based on a critical mobility number. The calculated closure depths were consistent with usual order-of-magnitude guidance and the limited specific field results on the seaward limit to significant wave effects on the nearshore profile (US coasts). Typical values for the Dutch coast with H_m = 1.0 m, T_m = 5.3 s (De Leeuw, 2005), D_{50} = 0.2 mm and s = 2.65 give a closure depth of 16.5 m. It is noted that the expression of Hallermeier (1981) is simple, supported by little field evidence and based on yearly median wave conditions (i.e. no effects of storm events). Furthermore, it does not account for the influence of currents (induced by waves, wind, tide and density-gradients).

Another approach is to look into the morphological envelope, i.e. until what water depths significant bed level changes occur (Figure 2.4).

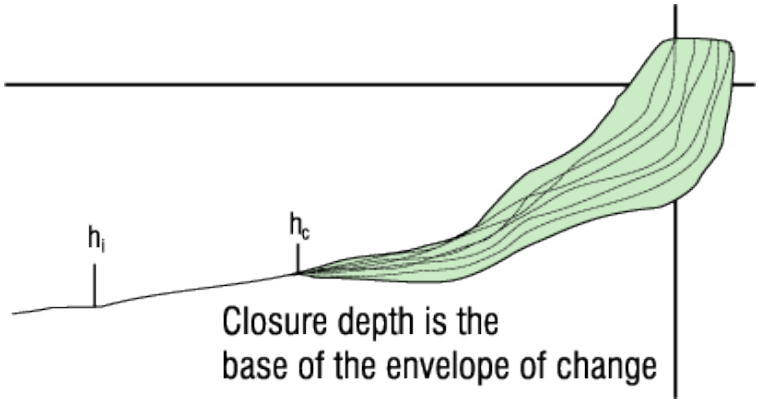

Figure 2.4 Illustration of the morphological envelope in order to define the closure depth.

This has been studied for the Holland coast using 1965-1997 JARKUS transect data by Hinton (2000). These so-scaled JARKUS “doorlodingen” extend further offshore than the regular JARKUS data, until a maximum water depth of about 17 m. Hinton (2000) computed the standard deviation of elevation as a function of the cross-shore distance for different periods, and took a value of 0.25 m (measurement accuracy) to distinguish an active from an inactive seabed (Figure 2.5).

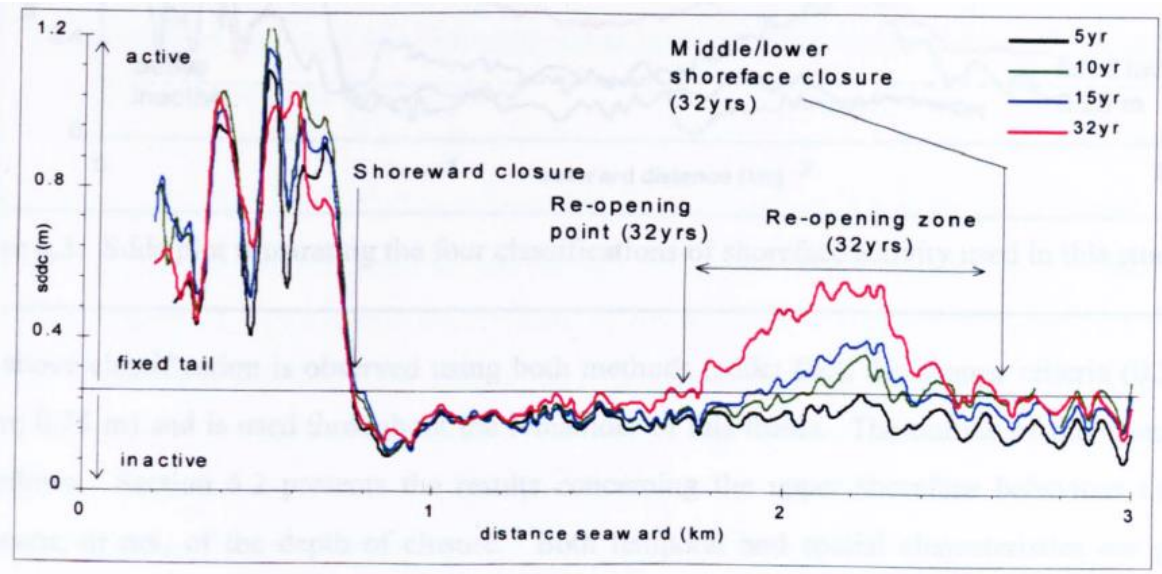

Figure 2.5 Standard deviation elevation as function of the cross-shore distance at Zandvoort. Figure taken from Hinton (2000).

This analysis resulted in a shoreward closure at water depths between 5 and 9 m. At some locations the profile re-opened and then usually re-closed towards its seaward limit. Re-opening was only observed over the longer time scales (>10 years) and at distances offshore greater than 1.5 km (starting at depths between 10-13 m). In addition, as the temporal period was increased the number of cases in which this behaviour occurs increased. This suggests that this behaviour is due to slow, cumulative change, rather than fast, infrequent events. Hinton (2000) suggests that re-opening is associated with a local shoreface steepening and refers to Roelvink & Stive (1990) and Stive *et al.* (1990) which have shown that the significant depth change observed on the shoreface represents the effect of the onshore transport of material to the active zone. The middle/lower shoreface closure is typically located at 12-13 m water depths.

More recently Vermaas *et al.* (2015, 2016) studied the Dutch lower shoreface morphodynamics using the RWS Vaklodingen data-set as well the more offshore-located (interpolated) data-set of the Hydrographic Office of the Royal Netherlands Navy for the period 1964-2013. The mean depths, mean depth range (difference between maximum and minimum depth) and linear trends were computed for selected areas at Westerschelde, Grevelingen, Haringviet, South-Holland, North-Holland, Texel, Terschelling (Figure 2.6) and Ameland, as well as for a subdivision of those areas. It was concluded that the transition from an active to a stable bed occurs at water depths between 10 and 15 m, i.e. where the depth range and bed level trend converge. Vermaas *et al.* (2015) computed that the coastal

foundation (and thus nourishment volume) would be 26% smaller with a NAP -15 m instead of a NAP -20 m depth contour as offshore boundary.

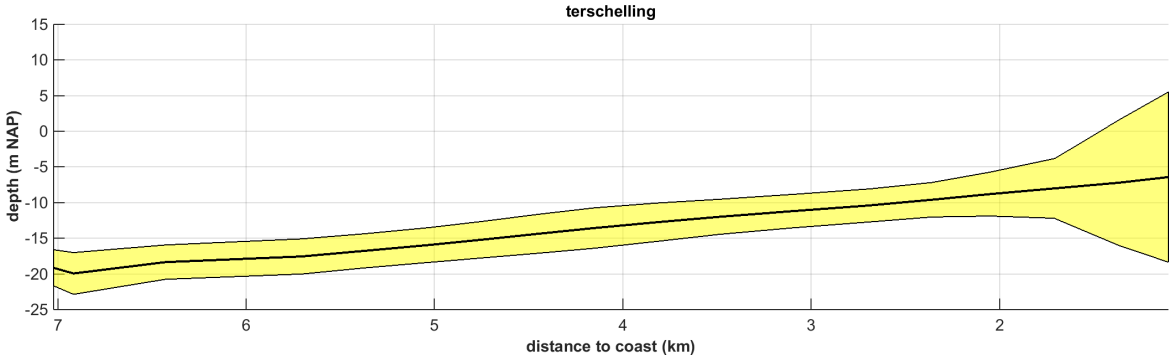

Figure 2.6 Mean depth (thick line) ± mean depth range (thin lines) as a function of cross-shore distance for the Terschelling area based on 1964-2013 bathymetry data. Note that the vertical scale of the mean depth range is 10x exaggerated for clarity reasons. Figure taken from Vermaas & Van der Spek (2016).

Koomans (2000) argues that the location with the maximum in heavy mineral concentration could be related to a depth of closure of the light mineral fraction (i.e. sand). This is based on laboratory experiments. In his large wave flume (GWK) experiments, heavy minerals were mainly concentrated in the region seawards of the breaker bar where net sediment transport rates became non-significant. Full-scale flow tunnel (LOWT) sheet-flow experiments showed a clear difference in transport rates of quartz and zircon (density of ~4650 kg/m^3) with a similar grain-size of 0.2 mm. Both fractions were transported in the direction of the larger onshore velocity (velocity skewness), but the mass transport rates of the zircon fraction were considerably smaller than for quartz. Based on this, Koomans (2000) argued that the increased concentration of heavy minerals on the profile of the GWK measurements resulted from lag formation. The location where the sediment transport of the light mineral fraction is initiated is thus characterised by the presence of increased concentrations of heavy minerals. Since most natural sediments contain only small amounts of heavy minerals (~1% for Dutch beach sands), depth of closure will in general depend on the sediment transport of light minerals. Therefore, the location with the maximum in heavy mineral concentration could be related to a depth of closure of the light mineral fraction.

As part of the NOURTEC nourishment programme (see Section 4.3.1), the depth of closure of the Dutch barrier island Terschelling was assessed by Marsh *et al.* (1998) based on profile measurements (i.e. where the maximum profile change became smaller than 0.25 m). They found that the 25-years depth of closure was not constant along the coastline but was located deeper in eastward direction (Figure 2.7). This figure also shows the distribution of this heavy mineral fraction, inferred from the radiometric measurements. The locations of maximum heavy-mineral fraction are similar to the closure depth computations, both at water depths between ~7 and ~10 m.

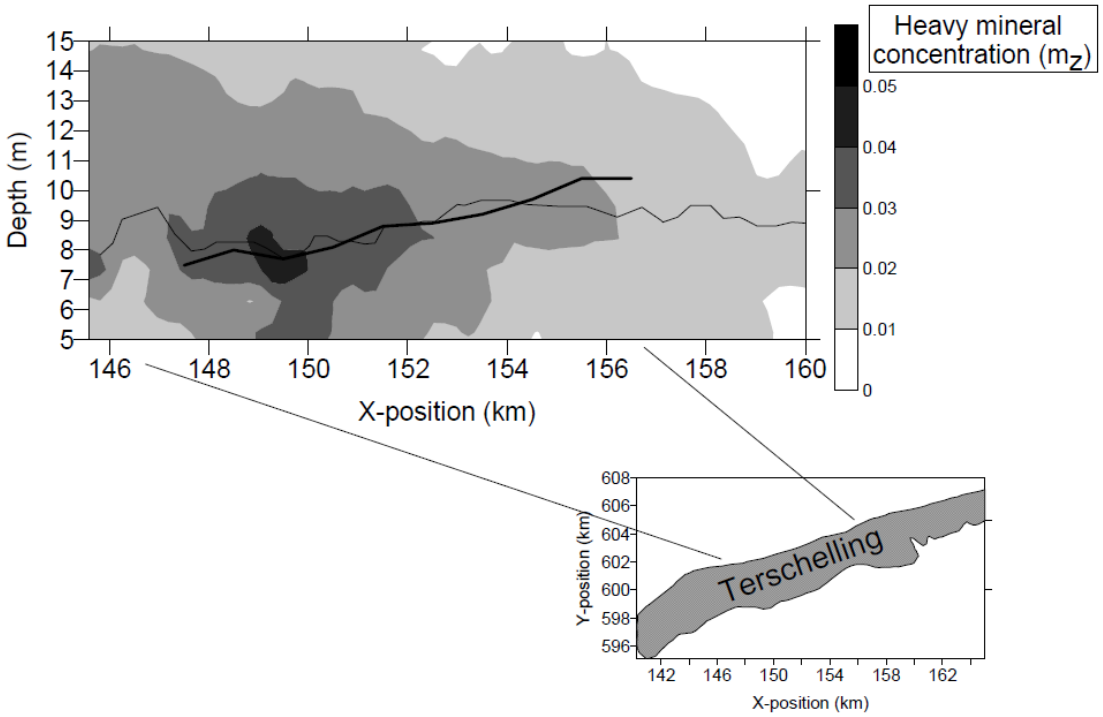

Figure 2.7 Longshore variation of the heavy-mineral concentration as function of water depth at Terschelling. The thin line represents cross-shore maxima in the heavy-mineral concentration. The thick line shows the variation of the 25-years depth of closure determined from profile measurements by Marsh et al. (1998). Figure taken from Koomans (2000).

The large-scale morphodynamic changes at the Holland shoreface were also studied by monitoring dredge disposal over time periods of 1-2 decades (Verhagen & Wiersma, 1991; Van Woudenberg, 1996). Morphological activity was observed up till a water depth of about 19 m, which coincides with the lower boundary of the active coastal profile. These studies are more elaborately discussed in Section 3.2.3.

2.5 Synthesis

In Dutch coastal policy, the nourishment volume for the coastal foundation to grow with sea-level rise is directly related to the coastal foundation area. In this computation it is currently assumed that there is no net sand transport at a decadal time scale across the seaward boundary, which is defined at the NAP-20m depth contour. This boundary is strongly linked to the onshore extent of the sand extraction zone to ensure there is a limited effect on the nearshore zone. The coastal foundation offshore boundary is not very well substantiated. Mainly the bed slope transition from ~1:100 to ~1:1000 was used as criterion. At the Delta and Wadden Coast, this slope transition occurs close to the NAP -20 m depth contour. In front of the central Holland Coast this transition is at around the NAP -16 m depth contour. The NAP -20 m depth contour is taken as seaward boundary here as well, because of the supposed positive effect of shoreface connected ridges at 16-20 water depths between Katwijk and Petten on coastal stability. Different ways of determining the depth of closure (based on wave action, morphological envelope and lag deposits of heavy minerals) indicate that the current 20 m water depth is a safe choice for the offshore boundary of the coastal foundation. However, direct monitoring of dredge disposals along the Holland coast over 1-2 decades showed that the transition of morphological active to inactive seabed occurs at a water depth of about 19 m.

3 Dutch lower shoreface morphodynamics

3.1 Introduction

The relevance of the shoreface was indicated by Wiersma & Van Alphen (1988) who stated that “the shoreface not only bears the vestiges of the geological history of the present coastline, but it is also the area whose shape is maintained or transformed by present-day hydrodynamic processes, to a large extent determining the future coastline”. This was before the start of the annual coastal maintenance using large-scale (shoreface) nourishments that would influence the shoreface evolution as well. The shoreface can be divided in the wave-dominated upper shoreface that is characterised by breaker bar morphodynamics and the lower shoreface that is thought to be predominantly active during storm events. This chapter concentrates on the lower shoreface morphodynamics.

The shoreface was subject of extensive studies during the Dutch coastal development research project *Kustgenese*, the predecessor of *Kustgenese 2* project as part of which this literature review was written. Comprehensive surveys of coastal bathymetry and geomorphology (Van Alphen & Damoiseaux, 1987), sediment composition and near-surface geology (Niessen & Laban, 1987; Niessen, 1989; 1990) were undertaken. Moreover, both the internal architecture and sediment-composition of, and the processes at the shoreface-connected ridges along the central Holland coast were studied (Van de Meene, 1994). The study of sediment cores revealed the geology of the present-day shoreface (Beets *et al.*, 1995) and of the mid-Holocene shoreface of the prograded beach barriers along the Holland coast (Van der Valk, 1996).

3.2 Large-scale sedimentology, morphology and geology

3.2.1 Shoreface sediments

The sea bed at the shoreface is predominantly sandy, with some clay deposits, and an admixture of gravel and mollusc shells. South of Bergen aan Zee, the mobile sea-bed layer consists of reworked alluvial sand of the rivers Rijn and Maas and reworked Pleistocene and older Holocene deposits. Median grain-sizes range from 250 to 300 µm. North of Bergen aan Zee the sea bed consists of reworked (peri-)glacial sands from the Pleistocene. Along the Wadden coast the median grain-size fines in the eastern direction from 210-300 µm offshore Texel to 63-150 µm offshore Schiermonnikoog (Niessen, 1990). Reworking of glacial tills near Texel and Vlieland produced gravel-rich layers. Large tidal channels near tidal inlets cut into the sea bed and excavate Pleistocene (Wadden area) and Tertiary deposits (Delta area), see Sha (1989a) and Van der Spek (1997) respectively. See Hijma (2017) for a comprehensive overview of both shoreface geology and the impact on tidal-channel migration.

The grain-size distribution of the sand on the shoreface is variable over time and reflects the variation in driving forces. Passchier (2003) and Passchier & Kleinhans (2005) described the variation in grain-size and small-scale sea-bed morphology of the central Holland shoreface over a one-year period. Guillèn & Hoekstra (1996) studied the changes in grain-size distribution in the upper shoreface of Terschelling caused by a pilot shoreface nourishment (Nourtec campaign, see Section 4.3.1). They concluded that the grain-size gradient over the shoreface quickly ‘recovered‘ from the disturbance by the comparatively coarse nourishment sand by redistribution of individual grain-size fractions to their “equilibrium” locations. Van Straaten (1965) and Van der Valk (1996) reported a double coarsening-upward sequence for mid- and late Holocene shoreface deposits in the prograded barrier sequence of the Holland

coast. However, this was not confirmed for the present-day situation (Niessen & Laban, 1987).

3.2.2 Shoreface morphology

Wiersma & van Alphen (1988) described the morphology of the shoreface of the Holland coast between Hoek van Holland and Den Helder. They concluded that the shoreface morphology and lithology vary considerably along the coastline, depending on the (1) coastal slope and (2) the superposition of ridges and tidal deltas. Van Alphen & Damoiseaux (1987) presented a series of 78 shore-normal depth profiles of the shoreface morphology between Cadzand and Rottumeroog, which extended about 20 km offshore with an alongshore spacing of approx. 5 km. These profiles were sounded in the summer of 1984 within the framework of the Kustgenese project. The profiles show a relatively flat sea bed beneath the 20 m isobath and a sloping shoreface. The shoreface shows a steep upper part with a slope gradient steeper than 1:100 and a lower part with gradients between 1:100 and 1:1000. These authors produced a morphological map of the shoreface of The Netherlands and the adjacent part of the continental shelf, scale 1:250,000, on the basis of these profiles and depth charts that were collected between 1977 and 1984. This map shows distinct differences between shorefaces of the Delta area, the Holland coast and the Wadden coast (Figure 3.1).

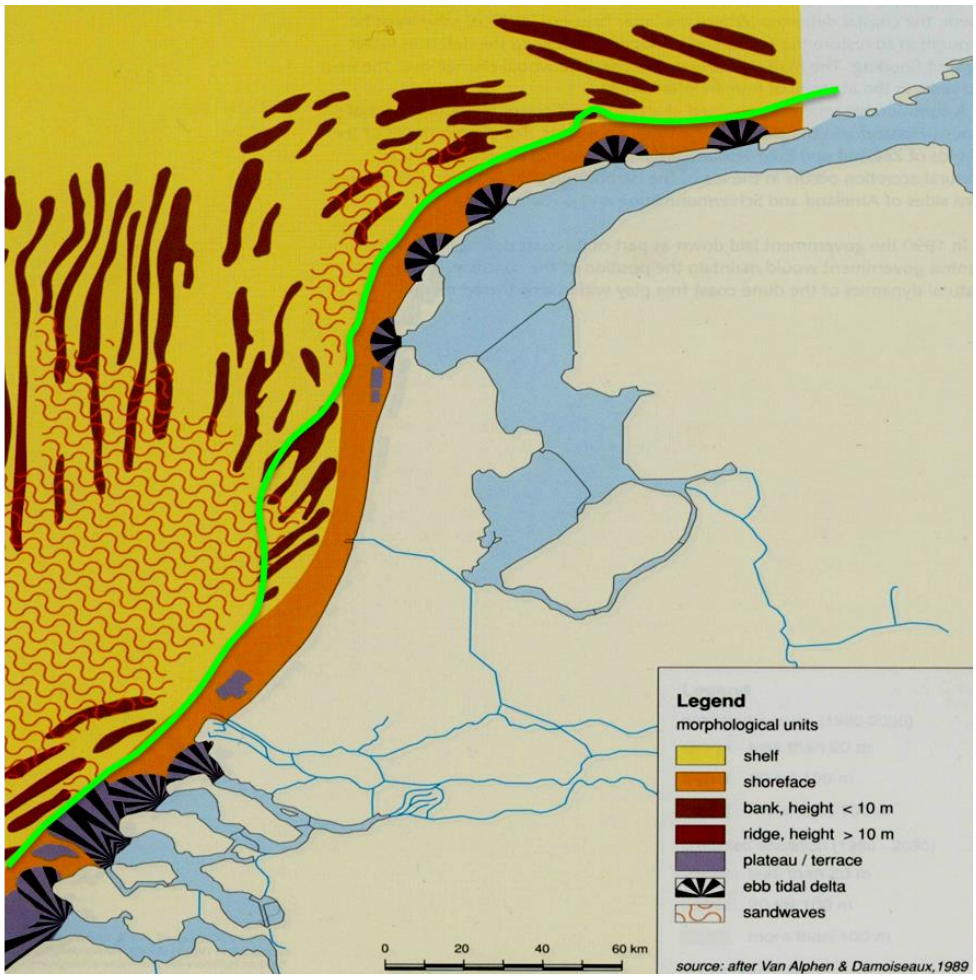

Figure 3.1 Simplified morphological map of the shoreface of The Netherlands and the adjacent part of the continental shelf. The green line indicates the 20 m isobath. After Van Alphen and Damoiseaux (1987). (https://www.arcgis.com/home/webmap/viewer.html?url=https%3A%2F%2Fgeoweb.rijkswaterstaat.nl%2Farcgis%2Frest%2Fservices%2FNoordzeeAtlas%2FNZ_NZA_geomorfologie%2FMapServer&source=sd)

Delta area
The shoreface of the Delta area consists of the contiguous ebb-tidal deltas of the (former) estuaries Westerschelde, Oosterschelde, Grevelingen and Haringvliet (from south to north), that are collectively indicated as the Voordelta. The ebb-tidal deltas have low-gradient platforms (slopes of less than 1:1000 to 1:100) that are dissected by ebb- and flood tidal channels and have inter- to supratidal sand bars on top. The gradients of the seaward slopes of the ebb-tidal deltas are ranging from 1:1000 to steeper than 1:100. Only the Oosterschelde ebb-tidal delta extends to the NAP -20 m contour, the others grade into a lower shoreface. Smaller-scale morphological elements such as plateaus, some of them with escarpments on their seaward side, and isolated bars, especially along the island coasts, occur. Offshore of the shoreface, the southwest-northeast running sand ridges of the Zeeland Banken and the Bollen van Goeree are situated. The northeastern tips of the Bollen van Goeree ridges connect to the lower shoreface offshore the island of Voorne. Sand waves do occur in all areas. In the northern part of the Delta area the constructed Maasvlakte 2 sits within the shoreface area. The Maasgeul navigation channel separates this area from the Holland coast.

Holland coast
The shoreface of the continuous, 120 km-long Holland coast consist of a comparatively steep (steeper than 1:100) surfzone that comprises shore-parallel breaker bars in most places and a less steep middle- to lower shoreface (gradients ranging between 1:100 and 1:1000). Between Hoek van Holland and Katwijk the shoreface is up to 8.5 km wide and extends to the NAP -20 m contour. A shallow plateau (up to approx. NAP-11 m) occurs between Hoek van Holland and Ter Heijde which is the former dredge-spoil dumping site Loswal Noord. Between Katwijk and Egmond the shoreface is less than 4 km wide and runs down to the NAP -16 m contour. Here, the shoreface is bounded by a series of 10 sand ridges that rise from a flat sea bed (slope < 1:1000). Four of these ridges connect to the shoreface between Zandvoort and Egmond. Sandwaves occur on most of the ridges. In the area with sand ridges the NAP -20 m contour lies up to approximately 20 km offshore. The dredged IJ-geul navigation channel dissects this area.

North of Egmond the shoreface widens and extends to the NAP -20 m contour again. Here, SW-NE oriented isolated bars occur on the shoreface. Besides, the shoreface includes two shallow plateaus between Petten and Groote Keeten, the southern of which is called Pettemer Polder. The occurrence of these plateaus is possibly related to Pleistocene relief in the subsurface (De Mulder, 1984). In the north, the shoreface is bounded by the ebb-tidal delta of Texel Inlet.

Wadden coast
The Wadden coast consists of barrier islands, separated by tidal inlets and their associated ebb-tidal deltas. In contrast with the Delta area, these ebb-tidal deltas do not meet. The ebb-tidal deltas have low-gradient tops (slopes of less than 1:1000) that are dissected by ebb- and flood tidal channels and have inter- to supratidal sand bars on top. The gradients of the seaward slopes of the ebb-tidal deltas are ranging from 1:1000 to steeper than 1:100 at their most seaward part. The ebb-tidal deltas are separated by the shorefaces of the barrier islands where distinct steep-sloped surf zones are lacking. The shoreface slopes down to the NAP -20 m contour with gradients between 1:100 and 1:1000 and has a width of 8.7 to 12.5 km. Smaller-scale morphological elements, such as isolated shore-oblique sand bars, reef-bow or saw-tooth bars at the downdrift sides of the ebb-tidal deltas offshore of Terschelling, Ameland and Schiermonnikoog, and elongated coast-parallel breaker bars, have been identified. Offshore Vlieland, a sand ridge and a plateau with an escarpment on its seaward

side are found. To the northwest of Ameland Inlet, the NAP-20 m contour shows a lobe-like seaward extension (which has been interpreted to be a subrecent ebb-tidal delta of the Borndiep by Sha, 1989b). The shoreface grades to the East into the mouth of the Ems estuary and the comparatively small ebb-tidal deltas of the inlet channels Lauwers and Schild, east of Schiermonnikoog. Sand waves can occur in all areas.

Ebb-tidal deltas

Ebb-tidal deltas form where the sediment-laden ebb current leaves the comparatively narrow tidal inlet and enters the sea/ocean, and as flow segregates, current velocities diminish beyond the sediment transport threshold. Hence, the sand is deposited and a shallow distal shoal called terminal lobe is formed. This process is counterbalanced by waves that impact on these shallow shoals and tend to move the sand landward, towards the inlet and bounding shores. Hence, the morphology of the ebb-tidal delta is essentially determined by the relative importance of wave- versus tidal energy. Wave-dominated ebb-tidal deltas are pushed close to the inlet throat, while tide-dominated ebb-tidal deltas extend offshore. See Elias *et al.* (2016) for an extensive summary of the relevant literature on ebb-tidal delta morphodynamics.

The main channels in tidal inlets along the Dutch coast are ebb-dominated and updrift oriented, which means that they turn left after leaving the inlet throat (Figure 3.2). This is caused by the tidal wave that travels from south to north to east along the Dutch coast. The ebb channels build terminal lobes that can expand seaward due to sediment supply and deposition. The right-hand side of the ebb-tidal deltas is shallow, since large channels are absent (Figure 3.2, nr. 6). These shallow sand masses where wave influence is larger or even dominates, are usually separated from adjacent island coast by a shortcut channel.

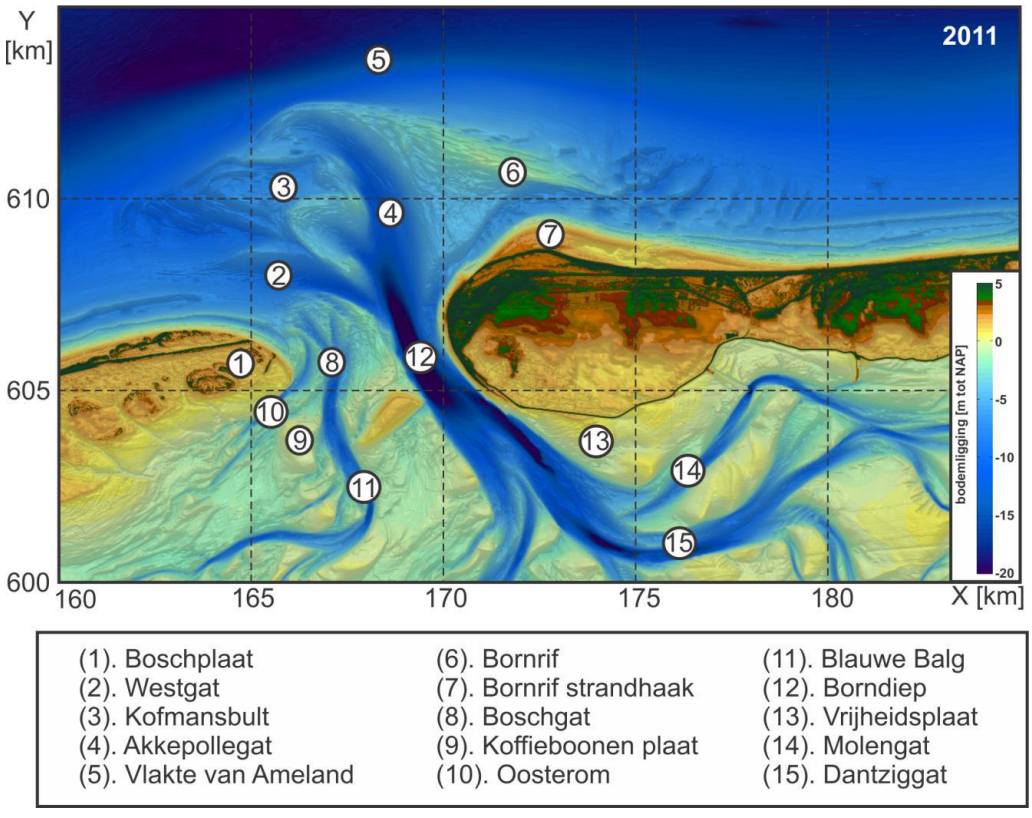

Figure 3.2 Ameland Inlet and its ebb-tidal delta in 2011, showing the general, characteristic channel and shoal morphology of ebb-tidal deltas along the Dutch coast. See text for details.

Most ebb-tidal deltas along the Dutch coast have been impacted by interventions in tidal basins such as partial or complete damming. These impacts can be arranged as follows:

1 Complete damming of a tidal inlet causes 'shrinkage' of ebb-tidal delta: erosion of the seaward slope by waves, predominantly above NAP-10 m, and building of intertidal sand bars at the edge. Moreover, the reduction in tidal current velocities results in a smaller sediment supply to the intertidal morphology, that causes erosion of the original intertidal bars, and infilling of channels with eroded sand and imported mud. Examples are the ebb-tidal deltas of Grevelingen, Haringvliet and Brielse Maas (see Elias *et al.*, 2016, for an overview).
2 A reduction of the tidal volume of the inlet leads to an increase of the impact of the shore-parallel North Sea tide. This leaves the large-scale lay-out of an ebb-tidal delta intact but causes local changes in channel orientation. The changes in channel orientation on the Banjaard shoal after the completion of the Oosterschelde storm surge barrier illustrate this (see Elias *et al.*, 2016, for more details).
3 A significant reduction of the tidal volume, caused by the damming of a large part of the tidal basin, leads to large-scale erosion of the ebb-tidal delta. The eroded sand is transported into the inlet and to the downdrift island. This sediment 'pulse' can trigger large-scale changes along the coast of the downdrift island. The evolution of the ebb-tidal delta of the Zoutkamperlaag and the North Sea shoreline of Schiermonnikoog after the closure of the Lauwerszee illustrates this (see Oost, 1995, for details).
4 Changes in phase difference between inlet tide and North Sea tide can impact the orientation of the main channels. The reduction in phase difference (without a significant change in tidal volume) in Texel and Vlie Inlet after the construction of the Afsluitdijk caused the main channels to rotate in updrift direction, diminishing the influence of the tidal flow in the shallow ebb-tidal delta platform and exposing it to increased wave attack. See Elias & Van der Spek (2006) for details on the changes in the ebb-tidal delta of Texel Inlet.

Shoreface-connected ridges

Van de Meene (1994) studied the shoreface-connected ridges along the central part of the Holland coast extensively. He collected bathymetric data along transects both perpendicular and parallel to the ridges, and boxcores on these transects for analysis of sediment grain-sizes and sedimentary structures. Moreover, he used side-scan sonar to produce mosaics of the top of the ridges, revealing the sea-bed morphology. The mosaics showed straight-crested sandwaves with heights (η) of 0.8-2 m and wave lengths (λ) of 600-750 m, with superposed straight- to sinuously crested megaripples (η=0.15-0.3 m; λ=5-12 m) on top of the ridges.

The shoreface sediment samples at NAP-10 m consisted of fine-grained grey sand (D_{50}=150-200 µm) with local admixtures of medium sand (D_{50}=250-300 µm). The median grain-sizes showed a jump at the lower shoreface to medium-grained brown sand at the shelf (D_{50}=250-300). Van de Meene stated that the distinct transition of the surface sediments from medium brown sand on the inner-shelf and lower shoreface towards fine grey sands higher up the shoreface has been described previously by Van Straaten (1965) and Van der Valk (1992). In addition to this data set, Van de Meene ran a seismic survey across the ridges and collected a set of closely spaced vibrocores along the seismic lines. The seismics showed signatures of infilling and migrating tidal channels, which was confirmed by the deposits in the vibrocores. On top of this, fine- to medium-grained, dark grey to yellowish brown sand containing an open-marine *Spisula* fauna occurred. Van de Meene concluded that the ridges are composed of marine sand (with exception of the most southern part), with 'older' sand at the landward side, whereas the tops and seaward sides of the ridges consist of 'young' sea sand. The

younging and thickening upwards of the sand indicate gradual outbuilding with time to northwest.

The most southern seismic line shows that in that part, the ridge topography has been carved out in older sediments, which indicates that the ridge morphology there is more an erosive feature than a depositional phenomenon, as it is along the seismic lines further north. Moreover, he concluded that the exposure of Pleistocene sediments in the troughs (at most overlain by a thin veneer of young sea sand) and the increased sorting of sediment at the ridge crests indicates that sediments are being eroded in the troughs and deposited at the ridge crests, which suggests that the ridges are still being maintained by the present hydrodynamic regime. Moreover, the thin and recent layer of young sea sand, marked by distinct shell lags, on the landward flank of the ridges suggests that sediment is being reworked at the landward flank and deposited on the seaward flank of the ridges. This indicates that the sand ridge system is migrating seawards very slowly. Migration rates are estimated at 0.5 to 1 m per year (which compares well with migration rates obtained from Van de Meene's model calculations).

3.2.3 Large-scale shoreface morphodynamics

In order to establish the large-scale morphodynamic changes at the shoreface, the North Sea Directorate of Rijkswaterstaat used dredged sand to build shore-normal sand dams on the shoreface and monitored their developments. Van Woudenberg (1996) described the evolution of a sand dam that was built on the southwest side of Loswal Noord near Hoek van Holland in 1981-1982, at depths of 15 to 23 m. The dam with an initial trapezoidal shape was 3600 m long, 250-370 m wide at its base and 1.30 to 4.05 m high. The part of the dam deeper than 19 m did not migrate over the period 1982-1995. However, the dam declined slightly in height and transformed to an asymmetrical, peaked profile with a mildly sloping southside and a steep northern side (resembling the profile of offshore sand waves). Moreover, the dam was covered with megaripples (η=0.2-0.5 m, λ=10 m). The upper part of the dam, shallower than 19 m, was not stable over the interval 1982-1995. This part migrated up to 150 m to the northeast and lost in height. A distinct asymmetry did not develop, possibly because of wave activity. Van Woudenberg concluded that the depth of transition from the stable to unstable part of the dam coincided with the lower boundary of the active coastal profile.

Verhagen & Wiersma (1991) analysed the development of a sand mound near Wijk aan Zee. The sand was dumped on the sea bed between NAP -10 and -15 m and had a maximum height of 1.2 m. Based on depth soundings they observed that the mound migrated to the northeast over the period 1982-1990 and that the migration rate was larger in the shallow parts than in the deeper parts. They concluded that the migration was caused by daily wave and current conditions and not by extreme events. Cross-shore sediment transport, either landward or seaward, could not be established.

Van Heteren *et al.* (2003) monitored 2 sites at the central Holland shoreface from March 2001 until April 2002, using a multibeam echo sounder, a side-scan sonar and a boxcorer. One site was situated on the margin of a sandwave area on a shoreface-connected ridge (Figure 3.3), the other at the transition of the lower shoreface to the inner continental shelf (Figure 3.4). For both areas 4 successive multibeam surveys were collected. The sand waves and megaripples on the shoreface-connected ridge seemed to be controlled by the longshore current. The megaripples superimposed on the sand waves were additionally influenced by wave activity, increasing the continuity of the megaripple crests. The variable size of the megaripples over time indicates that the shoreface is a dynamic environment, sensitive to strong wind conditions. During (minor) storm conditions the areas influenced by wave activity expand in the direction of the inner shelf and beam-trawl tracks are largely obliterated. See Passchier (2003) for more details.

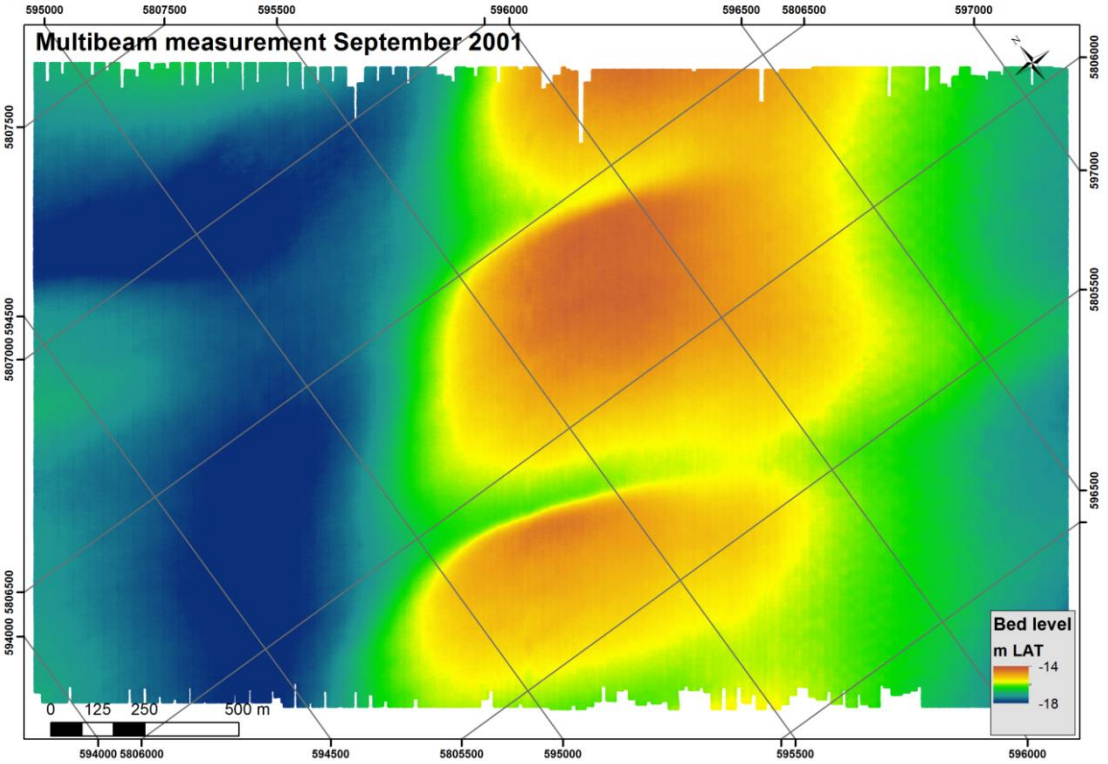

Figure 3.3 Multibeam sonar image of a shoreface connected ridge with sandwaves on top, located 5-10 km offshore Zandvoort and about 10 km south of the IJ-geul shipping channel. Landward is to the right. On the landward side, the area is dominated by a flat seafloor without major bedforms and a slope of less than 1:1000. On its seaward side, the area is characterised by sand waves that are 2-4 m in height and that have wavelengths of tens to hundreds of meters. A shoreface-connected ridge covered with sand waves on its seaward side occurs in the central part of the area.

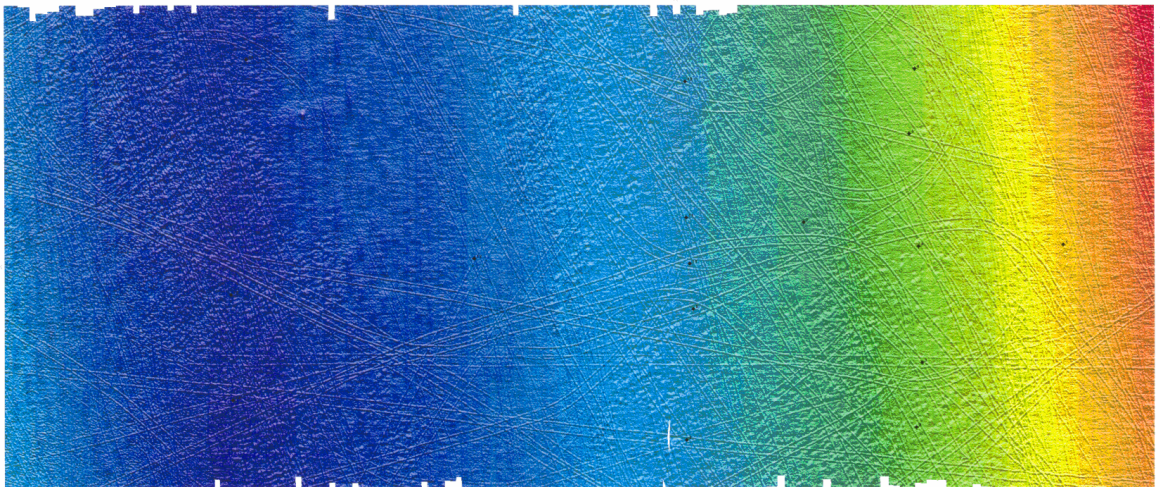

Figure 3.4 Multibeam sonar image of the transition of the lower shoreface to the inner continental shelf. The area is located 5-10 km offshore Noordwijk aan Zee, in water depths of 15 m (red colour) to 20 m (dark blue colour). Landward is to the right. The area is dominated by a flat seafloor (slope less than 1:1000) without major bedforms. Megaripples and tracks made by beam-trawling fishermen are found at the surface.

Analysis of profile changes at the middle and lower shoreface of the Holland coast (Vermaas, 2010; Vermaas *et al.*, 2015; Vermaas & Van der Spek, 2016) did not show an offshore-directed translation of sediment volumes, despite the addition of large volumes of sand to the upper shoreface in many locations.

3.2.4 Shoreface geology

A summary of the Holocene evolution of the Dutch coast is presented by Beets *et al.* (1994) and Beets & van der Spek (2000). Up until 5000 years before present (BP), the coast of The Netherlands showed an overall retreat, mainly due to the rapid rate of sea-level rise (SLR) caused by the melting of the land ice masses of the last glacial period. Around 5000 BP the SLR rate had dropped significantly and the sediment supply, predominantly from reworking of the shallow sea bed and erosion of the high-lying Pleistocene relief, was able to fill in the tidal basins, changing them into tidal flats, and subsequently into peat bogs, which resulted in (gradual) closure of the tidal inlets and stabilising of the coastline. The Wadden area is an exception to this, since in the western part there were no tidal basins due to the high-lying Pleistocene and in the eastern part the sediment supply was too small to fill in the tidal basins completely.

After 5000 BP the Delta, Holland and Wadden coast all showed a different evolution. The Delta coast had stabilized by 3500 BP but was breached and changed into a series of distributaries of the rivers Rhine, Meuse and Scheldt in the early medieval period. The Holland coast from south of Den Haag to Egmond, gradually changed into a beach-barrier-dune coast that prograded seaward until the Middle Ages. The northern part of Holland from Egmond to Texel, where the coastal evolution was dominated by the gradual erosion and submersion (because of SLR) of the high-lying landscape of Pleistocene origin, was gradually flooded in the early medieval period, which resulted in establishment of new tidal inlets and rapid expansion of the western part of the Wadden Sea.

The shoreface geology of the Delta coast has not been studied comprehensively. Details are given by Ebbing et al. (1993), Ebbing and Laban (1996) and Van der Spek (1997). The subsurface of the shoreface of the Holland coast has been surveyed extensively with seismics and sediment cores. Moreover, the shoreface deposits of the prograding beach-barrier coast have been studied in great detail. The shoreface of the Wadden coast has been studied predominantly through seismic surveys, complemented with analyses of sediment cores. The general picture is as follows:

1 The seabed consists of an active sand layer, active meaning that it is mobile due to smaller-scale bedforms such as megaripples that migrate over the seabed. This layer consists of brown sand and is rich in shells.
2 Below the active layer remnants of the transgressive coastal system are found. Coastal retreat causes erosion, predominantly by waves. The retreating shoreline transgresses over its back-barrier, exposing back-barrier deposits at the shoreface. The eroding waves will remove the upper parts of the back-barrier deposits and hence only the lower (sandy) parts, that are usually cut into the subsurface are preserved. In many places along the Dutch coast (from the Maasvlakte, along the Holland and Wadden coast, to the Ems estuary), the lower parts of the deposits of migrating tidal channels are found, both in seismic surveys and cores.

Between Voorne and Monster, channel deposits of the Late-Pleistocene and early-Holocene river Rhine are found (see Van Heteren *et al.*, 2002; and Hijma *et al.*, 2010; for details). The shoreface of the Holland coast between Hoek van Holland and Zandvoort has been studied in detail. Beets *et al.* (1995) demonstrated the variety of deposits to be found here. Rieu *et al.* (2005) reconstructed the channel patterns of the mid-Holocene tidal basins that occur

offshore the area between Scheveningen and Zandvoort. Van Heteren & Van der Spek (2008) described the remnants of the delta of the 'Oude Rijn' that is found offshore Katwijk and Noordwijk aan Zee, whereas Van Heteren *et al.* (2011) explained how the shoreface of the prograding beach barriers was supplied with sand from the eroding lower shoreface.
Seismic surveys along the Wadden coast revealed the migration of the predecessors of the present-day tidal inlets (see Sha, 1989b; Sha & de Boer, 1989; and Sha, 1992). Van Heteren & Van der Spek (2003) reconstructed the tidal basin of an earlier stage of the Lauwerszee which extended to an area north of Ameland. The western part of the Wadden Sea is situated on high-lying Pleistocene and, consequently, comparatively young. Offshore this part, predominantly erosion products of Pleistocene deposits (boulder fields) and limited traces of channels occur (Sha *et al.*, 1996).

3 The series of prograded beach barriers between Monster and Egmond allows for detailed study of shoreface deposits. Transects near Den Haag, Wassenaar and Haarlem were studied by Van Straaten (1965), Van der Valk (1996), Van der Spek (1999) and Cleveringa (2000). The sediment sequences showed that the shoreline was prograding over eroded tidal basin/tidal channel deposits. The upper shoreface deposits showed the influence of frequent wave activity that decreased with depth. Lower shoreface deposits showed evidence of transport by tidal currents whereas the middle shoreface was a relatively quiet environment where bioturbation by benthic organisms dominated. Storm events resuspended shoreface sediments down to the lower shoreface that were subsequently settling from suspension, producing fining-upward sequences with coarse shell layers at their bottom and grading upwards into sand and clay. The completeness of these storm sequences at the lower shoreface confirms that reworking by storm waves at these depths was only an occasional event.

These conclusions are summarised in Figure 3.5. The validity of this conceptual model of shoreface processes and evolution for the present-day situation needs to be tested.

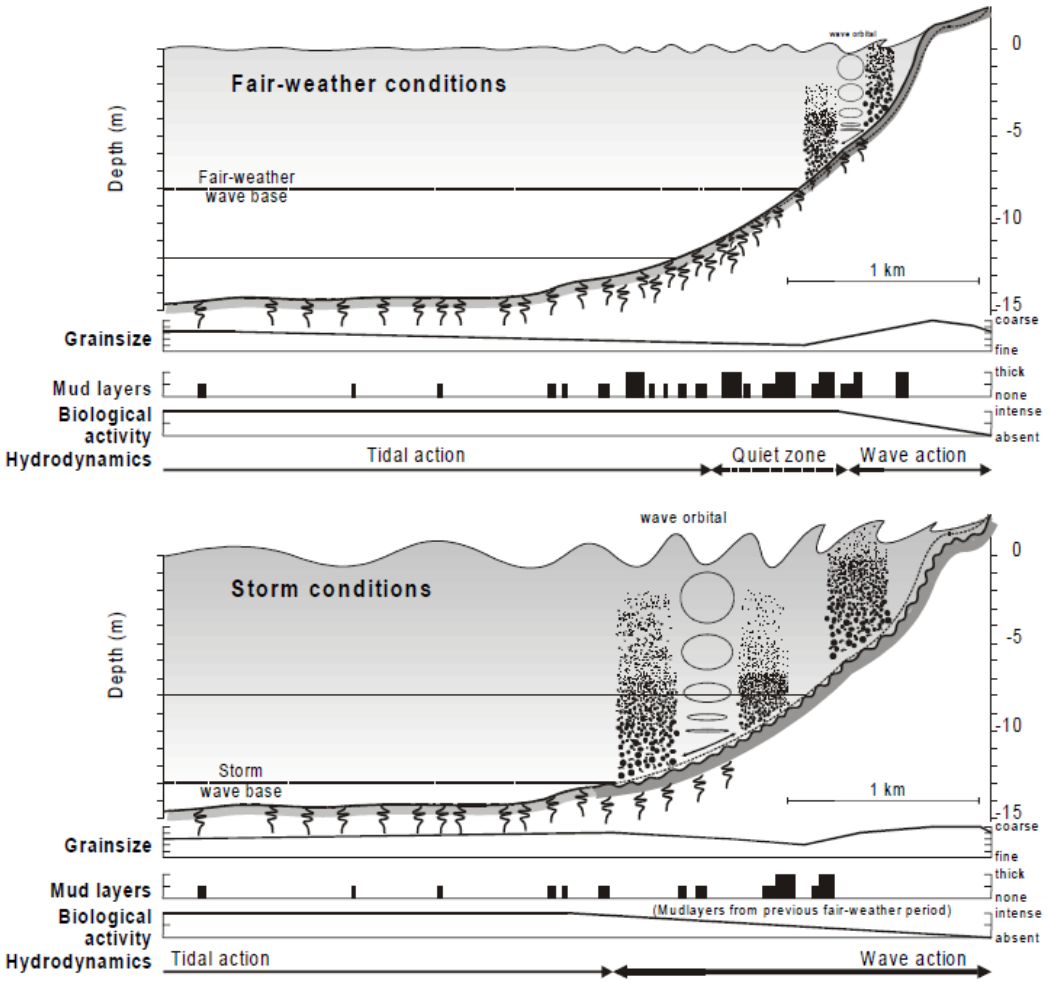

Figure 3.5 Conceptual model of shoreface processes based on the interpretation of subrecent shoreface deposits from the Holland coast. From Cleveringa (2000).

3.3 Hydrodynamics

The hydrodynamic conditions on the shoreface result from tide-, wind-, density gradient-driven and wave-induced currents, and the wave-induced orbital motion.

3.3.1 Currents

The mean tidal range decreases from Vlissingen (3.8 m) to Den Helder (1.4 m), after which it increases again in eastern direction (2.2 m at Schiermonnikoog), Figure 3.6.

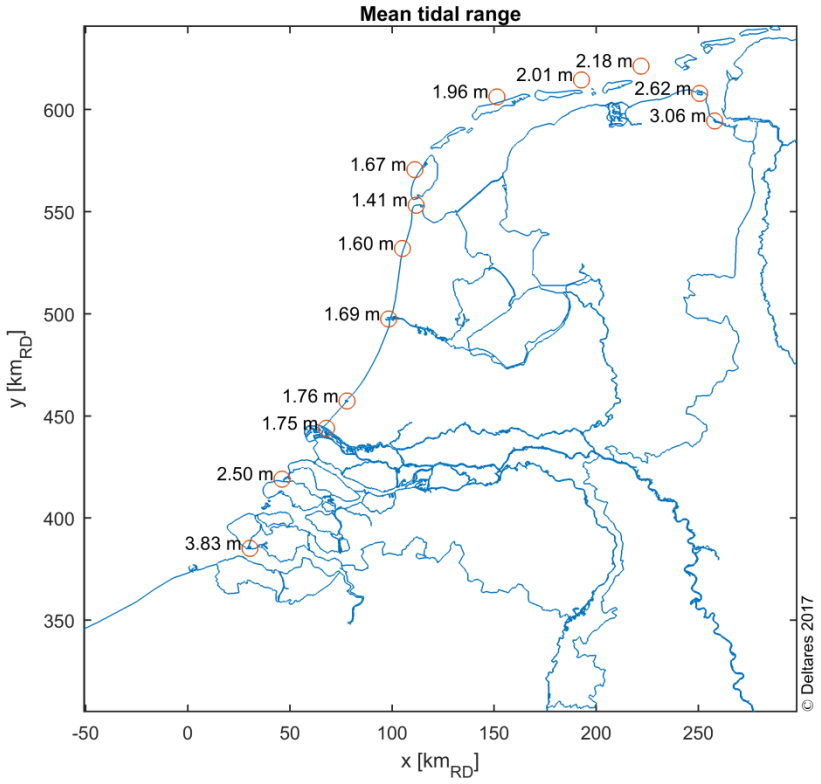

Figure 3.6 Mean tidal range along the Dutch North Sea coast (Data: Rijkswaterstaat, 2013).

Typical peak tidal current velocities are ~1.0 m m/s at the surface. The north-easterly flood current is somewhat larger (0.05-0.1 m/s) than the south-westerly ebb currents. The tidal current is mainly alongshore-directed, but the Coriolis force deflects the current to the right (Northern Hemisphere, NH), i.e. the flood current is bended onshore and the ebb current offshore. The limited vertical mixing due to density-stratification strengthens tidal ellipticity (De Boer, 2009). The vertical flow structure due to density effects is more elaborately discussed in Appendix A, based on the work of De Boer (2006, 2009), Moreover, the tidal current can have a stronger cross-shore component offshore from the ebb-deltas (Western Scheldt, in between Wadden Islands) related to the filling and emptying of the tidal basins.

The dominant wind direction is from the southwest, but large storm events are frequently associated with northwesterly winds. In shallow water (depths smaller than ~10 m; friction-dominated zone), the current responds rapidly to the wind stress and the surface current tends to be aligned with the wind direction. The shore-normal wind stress component causes water level set-up or set-down at the shore depending on the wind direction. The resulting pressure gradient yields an onshore (upwelling) or offshore (downwelling) bottom current. At deeper water (depths larger than ~20 m; geostrophic zone) wind-induced currents are affected by the Coriolis force. This results into the Ekman spiral flow with a 45^{o} clockwise (with respect to the wind direction, NH) surface current curling down to 225^{o} clockwise current at the bed. The (depth-averaged) mass flux is perpendicular (clockwise, NH) to the wind direction, and its shore-normal component also results into set-up or set-down depending on the wind direction. A typical south-westerly, alongshore wind results into an onshore-directed surface current and an offshore-directed near-bed current in the North Sea (downwelling) due to the Coriolis effect. A northerly wind can result in an onshore-directed near-bed current (upwelling). Near-bed wind-induced currents are typically between 0 and 0.1 m/s.

Density-induced currents are related to spatial density gradients of the fluid-sediment mixture due to variations of temperature, salinity and/or sediment concentration. The density variation due to salinity variations is mainly related to outflow of the Rhine river near Hook van Holland. The behaviour of salinity and density gradients is strongly related to the magnitude of the Rhine discharge which varies between 800 and 10,000 m^3/s, and with an average annual discharge of 2,200 m^3/s. Fluid density variations over longshore distance of 100 km (up to ~ Callantsoog) and a cross-shore distance of 30 km from the Rhine river mouth have been observed (De Ruijter *et al.*, 1992). The onshore pressure gradient due to the more salty and denser offshore water leads to onshore near-bed velocities of 0.02-0.04 m/s at Noordwijk (De Ruijter *et al.*, 1992).

3.3.2 Waves

The onset of breaking of irregular waves appears to be when the ratio of the (significant) wave height to the wave depth is around H_s/h = 0.4 (Van Rijn, 2013). This means that for a typical storm with a wave height of 5 m, wave breaking starts at around water depths of 12-13 m. In this shallow part of the lower shoreface, wave breaking during high-energy events drives a longshore current (in case obliquely incident waves) and a near-bed offshore return current (undertow). The currents are generated by spatial gradients of the radiation stress which is the wave-induced momentum flux, and (in the cross-shore direction) the balancing pressure gradient due to water level set-up. Houwman & Hoekstra (1994) measured maximum near-bed (about 0.5 m above the bed) offshore cross-shore current velocities of 0.2 m/s at a water depth of 10 m offshore from Egmond, associated with a 4.7 m significant wave height.

Another potentially relevant near-bed wave-induced current (“streaming”) at the lower shoreface is determined by two competing mechanisms: an onshore streaming resulting from the horizontal non-uniformity of the velocity field under progressive free surface waves (known as Longuet-Higgins (1953) streaming), and an offshore streaming related to the nonlinearity of the waveshape (Kranenburg *et al.*, 2012). More specifically, the Longuet-Higgins streaming results from an onshore bed shear stress due to the fact that the horizontal and vertical orbital motions are not exactly out of phase in the bottom boundary layer. The offshore wave shape streaming results from the necessity of an offshore-directed near-bed current-related bed shear stress to balance the onshore-directed wave-related bed shear stress due to larger turbulence in the onshore than in the offshore wave-cycle (velocity skewness). Note that in the special case of steep, 2D, vortex ripples this waveshape streaming can become onshore-directed very close to the bed (Davies & Villaret, 1999). The boundary layer streaming increases with wave height and period, decreases with water depth, and has typical theoretical magnitudes of 0-0.05 m/s (see also Table 3.1).

Wind and wave climate are closely related in the semi-enclosed North Sea where waves are mainly determined by local seas instead of swell. This means that the waves are dominantly incident from the southwest and northwest; large storm waves are generally coming from the northwest. Table 3.1 show typical high-frequency wave characteristics at deep water (h = 20 m) and the associated near-bed horizontal orbital velocity based on linear wave theory and Longuet-Higgins (1953) streaming according to:

$$\langle u \rangle_{LH} = \frac{3\hat{U}^2}{4c} \tag{3.1}$$

with $\hat{U}$ the horizontal orbital velocity amplitude and *c* the wave celerity. This table shows that wave orbital motion is small for the 50% wave condition, and that the Longuet-Higgins streaming is very small for the 50% and 10% wave conditions.

Table 3.1 Deep water (h = 20 m) high-frequency wave statistics of De Leeuw (2005) and computed horizontal orbital velocities amplitudes, near-bed Longuet-Higgins streaming and velocity skewness parameter R.

Exceedance	***H*** **(m)**	***T*** **(s)**	$\hat{U}$ **(m/s)**	$\langle u \rangle_{LH}$ **(m/s)**	***R*** **(-)**
50%	1.0	5.3	0.07	0.00	0.50
10%	2.4	7.0	0.39	0.01	0.50
1%	4.2	8.9	0.97	0.06	0.51
0.1%	5.5	10.7	1.47	0.13	0.54

Once the waves “feel” the bed, they deform. The wave crests become higher and shorter, and the wave troughs longer and less deep. This results in larger onshore-directed velocities under the wave crest and smaller offshore-directed velocities under the wave trough. This so-called velocity skewness is important for sediment transport: the non-linear relation between sediment transport and velocity generally leads to a net onshore transport. The velocity-skewness can be expressed through the ratio of the on- and offshore orbital velocity peaks, $R = U_{on} / (U_{on} + U_{off})$, with $R = 0.5$ corresponding to symmetric velocities. These are included in Table 3.1, computed using second-order Stokes theory. This shows that the waves are nearly symmetric at this water depth, except for the wave condition with a probability of exceedance of 0.1% (~once per 3 years). In more shallow water, wave skewness becomes significant at lower wave heights.

The interaction between high-frequency waves and the coast generates long period or low-frequency wave motions (infragravity waves). As a result of short wave height variations so-called bound long waves are generated due to spatial radiation stress gradients. These long waves travel with the wave group velocity and are out of phase with the short wave envelope (correlation coefficient of -1). These bound long waves may be released (free long wave) when the short waves break and are generally reflected on the beach and either escape to deep water (“leaky waves”) or are trapped in the surf zone by refraction (“edge waves”). At deep water, low-frequency wave heights are typically 10% of the high-frequency wave height, and the ratio of peak orbital velocities is 0.1-0.2 (Van Rijn, 2013). Low-frequency waves only play a role in the shallow part of the lower shoreface in the case of storm events, in line with wave breaking effects. For sediment transport the correlation between the low-frequency waves and short wave envelope is relevant. Bound long waves (correlation coefficient of -1) are out of phase: low-frequency wave troughs coincide with large high-frequency wave heights, which is a mechanism for offshore-directed sediment transport. Ruessink (1998) studied low-frequency motions at the dissipative coast of Terschelling (The Netherlands); the Nourtec measurement campaign (see also Section 4.3.1). For a high energy event he measured a low-frequency wave height of 0.5 m at a water depth of 9 m, and the correlation coefficient was -0.2, meaning the bound long waves were not very important.

3.4 Sand transport processes

3.4.1 General

Sand can be transported in close contact with the bed (bedload) and suspended in the water column (suspended load), depending mainly on the sediment size, near-bed velocity, turbulence levels and bed roughness. Sand transport by the tide-, wind-, density gradient-

driven, wave-induced currents is referred to as current-related sand transport, whereas wave-related sand transport is due to the orbital motion under a non-linear wave with higher onshore than offshore peak orbital velocities (velocity skewness). The current-related transport is in the current direction, which has both a cross-shore and alongshore component. The wave-related transport in the direction of wave advance, i.e. mainly in the cross-shore direction. In the special case of large phase lag effects between velocities and sand concentrations (fine sand, vortex ripples), the wave-related sand transport can be against the direction of wave advance (see Ribberink et al., 2008). There is a mutual interaction between small-scale bedforms (of the order of centimetres to meters), near-bed flow and sand transport. The bedform-related roughness enhances sediment suspension.

3.4.2 Small-scale bedforms and sediment suspension

Dolphin *et al.* (2005) measured bedform type and length using sonar data from a Sand Ripple Imaging Logging System (SRILS). The bed was scanned 4 times per hour and the scanned area had a radius of 2.5 m. At the same time the suspended sand concentrations were measured using an ABS. These instruments were deployed 2-km offshore of the coast of Noordwijk aan Zee at a water depth of 13 m (SANDPIT measurements, see also Section 4.3.5). A series of bedforms types was detected:

- Non-planar bed: patchy, bumpy surface with low gradients at low flow velocities.
- Tidal ripples during spring peak ebb tidal flows of 0.26-0.33 m/s and in absence of waves (root-mean-square orbital velocity U_{rms} <~ 0.2 m/s).
- Long wave ripples (2D/3D) with wave lengths of 0.35-2.0 m during moderate to high wave-orbital flow (0.3 <~ U_{rms} <~ 0.7 m/s). These were present 52% of the time sand was in suspension.
- Short wave ripples with lengths of 0.05-0.25 m were less common. These formed during low-moderate near-bed orbital motion (0.2 <~ U_{rms} <~ 0.3 m/s).
- Flat-bed/sheet-flow at high wave orbital velocities (U_{rms} >~ 0.7 m/s, corresponding to significant wave heights between 2 and 3 m).

The measured near-bed reference concentrations (about 1 cm above the bed) varied between 0.01-1 g/l. Sand suspension was dominated by wave events. Even under the strongest tidal flows, suspended sand transport was confined to a 0.02-0.03 m thin near-bed layer with low concentrations (< 0.07 g/l). The tide did transport sand as bedload.

Meirelles *et al.* (2016) measured small-scale bedforms using an Acoustic Ripple Profiler (that covered a circular area of ~11 m^2 at an hourly rate) offshore from the Sand Motor at a water depth of ~12 m (Section 4.3.7); median grain size was between 0.25 and 0.35 mm. He distinguished visually six bed states: current ripples (C), wave ripples (W), wave-current ripples (WC), current ripples with subordinate wave ripples (Cw), wave ripples with subordinate current ripples (Wc) and poorly developed ripples (P). The ripples were typically 0.02-0.04 in height and 0.4-0.6 m in length. During the ~30 days observation period the C-type, governed by tidal currents, prevailed. Wave ripples only dominated during a storm with waves higher than 2 m. The ratio of the wave and current mobility number appeared to be a simple and quick way to distinguish between the observed bed states.

3.4.3 Sand transport processes

Van de Meene & Van Rijn (2000) measured bedload transport, velocities and suspended sediment concentrations at the shoreface-connected ridges off the coast of Zandvoort with water depths between 14 and 18 m (see Section 4.3.2). They concluded that sediment transport during fair-weather was very episodic, with bedload transport slightly dominant over suspended load transport. The suspended sediment transport during storms was dominated by the mean fluxes, with waves acting as a stirring mechanism. The contribution of wave-

oscillatory fluxes could not be neglected; the largest values were directed with the waves, but also wave-related sediment fluxes against the wave direction were measured. The long-wave fluxes were present and mostly opposite to the direction of wave advance, but very small.

During the SANDPIT measurement campaign, Grasmeijer et al. (2005ab) measured current-related suspended transport rates between 0.01 and 1.0 m above the bed using ABS and ASTM. The suspended loads were reasonably well predicted by existing transport models. They fitted the following empirical formula to these depth-integrated, current-related suspended transport rates (in kg/m/s):

$$q_{sc} = c_3\theta_c\left[\left(c_1\theta_w + c_2\theta_c\right) - \theta_{cr}\right] \tag{3.2}$$

with θ_c, θ_w, θ_{cr} the wave-related, current-related and critical Shields number and [c_1, c_3, c_3] = [0.85, 0.51, 0.74 kg/m/s] empirical coefficients to match the ASTM data best. This resulted in flood-directed transport of +13.4 m^3/m/year, an ebb-directed transport of -12.2 m^3/m/year and thus a net transport in flood direction of +1.2 m^3/m/year (all values including pores[2]). These annual transport rates were much smaller than those predicted by Van Rijn (1997) and Van Rijn *et al.* (2005) using the 2DV Unibest-TC numerical model (see also Section 3.4.4), which is according to Grasmeijer et al. (2005a) likely due to differences between the model-imposed and measured velocities.

Kleinhans & Grasmeijer (2006) measured bedload transports with a calibrated sampler in spring tidal conditions without waves at a water depth of 13–18 m with fine and medium sands offshore from Noordwijk in the framework of the SANDPIT project. They concluded that the measured bedload in tidal current conditions was very near incipient motion. The measured transport rates were a factor of 5 smaller than well-known bedload models predict, which was possibly explained by the mud effects (cohesion and turbulence damping). Annual transport rates were calculated using an empirical North Sea bedload predictor derived from the data fed with empirical probability distributions of near-bed current and orbital velocities. This resulted in an annual flood bedload transport of ~2 m^2/year, an ebb transport of ~1.5 m^2/year and a net transport of ~0.5 m^2/year. These are of the same order as the suspended load transport rates of Grasmeijer et al. (2005a); bedload and suspended load are thus both important at the lower shoreface.

3.4.4 Net transport rates

Van Rijn (1997) predicted net (yearly-averaged) sand transport rates at the NAP -20 m and NAP -8 m depth contours of the JARKUS profiles at Callantsoog, Egmond, Noordwijk and Scheveningen using the 2DV Unibest-TC numerical model. The imposed tide- and wind-induced water levels and depth-averaged velocities were computed using a depth-averaged 2DH flow model. Fluid-density gradients were derived from field measurements. The model approach of Van Rijn (1997) will be discussed in more detail in Section 5.2.2.

Table 3.2 shows that the predicted cross-shore transport rates at 20 m water depth was dominated by the onshore contribution due to the near-bed onshore current driven by spatial density gradients. At the 8 m water depth, also transport contributions due to velocity skewness (onshore), bound long wave effects (offshore), Longuet-Higgins streaming

[2] *The seabed contains sand and pores filled with water. The typical pore volume fraction, ε_p, is 40%. This means that a net sand transport of 1 m^3 in a certain period corresponds to a bed volume change of 1/(1- ε_p) ≈ 1.7 m^3 in that same period. Net sand transport rates including pores are 1/(1- ε_p) ≈ 1.7 higher than without pores, and enable a more direct translation to bed level changes.*

(onshore) and breaking-induced undertow (offshore) became important. The resulting total net cross-shore sand transport was in the onshore direction, also for the other transects (Table 3.3), and dominated by the bedload contribution. At the 8 m water depth the offshore and onshore contributions were comparable resulting in a net transport close to zero. With a coastal length of 110 km between Hook van Holland and Den Helder, the typical predicted values of 0-20 m^3/m/year correspond to a net sand import into the coastal foundation of 0-2 million m^3/year.

Table 3.2 Contribution of various hydrodynamic processes to net (yearly) cross-shore transport rates at Noordwijk according to Van Rijn (1997). Positive values indicate onshore sand transport.

Process	**Contribution to net cross-shore sand transport (m^3/m/year, including pores)**	
	20 m water depth	8 m water depth
Velocity skewness	0	+15
Bound long waves	0	-15
Longuet-Higgins streaming	0	+15
Reduced (50%) undertow	0	+25
Fluid density-gradient effect	+10-25	+10

Table 3.3 Estimates of net (yearly) cross-shore transport rates according to Van Rijn (1997). Positive values indicate onshore sand transport.

Location	**Net cross-shore sand transport (m^3/m/year, including pores)**	
	20 m water depth	8 m water depth
Callantsoog	+5 ± 10	0 ± 10
Egmond	+15 ± 10	0 ± 10
Noordwijk	+10 ± 10	0 ± 10
Scheveningen	+0 ± 10	0 ± 10

Van Rijn *et al.* (2005) repeated these computations by using the updated Unibest-TC model and the same wave and current regime focussing on the NAP-20 m depth contour of the Noordwijk profile. The updated Unibest-TC model included the TR2004 transport model (Van Rijn, 2007ab) instead of the bedload model of Ribberink (1998) and the suspended load model of Van Rijn (1993). The resulting annual cross-shore transport was very similar to the value presented Van Rijn (1997), with close to zero transport without density gradient effects and a net onshore transport of 10-15 m^3/m/year with a near-bed current of 0.05 m/s representing density gradient effects. Next to the near-bed current, predicted values were sensitive to the sediment grain size. The TR2004 bed roughness predictor had only little effect on the predicted transport rates.

De Leeuw (2005) computed net cross-shore transport rates at the lower shoreface with different empirical and numerical models in a relative simple way, focussing on effects of velocity skewness and Longuet-Higgins boundary layer streaming. He concluded that the annual transport rates were dominated by high-wave sheet-flow events, despite the low frequency of occurrence. The onshore-directed net cross-shore transport induced by velocity skewness was 2-16 m^3/m/year and enhanced by the onshore Longuet-Higgins streaming to 11-35 m^3/m/year. These results are very different than those from Van Rijn (1995) and Van Rijn *et al.* (2005). De Leeuw (2005) was not able to explain these differences fully, but

hypothesised that this was related to his relatively simple model approach (neglecting currents, assuming coast-perpendicular waves) and differences in the applied wave climate and sediment grain size. Nevertheless, this study emphasises the difficulty in predicting the relatively small cross-shore transport rates at the lower shoreface, given the uncertainties in the model formulations, parameter settings and input.

3.5 Synthesis

Large-scale morphology, sedimentology and geology
Analysis of profile changes at the middle and lower shoreface of the Holland coast did not show an offshore-directed translation of sediment volumes, despite the addition of large volumes of sand to the upper shoreface in many locations.

The shoreface of the Dutch coast is a complex area. Its composition is partly determined by its evolution in the past, whereas present-day processes are influencing or even changing this. The present situation and large-scale artificial supply of sediment will determine its future development. The observed variation in grain-size distributions and shape and size of small-scale sea-bed features with time at the lower shoreface reflect the impact of varying wind and waves conditions.

The shoreface morphology varies along the Dutch coast, depending on the coastal slope and superposition of shoreface-connected ridges (central Holland coast) and ebb-tidal deltas (Delta area, Wadden Sea). The architecture of the shoreface-connected ridges off the central Holland coast indicates that they are still active today. These ridges are prograding to the northwest at their seaward sides, although they turn out to be erosive features at their southern edge. The development of most ebb-tidal deltas along the Dutch coast is largely influenced by interventions in the tidal inlets and -basins.

Man-made, shore-normal sand bodies on the shoreface show deformation and migration on the decadal time scale, with decreasing magnitudes with depth. Below 19 m water depth, the sand bodies are in stable position but show morphodynamics comparable with sand waves on the continental shelf.

The lower part of the shoreface is formed by tidal-basin- and river deposits stemming from the transgressive phase before 5500 BP. These deposits are overlain by an active sand layer that responds to variations in tidal, wave and wind conditions.

Shoreface deposits of the prograding beach barriers of the Holland coast indicate dominance of wave processes that decreases with depth at the shoreface. Moreover, they indicate that resuspension by storm waves impacted the middle and lower shoreface, with a frequency decreasing with depth. The validity of this conceptual model of shoreface processes and evolution for the present-day situation needs to be tested.

Sand transport processes
Most knowledge of Dutch lower shoreface sediment dynamics originates from field and modelling studies of the relatively straight, closed and wave-dominated Holland coast. Even for the Holland Coast the number of detailed studies into lower surface sand transport processes is limited.

From these studies it is concluded that lower shoreface sand transport is episodic with annual transport determined by high-wave events. Bedload is dominant at water depths of 20 m; moving into more shallow water suspended load becomes important too. Except for storm

events, current- (mainly tide) and wave-induced small-scale bedforms with typical heights of 0.02-0.04 m and lengths of 0.4-0.6 m were frequently observed on the lower shoreface. These ripples are important for sand transport processes as these generate drag roughness that is an important sand suspension mechanism.

Potential cross-shore transport mechanisms are:

- Onshore: density gradient driven near-bed current, velocity skewness, Longuet-Higgins boundary layer streaming and upwelling.
- Offshore: undertow, (bound) long wave effects (both more important at shallow water), offshore turbulence asymmetry streaming and downwelling.
- On- or offshore: cross-shore tidal current component.

The importance of offshore turbulence asymmetry streaming and up- and downwelling on cross-shore sand transport has not yet been quantified. Furthermore, it is unclear how cross-shore tidal current components contribute to the on- and offshore sand transport. This could especially be important for the Delta and Wadden Coast. The density-driven current seems to be very important for the net cross-shore transport at the 20 m water depth, but might not be so at the Delta and Wadden Coast since these are relatively far away from the Rhine river mouth.

Typical estimates of the annual net cross-shore transport rates are 0-20 m^3/m/year (including pores) in the onshore direction, which amount to 0-2 million m^3/year into the Holland Coast area. At the 8 m depth contour on- and offshore contributions seem to cancel each other out, leading to a nearly zero net cross-shore transport along the Holland Coast. It is unclear what typical net transport rates are in between the 20 and 8 m depth contours. Furthermore, we could not find estimates of lower shoreface transport rates along the Delta and Wadden Coast.

The episodic nature, relatively low values and the important bedload contribution make it very difficult to accurately measure and predict lower shoreface sand transport processes.

4 Field measurements

4.1 Introduction

This chapter presents an overview of available measurements of sand transport processes, morphodynamics, and the subsurface of the Dutch shoreface. It also includes recent campaigns that were more focussed on fine sediment dynamics. The field studies are presented in chronological order. This chapter starts with a short description of standard meteorological and hydrodynamic measurements on the Dutch shoreface. An overview of the measuring instruments can be found in Appendix B; meta-data of the measurement campaigns is presented in Appendix C. This chapter is an update of the memo by Van der Werf *et al.* (2017).

4.2 Standard meteorological and hydrodynamic measurements

Water levels, wind velocities and waves are continuously measured at a large number of stations along the Dutch Coast (Table 4.1, Figure 4.1). These are long time-series; some even go back to the end of the 19th century. The data can be downloaded from the website waterberichtgeving.rws.nl

For the shoreface the stations (from south to north) Schouwenbank (wind, waves excl. direction), Europlatform (water levels, wind, waves incl. direction), Lichteiland Goeree (water levels), IJmuiden Munitiestortplaats (water levels, wind, waves incl. direction), Platform Hoorn Q1B (water levels, wind, waves excl. direction), Eijerlandse Gat (water levels, wind, waves incl. direction), L09 platform (wind, waves excl. direction), Amelander Westgat (water levels) and Schiermonnikoog Noord (water levels, wind, waves incl. direction) are especially relevant.

Table 4.1 Observations stations on the Dutch shoreface from south to north.

Station	**Measured parameters**			
	Water levels	Wind	Wave height and period	Wave direction
Schouwenbank		X	X	
Europlatform	X	X	X	X
Lichteiland Goeree	X			
IJmuiden Munitiestortplaats	X	X	X	X
Platform Hoorn Q1B	X	X	X	
Eijerlandse Gat	X	X	X	X
L09 platform		X	X	
Amelander Westgat	X			
Schiermonnikoog Noord	X	X	X	X

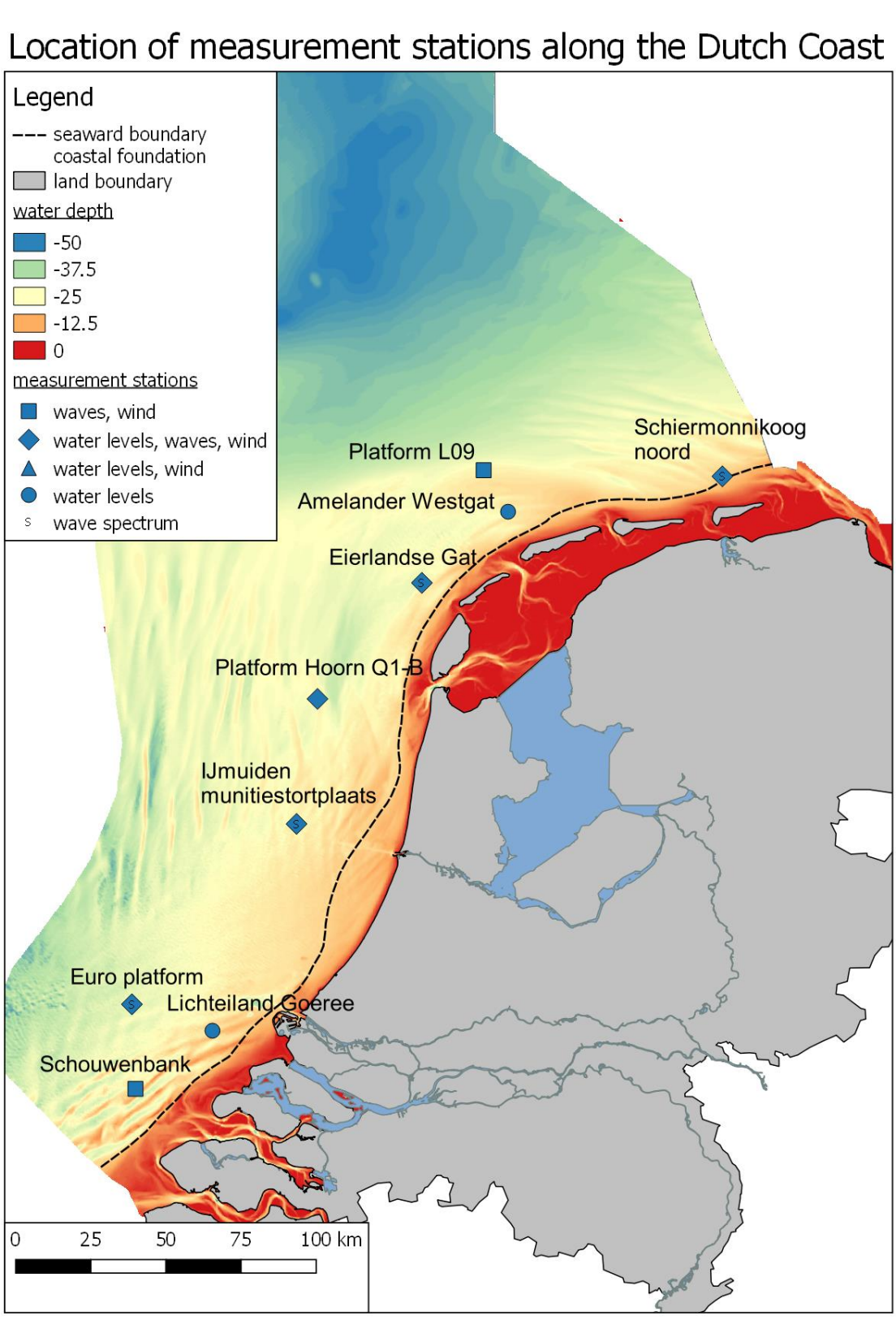

Figure 4.1 Location of measurement stations with long time-series of water levels, wind and waves in the vicinity of the seaward boundary of the coastal foundation (dashed line). "Wave spectrum" indicates directional waverider buoy measurements that include wave direction information.

4.3 Sediment transport processes

4.3.1 Nourtec measurements (Houwman, 2000)

These data were collected in periods between 1993 and 1995 at several positions with water depths between 3 and 10 m in the barred nearshore zone in front of the barrier island Terschelling (Figure 4.2). The measurement campaign was part of the Nourtec project that investigated innovative (shoreface) nourishment techniques, jointly in Denmark, Germany and The Netherlands. The instrumented tripods contained EMFs (Electronic Magnetic Flow meters), pressure sensors and OBSs (Optical Backscatter Sensors). The deepest location was at a water depth between 9 and 10 m, ~1.7 km off the coast; there was no OBS sensor on this tripod. There was also a wave buoy at 15 m water depth, 4.6 km from RSP (*Rijksstrandpalenlijn*). Houwman (2000) did not analyse the OBS data.

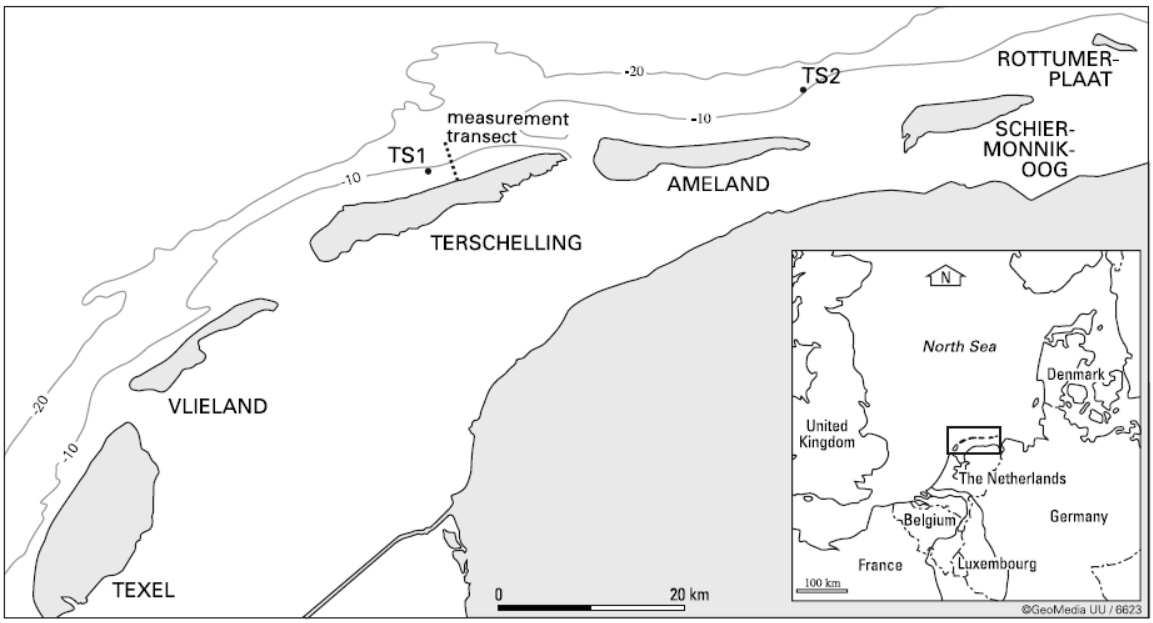

Figure 4.2 Location Nourtec measurements Houwman (2000). Figure taken from Ruessink et al. (2006).

4.3.2 Van de Meene & Van Rijn (2000)

Van de Meene & Van Rijn (2000) measured the three-dimensional current structure across shoreface-connected ridges along the central Dutch coast (Figure 4.3) with an acoustic Doppler current profiler (ADCP) and several short- and long-term current meter deployments. In addition, vertical salinity distributions along the ADCP-transects were measured with a CTD probe (Conductivity, Temperature and Depth). Supporting data include wind velocities recorded routinely near Meetpost Noordwijk and discharge data of the river Rhine.

The ADCP data were collected between 30 May and 1 June 1990 during fair-weather, spring tidal conditions. The measurements were done with a ship-borne 1200 kHz ADCP along transect 28 for one tidal period (13 h). Traverses along this line were repeated once every hour. Long-term current and water-level measurements were done near the locations depicted in Figure 4.3. The measurements were carried out with NBA-2DNC current meters and Dag6000 pressure sensors. The instruments were deployed during six different periods between 1989 and 1991. The duration of the deployments was usually one month, but it varied between two weeks and two months. One experiment was done during fair-weather

conditions (May-June 1990), the other five during generally stormy winter conditions (November-February).

Fair-weather transport measurements were carried out at the crest of one of the shoreface-connected ridges, between locations 151 and 161 (Figure 4.3), on 14 and 15 August 1990. The measurements were done with a Total Load Sampler, developed by Delft Hydraulics (Van Rijn & Gaweesh, 1992). The sampler was equipped with a bag-type bed load trap, a vertical array of intake nozzles connected to a series of pumps to obtain suspended sediment samples and three current meters (two propellers and one electromagnetic flow meter). The sampler allowed for the measurement of time-averaged sediment transport rates, based on direct sampling of the sediment.

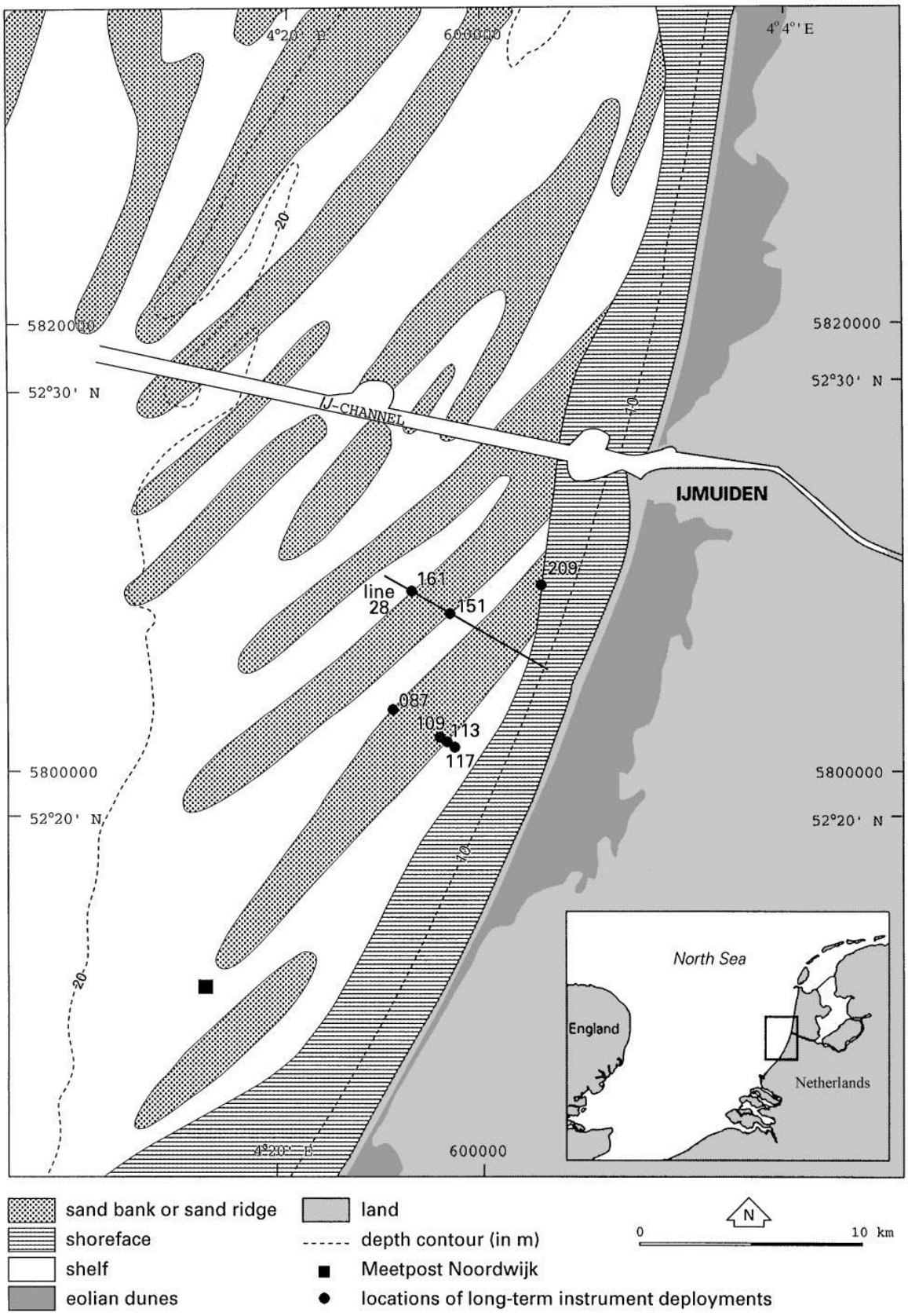

Figure 4.3 Measurement locations around the shoreface-connected ridges along the central Dutch coast. Figure taken from Van de Meene & Van Rijn (2000).

4.3.3 CEFAS/RIKZ campaign at Noordwijk (CEFAS, 2003; Hartog & Van de Kreeke, 2003)

This joint research programme of CEFAS (UK) and RIKZ (NL) consisted of a measurement campaign at Noordwijk aan Zee. Over the course of 2 years, from March 2000 till April 2002, a Smartbuoy was moored at three different locations, 2, 5 and 10 km offshore (Figure 4.4). The Smartbuoy measured SPM (suspended particulate matter) concentrations, salinity, temperature and chlorophyll-a concentrations, 1 m below the surface.

Additionally, a measurement frame was deployed (i.e. the CEFAS Minipod). This frame was developed in-house by CEFAS. The frame was deployed from 20-11-2001 until 2-1-2002 at Noordwijk 2, and from 5-3-2002 until 22-04-2002 at Noordwijk 5. The digits 2 and 5 correspond to offshore distances. During the mentioned periods, the Smartbuoy was also moored at the corresponding locations. Prior to these measurement periods, the Smartbuoy was moored at Noordwijk 10. Water depths vary between 10 m (Noordwijk 2) and 16 m (Noordwijk 10).

The Minipod was equipped with an ADV to measure near-bottom flow, OBS en ABS sensors to measure suspended fines and sand, pressure sensors for wave heights and tidal elevations, a Fluorometer for chlorophyll-a, a LICOR light sensor to measure light intensity and an oxygen sensor for oxygen profiles.

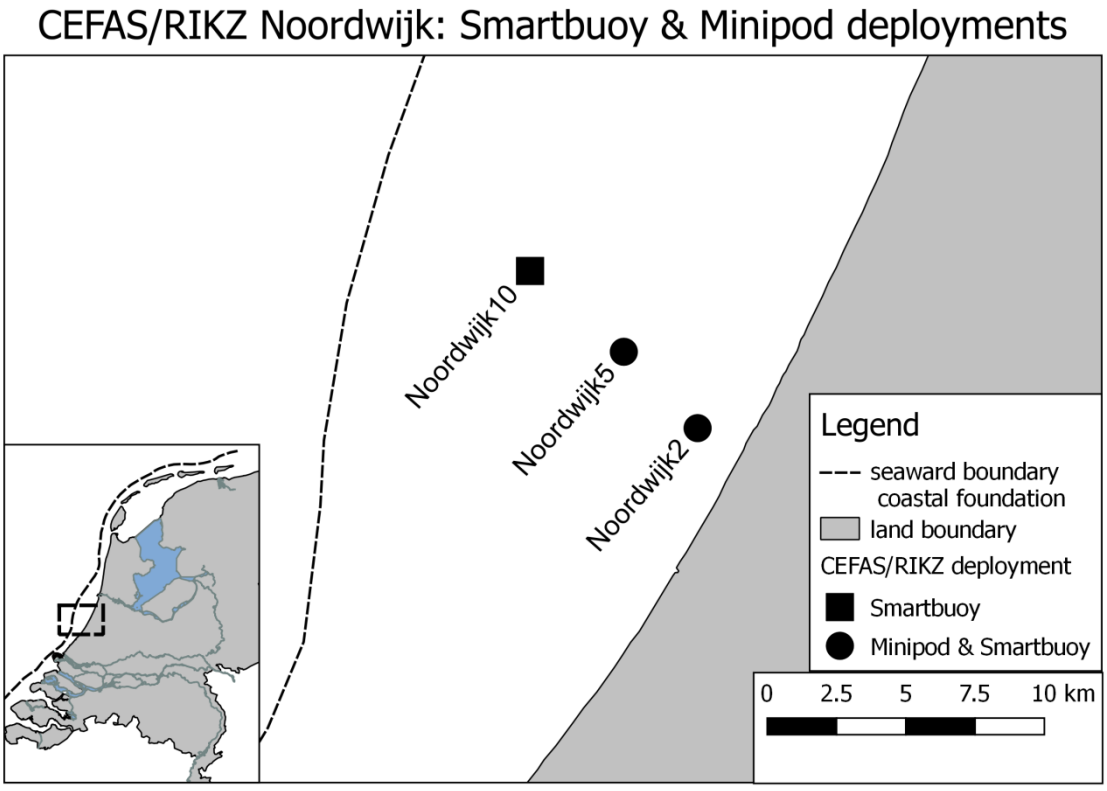

Figure 4.4 Measurement locations of the CEFAS/RIKZ 2002 campaign at Noordwijk.

4.3.4 BwN transects (Van der Hout *et al.*, 2015)

These field measurements were carried out as part of the Building with Nature (BwN) project, in order to contribute to a better insight in cross-shore variations in current velocity, stratification and SPM concentrations. In 2003, 2010 and 2011, measurement campaigns

were performed with the RV Navicula (NIOZ). The main goal of these campaigns was to collect vertical profiles of current velocity, density and SPM concentrations. Current velocity was measured with a vessel-mounted ADCP, whereas density and SPM concentrations were measured by lowering a lightweight frame from the vessel with CTD (Seapoint Seabird SBE911 plusCTD) and OBS sensors (Seapoint OBS) mounted to it. To validate OBS sensor measurements, water samples were taken with Niskin bottles on the same locations as the frame was lowered. The measured transects are all located in the Northern part of the Holland Coast (Figure 4.16). These are, from South to North: Wijk aan Zee, Egmond, Camperduin and Callantsoog. The transects span an offshore distance of 0.5 to 7 km offshore. Water depths varied between 5 and 20 m, and significant wave heights varied between 0.3-1.5 m. The operational limits of the RV Navicula restricted the operation of the ship, and therefore measurements, to a maximum significant wave height of 1.5 m.

4.3.5 SANDPIT measurements (Van Rijn *et al.*, 2005)

The SANDPIT ("Sand Transport and Morphology of Offshore Sand Mining Pits") field measurements were carried 2 km off the coast of Noordwijk aan Zee, in spring and autumn 2003 (Figure 4.5). Water depths varied between 12 and 16 m. Reasons for choosing the Noordwijk field site include i) natural shoreface, i.e. no nearby navigation channels and constructions, ii) nearby presence of observation platform Meetpost Noordwijk (wind, waves, tides), iii) limited mud transport (e.g. no nearby dredging and dumping), iv) Noordwijk transect has been used before in modelling studies (e.g. Van Rijn, 1997).

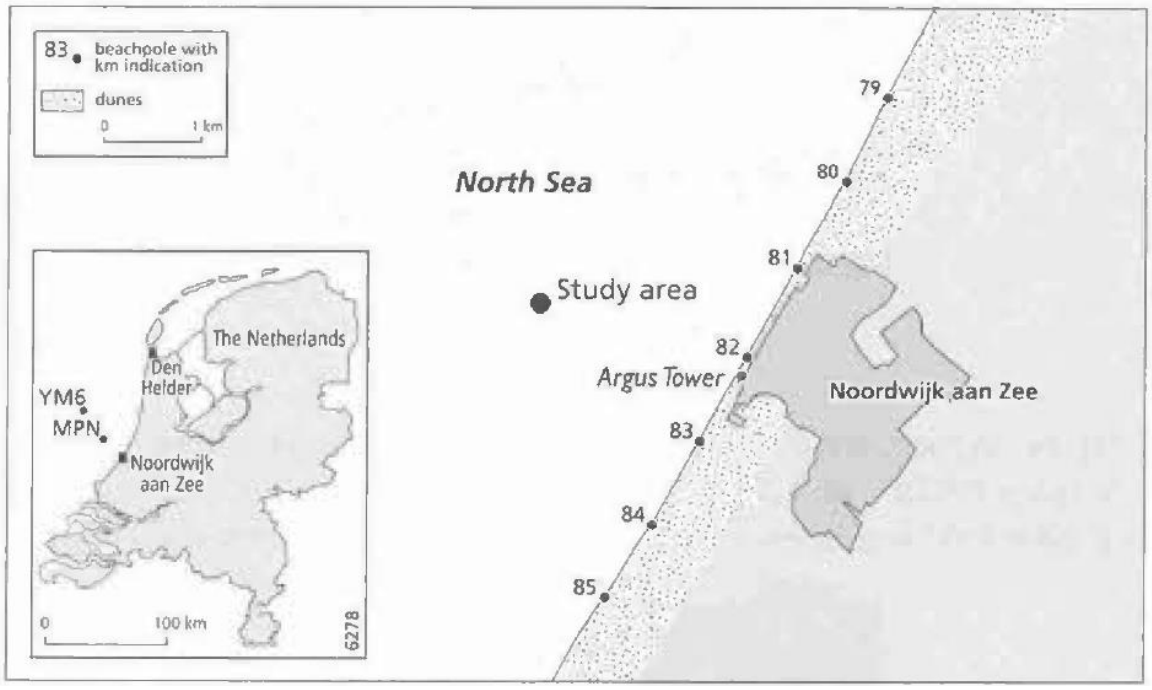

Figure 4.5 Location SANDPIT field measurements 2 km off the coast of Noordwijk aan Zee. Figure taken from Van Rijn et al. (2005).

At the location 2 km off the coast the following measurements were carried out from 4 different, collocated tripods:

- water levels (pressure sensor)
- velocities (EMF, ADCP)
- suspended sediment concentrations (OBS, ABS (acoustic backscatter system))

- sediment fluxes (ASTM; acoustic sand transport meter, suspended sediment trap)
- bedforms (ripple profiler, rotary side-scan sonar)

During the autumn 2003 campaign the significant wave heights varied between 0.1 and 4.0 m, spectral peak periods were between 7.5 and 11.6 s and maximum tidal current velocities were ~0.6 m/s. The D10, D50 and D90 of the bed material were 0.19, 0.23 and 0.31 mm, respectively.

Current-related bedload transport was measured at the 13 and 18 m water depth locations during 10-40 minutes sampling periods with a basket-type bedload 'Nile' sampler during two spring tidal flood peaks and one ebb peak. Flow velocities were simultaneously measured with 1-2 OTT propeller type current meters on the bedload sampler.

4.3.6 LaMER Egmond lander (Witbaard *et al.*, 2015)

Within the framework of the Monitoring and Evaluation Programme (MEP) of Rijkswaterstaat and the LaMER foundation field data were collected to assess the predicted effects of sand mining on fine sediment dynamics. A measurement frame was deployed 1 km offshore at Egmond aan Zee, from March 2011 until December 2012 to quantify near-bed fine sediment dynamics (see Figure 4.16 for the location).

Two (almost) identical frames were deployed during alternating periods. This procedure was necessary for such a lengthy deployment, as battery life of instruments does not allow for deployments longer than approx. 2 months. Furthermore, instruments are affected by biofouling during summer, and need to be maintained regularly. The measurement frame was placed at an average depth of 11 m, and was equipped with: two ADV sensors to measure current velocity and turbulence intensity, an upward-looking ADCP to measure current velocities over the full water column (except for the lower 2 m), a CTD sensor to measure salinity, and 4 OBS sensors to measure suspended sediment concentrations near the bottom (0.3, 0.8, 1.4 and 2m from the bottom). Apart from the measurements that were collected with the measurement frame (also called 'bottom lander'), bed samples were collected in the vicinity of the measurement frame with boxcores. For the upper 5 cm of the boxcore samples the grain size distribution was determined. Additionally, the company MEDUSA collected samples to analyse the mud content of the bed near the study site.

4.3.7 STRAINS I & II (Henriquez *et al.*, 2013; Meirelles *et al.*, 2014)[3]

The STRAINS projects aim to quantify the influence of the Rhine ROFI on sediment transport on the shoreface. There were two separate measurement campaigns, i.e. STRAINS I and STRAINS II. The STRAINS I measurements were carried out with an instrumented bed-frame, named the NEMO lander, deployed at -12 m NAP in February 2013 for 21 days, 1 km offshore from the tip of the Sand Motor. Current profiles were estimated from a downward-looking ADCP (Nortek Aquadopp HR) mounted 50 cm above the bed. Current profiles throughout the water column were recorded from an upward-looking ADCP (Nortek Aquadopp). Near-bottom flow velocities were also measured with two ADVs (Nortek Vector) positioned 0.56 m above the bed and sampled with 8 Hz. The ADVs measured one after another with an overlap of 6 days. Other instruments (CTD, OBS, ADCP, LISST) were mounted on two additional frames and two additional moorings (Henriquez *et al*., 2014). Additionally, the area was monitored with radar, Wave Rider buoys and the ARGUS video system to determine flow velocities, bed levels and wave heights.

[3] *The overview of the STRAINS II project originates from Sabine Rijnsburger, PhD student Technical University of Delft.*

During the STRAINS II campaign measurement frames were deployed at 1, 1.5 and 5.5 km offshore from the Sand Motor tip, with corresponding depths being 8, 12 and 18 m, respectively (Figure 4.6). This second campaign took place in September and October 2014. At the 8 m water depth, a frame was deployed which measured current velocities (ADV), suspended sand (Aquascat ABS) and SPM (OBS sensors). At the 12 m depth, one frame measured velocities over the entire water column with an ADCP, near-bed salinity with a CTD sensor and SPM concentrations with an OBS. A second frame at 12 m depth measured near-bottom velocities at three heights (ADVs at 0.25, 0.5 and 0.75 m), near-bottom salinity (CTD at 0.25, 0.5 and 0.75 m), near bottom SPM concentrations (OBS at 0.33, 0.58, 0.83 m) suspended flocs with LISST (size and concentration). The frame was also equipped with 4 ABS sensors to measure suspended sand concentrations and a 3D ripple scanner. A fourth frame, at 18m water depth, measured velocities over the entire water column with an ADCP, near-bed salinity with a CTD sensor, SPM concentrations with an OBS and suspended flocs with a LISST. Furthermore, vertical profiles of salinity, suspended sediment and chlorophyll-a were collected by placing moorings at 12 and 18 m water depths. 5 OBS and 5 CTD sensors were mounted on a steel cable at each location. Spacing between the sensors increased with height above the bed.

During the second campaign there was also a measurement cruise with the RV Navicula, primarily focusing on measuring suspended fine sediment, by deploying two different floc cameras (one from HR-Wallingford, one from TU Delft). Furthermore, CTD and OBS profiles were taken by deploying a lightweight frame as was also done in the BwN-transect project (Section 3.3.4).

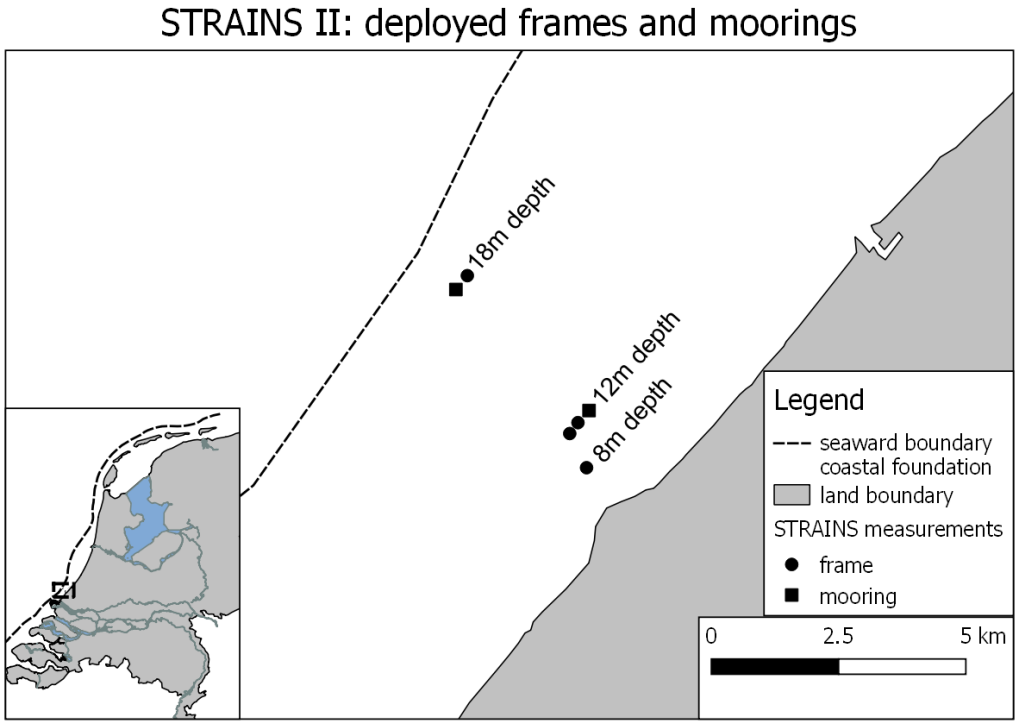

Figure 4.6 Location of deployed moorings and frames during the STRAINS II campaign 1, 1.5 and 5.5 km offshore from the Sand Motor, corresponding to water depths of 8, 12 and 18 m.

4.3.8 MegaPex experiments

MegaPex stands for MEGA Perturbation EXperiment and is a six weeks field experiment in the fall of 2014 within the framework of NeMo and NatureCoast research projects. The aim was to obtain insights into the feedback between coastal processes related to hydrodynamics, morphology, aeolian transport, dune formation, hydrology and ecology with special focus on the development of the mega nourishment called The Sand Motor, constructed in 2011.

Next to many shallow water measurements, Saulo Meirelles Nunes Da Rocha (TUD PhD student within NEMO project) measured velocities (ADV's, ADCP), salinity, suspended sediment concentration (ABS), suspended particle size (LISST) and bedforms (3D side-scanning sonar) at a water depth of 12 m offshore from the tip of the Sand Motor (Meirelles *et al.*, 2016) similar to as was done the in the STRANS experiments (Meirelles *et al.*, 2014).

4.4 Morphology

4.4.1 Bedforms

Passchier & Kleinhans (2005)

Passchier & Kleinhans (2005) studied bedforms, vertical bed structure and grain size at three sites on the Dutch shoreface (Figure 4.7); Areas 1 and 2 have dimensions of 1 km x 2.5 km, and Area 3 1 km x 5 km. Area 1 is part of a shoreface-connected ridge, approx. 10 km West of Zandvoort with water depths of 15–18 m. Area 2 is a sloping surface landward of the shoreface-connected ridges, approx. 5 km west of Noordwijk with water depths 14–18 m. Area 3 is located 55 km west of Bergen aan Zee in water depths of 25–30 m. It is characterised by 1–3 m high sand waves with a wavelength of ~200 m.

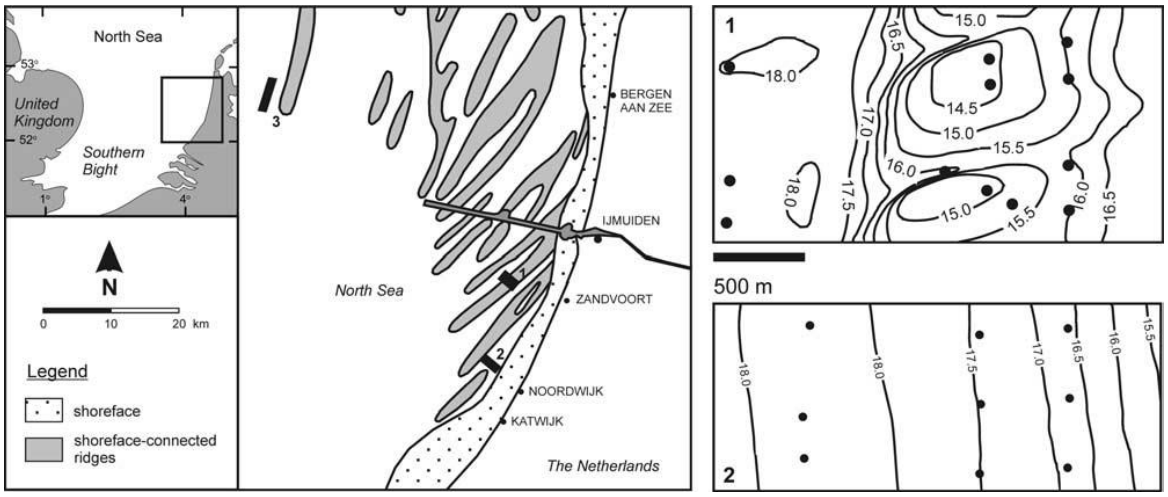

Figure 4.7 Left: location of study areas in the Netherlands coastal zone. Right: detailed bathymetry of the study areas on the lower shoreface; dots are sample locations. Area 3 is situated in water depths of 25–30 m. Figure taken from Passchier & Kleinhans (2005).

Data acquisition at the three areas occurred during fair-weather conditions in 2001 (Figure 4.8). The multibeam data were obtained using 20 m track line spacing creating a minimal overlap. The SANDPIT sites were mapped with multibeam and sonar-imaging techniques in October 2002 (sonar only) after a large storm (H_{sig} < 6 m) and in February 2003 (sonar and multibeam) during fair weather conditions.

The standard error in the bathymetry related to the conversion of the acoustic signal to water depth and the application of the tide and velocity correction is in the order of 0.15 m, which is important when comparing data from different surveys. However, local changes in the bed morphology measured during one survey (with the same standard error), and thus bed form amplitudes, are precise on a centimetre-scale resolution. The positioning error is up to a few meters and the horizontal resolution of the multibeam data is 1 x 1 m, which is sufficient to observe bed forms of megaripple scale (meter-scale wavelength), but insufficient to resolve ripples (centimetre-scale wavelengths).

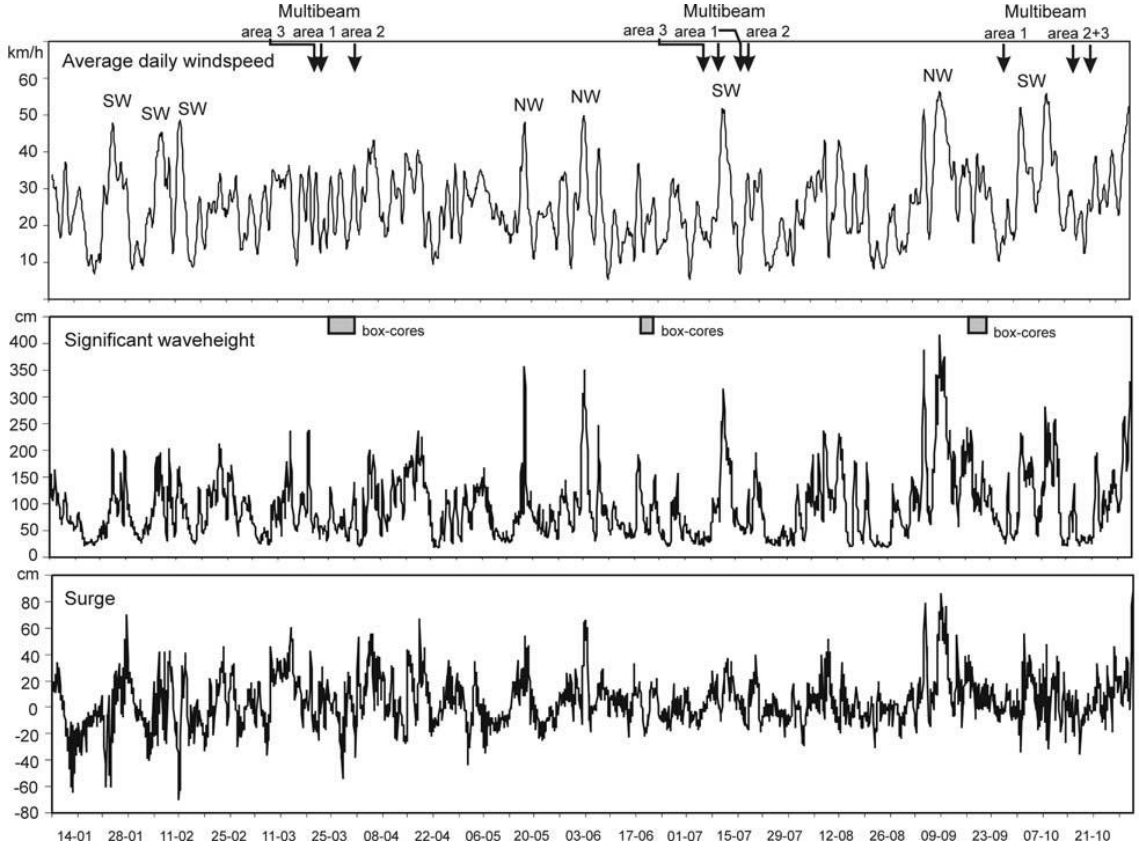

Figure 4.8 Average daily wind speed (SW = wind from the southwest, NW: wind from the northwest), significant wave height and surge height as 3-hour averages, measured at Meetpost Noordwijk (h = 18 m) for the period 7 January until 31 October 2000. Figure taken from Passchier & Kleinhans (2005).

In 2001, bottom samples were obtained using a cylinder-shaped box corer with a diameter of 32 cm. The March and June corings can be considered a fair-weather situation, whereas the September campaign occurred after a seasonal storm (Figure 4.8). Penetration varied between 0.2 and 0.3 m. Lithology, structure and sedimentological features of the seabed were monitored in 10 cm diameter core samples covering 12 sampling stations in area 1, 9 stations in area 2, and 11–16 stations in area 3. Grain size distributions (<2 mm) of the top lithological units were analysed using untreated samples in a Malvern particle sizer. Reineck boxcores were collected from the SANDPIT sites in November 2002 (post-storm) and in September 2003 (fair-weather situation). Lacquer profiles of the (vertical) stratification of the top 0.2 m of the bed were made from a near-vertical section (scraped clean) of undisturbed boxcore sediment.

Van Dijk & Kleinhans (2005)

The seabed morphology was measured using multibeam and side-scan sonar at a coastal site (1770x1326 m) in an area with shoreface-connected ridges and water depths of 14-18 m, 6-8 km west of Zandvoort, and at an offshore site (5510x1100 m) in a sand wave field, with water depths of 27-30 m, 50 km west of Egmond aan Zee (Figure 4.9). These are the same areas as Areas 1 and 3 by Passchier & Kleinhans (2005). Data were acquired on 4 expeditions in March, June/July and September/October 2001 and April 2002, and for the offshore site also in September 2002. During the above 4 expeditions, the seabed was sampled using a cylindrical box corer with a diameter of 32 cm, from which cores of 10 cm diameter were resampled. The total number of samples per expedition varying between 13 and 17 at the coastal site and 12 and 19 at the offshore site. Grain size samples for grains <2 mm were analysed by laser diffraction, using a Malvern 2000.

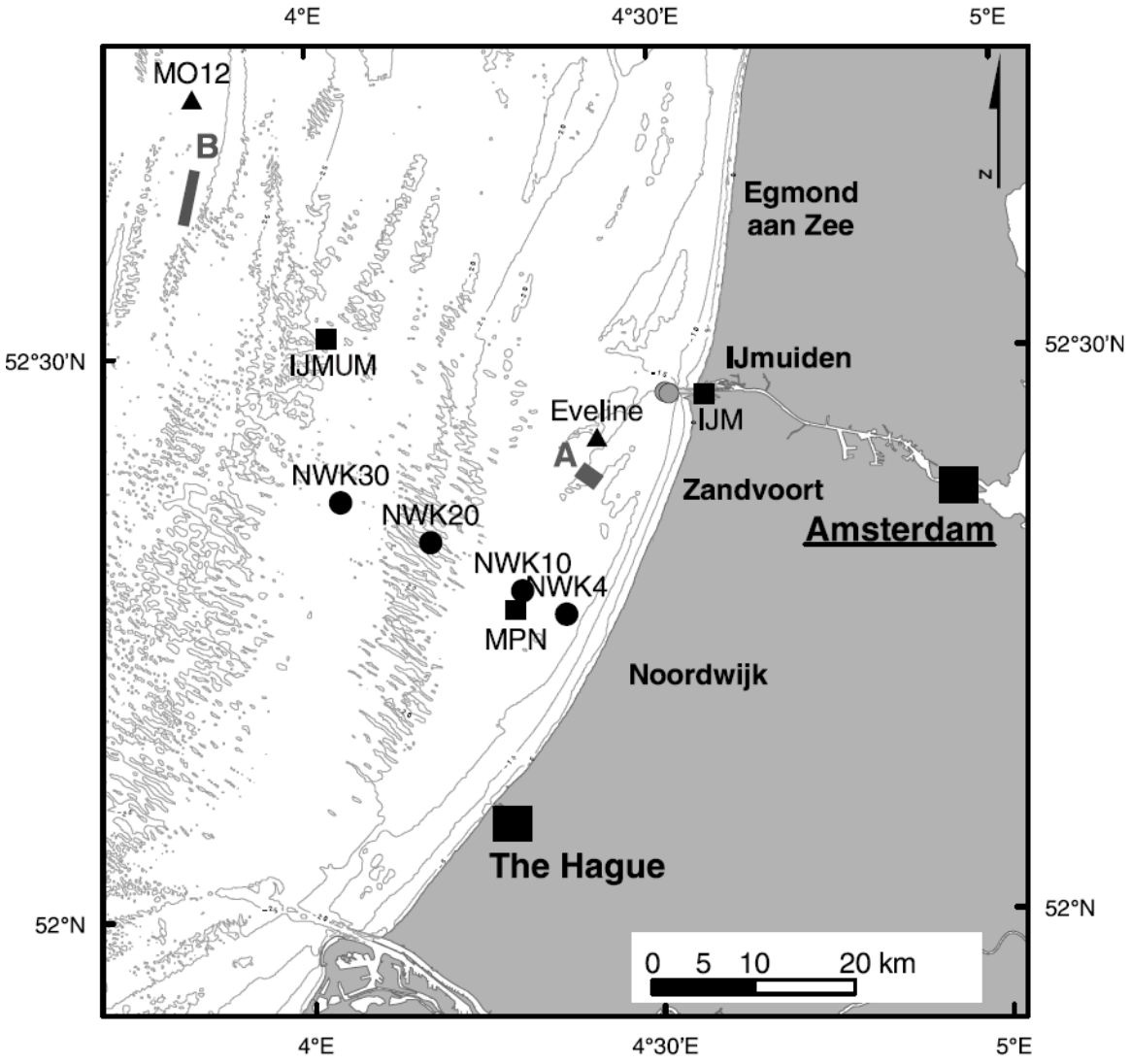

Figure 4.9 Location of the coastal site (A) in the shoreface-connected ridge area and the offshore site (B) in a sand wave field. Monitoring stations and tide gauges are also indicated. Figure taken from Van Dijk & Kleinhans (2005).

4.4.2 JARKUS and Vaklodingen

JARKUS ("Jaarlijkse Kustmetingen") are yearly measurements of bed levels along about 2500 cross-shore transects with an alongshore distance of ~200-250 m. Standard these transects runs offshore to a depth of ~8 m. Before 1991, longer transects were occasionally measured covering the shoreface.

Vaklodingen are 20 x 20 m bed level data based on interpolation of single-beam measurements with a transect distance of 200 to 1000 m, depending on the location, and (since recently) detailed LIDAR measurements of subaerial parts. The Vaklodingen data cover the entire coastal system until a water depth of ~20 m (Figure 4.10). Typically, the Vaklodingen measurements are acquired every three to six years, depending on the area. The Vaklodingen data are organized in tiles of 10 km x 12.5 km.

Figure 4.11 presents an overview of the available Vaklodingen en JARKUS data for the Holland Coast for the year 2011. The same figures are available for all other years and areas.

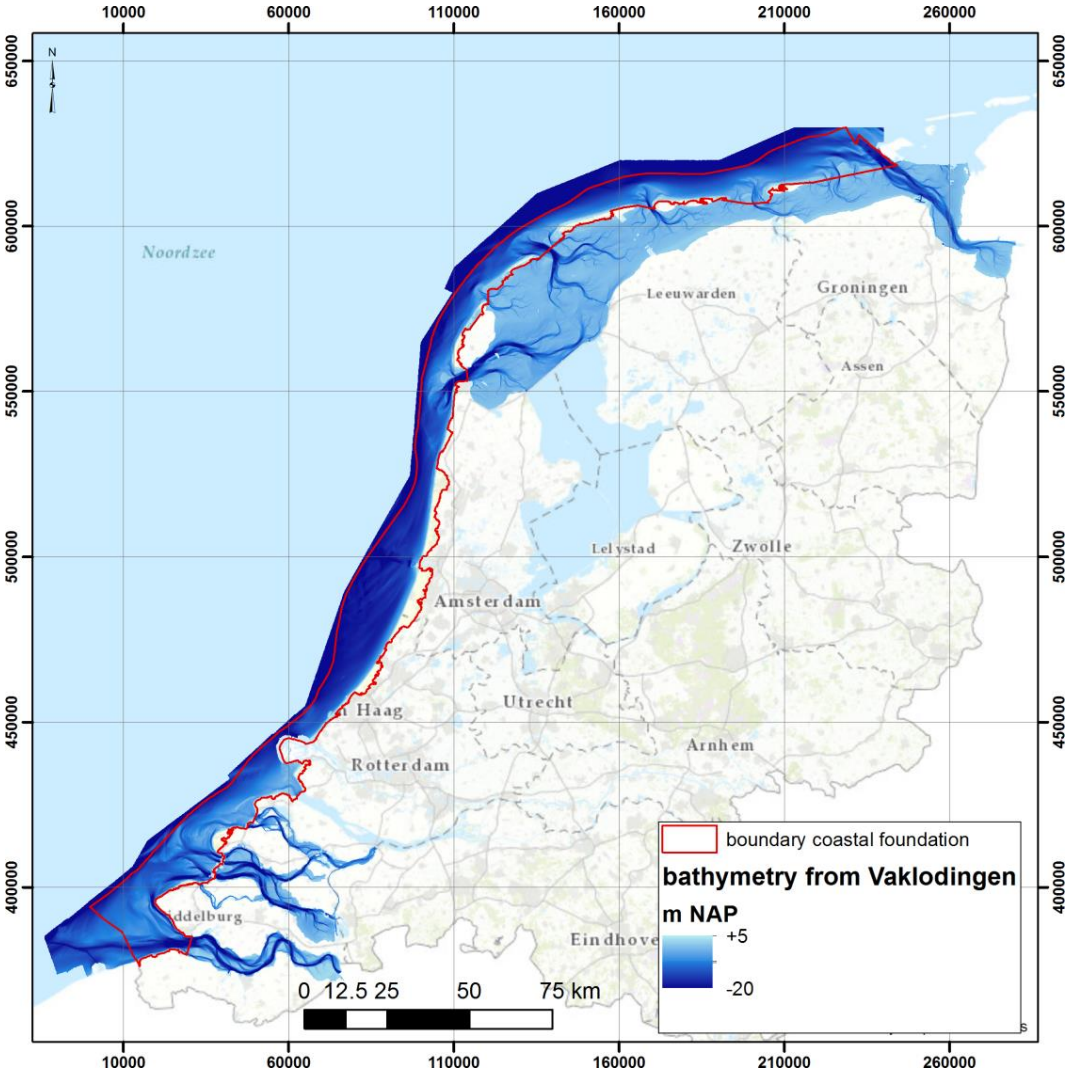

Figure 4.10 Position of coastal foundation and bathymetry from Vaklodingen measurements between 2009 and 2014.

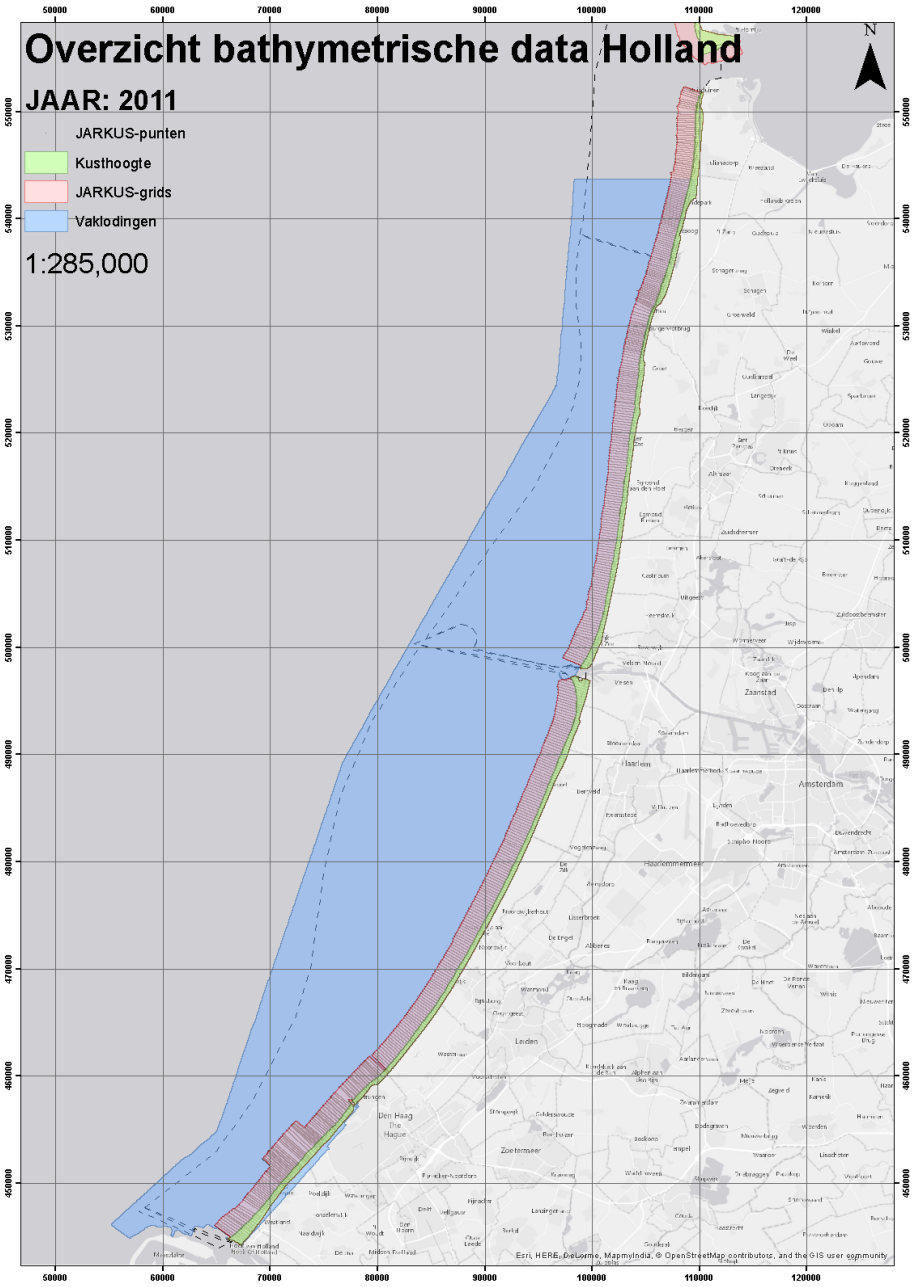

Figure 4.11 Available datasets along the Holland coast in 2011. "Kusthoogte" refers to LIDAR measurements.

4.4.3 Bathymetric surveys by Hydrographic Office of the Royal Netherlands Navy

Rijkswaterstaat is responsible for the Vaklodingen and JARKUS data. The Hydrographic Office of the Royal Netherlands Navy is responsible for most other and deeper parts of the Dutch continental shelf. In the 2003 survey policy, the Dutch shoreface was typically measured every 6 years (Figure 4.12).

An overview of the bathymetric surveys is given by maps per decade (see Figure 4.13 as an example). The source data can be requested at www.hydro.nl. The spatial resolution varies between the surveys. Until 2000 only single-beam measurements were performed, with resolution depending on line spacing. After 2000 multi-beam is used more often, giving a

much higher resolution. For each survey the raw data (at 3x5 m detail level) was interpolated to a 25 m raster dataset by Deltares. These are available through OpenEarth: https://publicwiki.deltares.nl/display/OET/Dataset+documentation+bathymetry+NLHO.

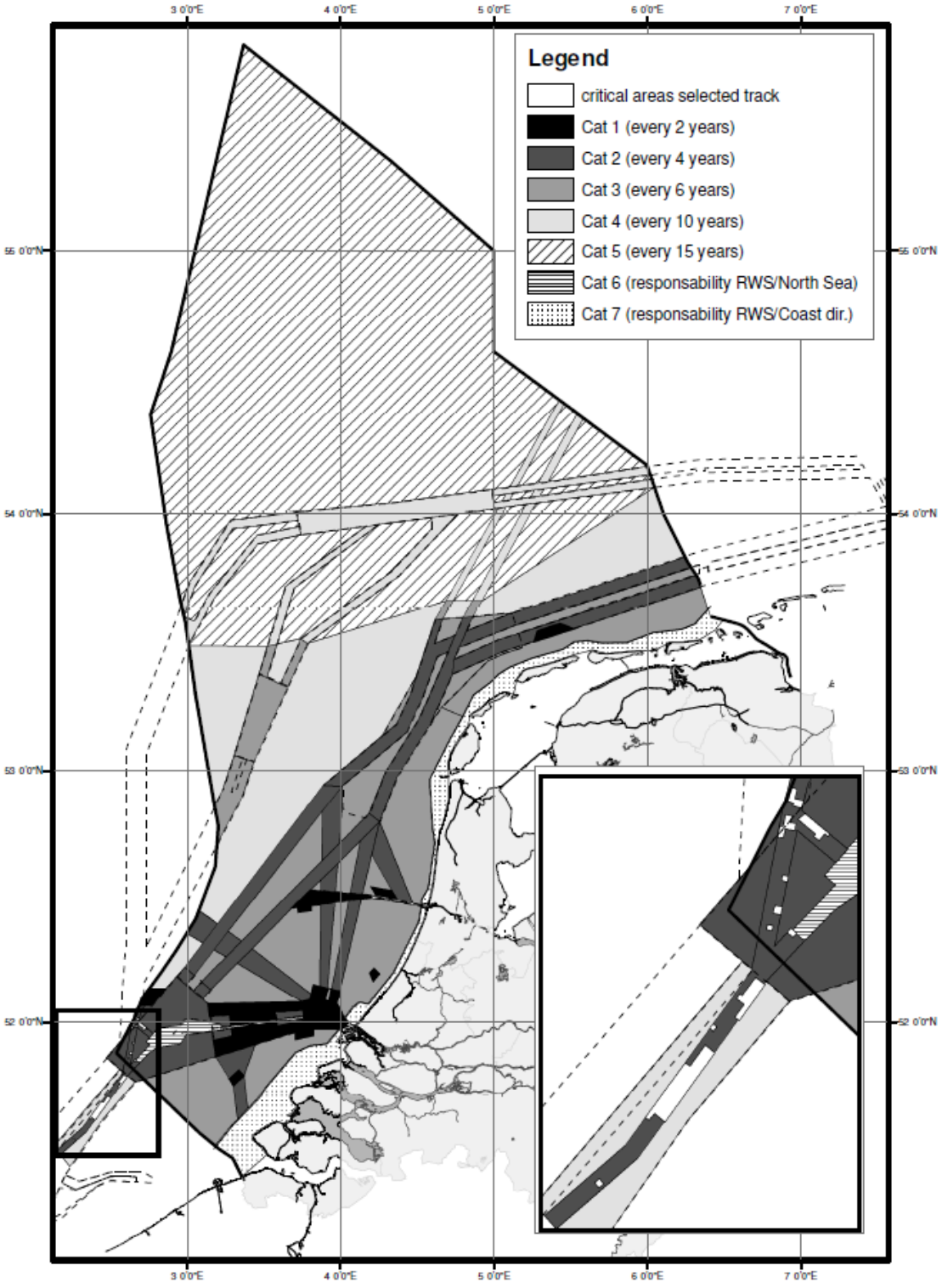

Figure 4.12 The 2003 survey frequency policy of the Hydrographic Office of the Royal Netherlands Navy. Figure taken from Dorst (2009).

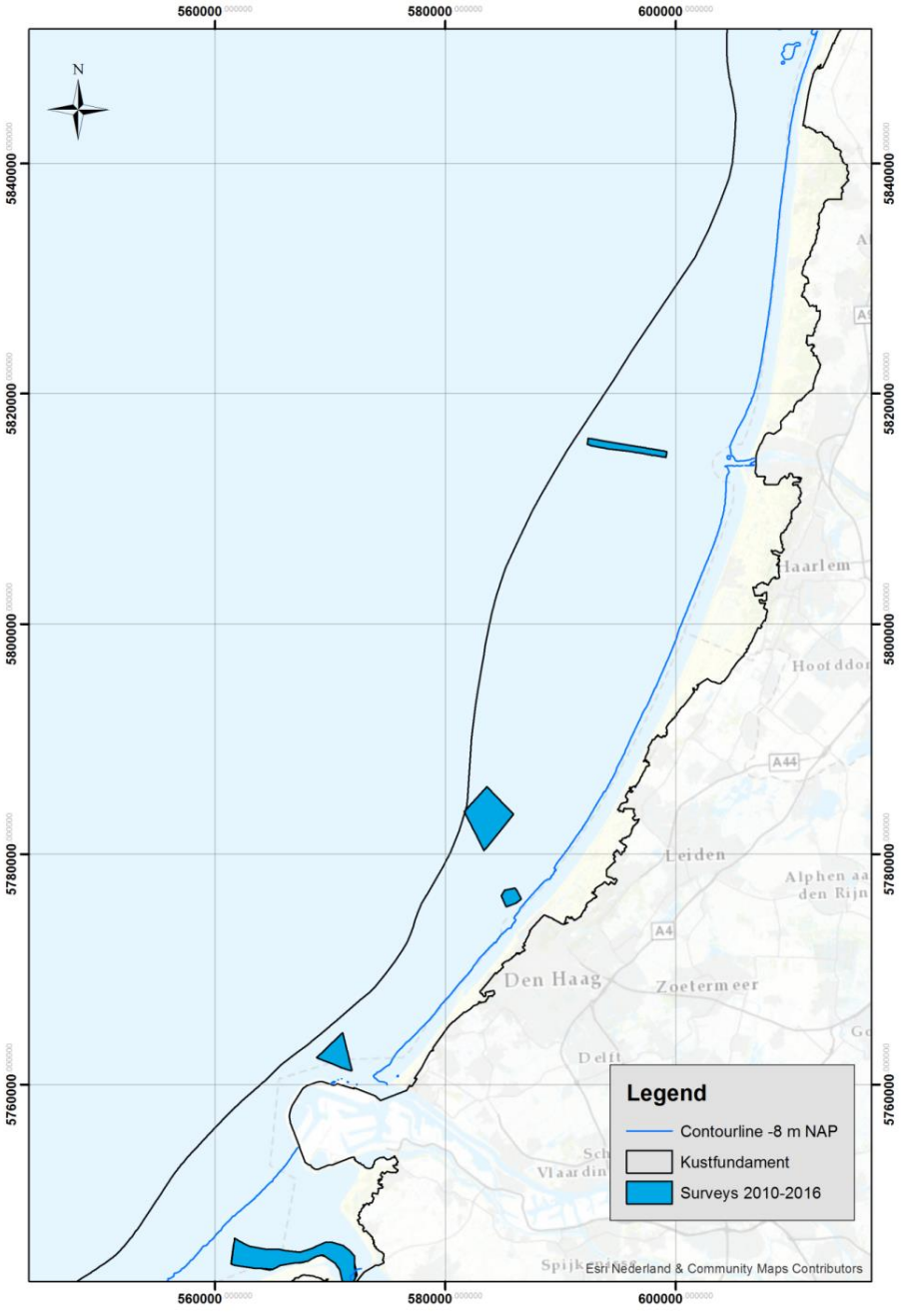

Figure 4.13 Surveys performed by the Hydrographic Office of the Royal Netherlands Navy within the coastal foundation for the period 2010-2016.

4.4.4 Side-scan sonar

The Hydrographic Office of the Royal Netherlands Navy acquires side-scan sonar data along the entire Dutch Continental Shelf. An example overview of the available side-scan sonar data can be found in Figure 4.14. The data are stored at TNO Geological Survey, Utrecht. Overall, the resolution is low, of the order of 150 m. The side-scan sonar data gives information of objects and characteristics of the seafloor, but generally no information of the absolute depth (bathymetry).

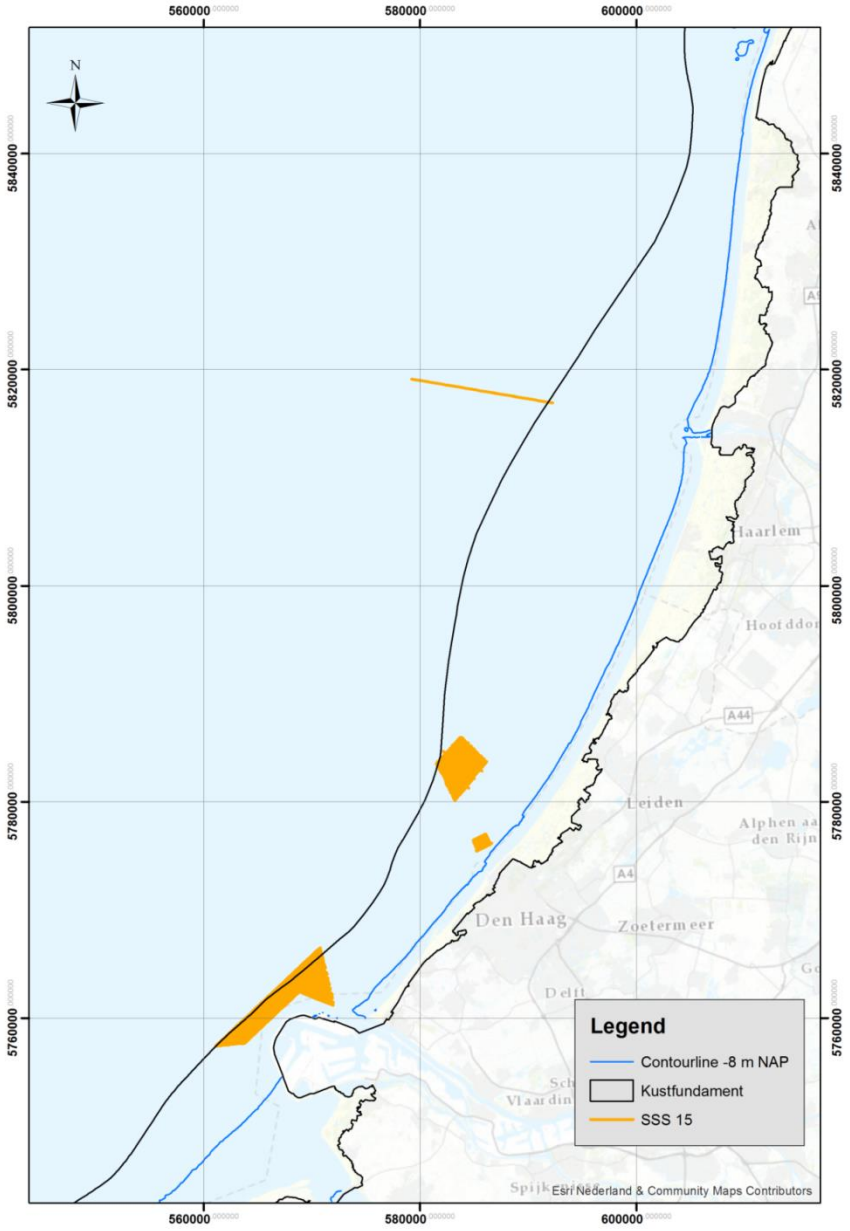

Figure 4.14 Available side-scan sonar data within the coastal foundation of the Holland coast for the year 2015.

4.5 Subsurface sampling

An example overview of publicly available boreholes can be found in Appendix D. The boreholes are available at TNO Geological Survey through www.dinoloket.nl. For the coastal areas Wadden, Holland and Delta overview of the boreholes were made per depth-class (depth below seafloor).

In the area of the lower shoreface, between NAP -8 and -20 m, the depth of most boreholes is limited (less than 0.2 m). Most boreholes deeper than 5 m have a relatively poor quality since they are flushed borings (mostly a low vertical resolution). The density of the boreholes per km^2 decreases with depth. Besides depth, the quality and usability of the boreholes depends on several factors, including:

- vertical resolution

- presence and quality of stratigraphic description
- presence and quality of borehole photographs
- presence of grain-size analyses and number of analyses per borehole
- presence of chemical/mineralogical analyses

Examples of boreholes showing the variability of available information are shown in Appendix D. Borehole B01D0287 has very limited information; B24H0136 has many parameters described and an elaborate description, but lacks information on the stratigraphy; BQ140002 has fewer parameters, a good description which occasionally contains information on the stratigraphy, although for most layers not very specific (only period, no geological formation).

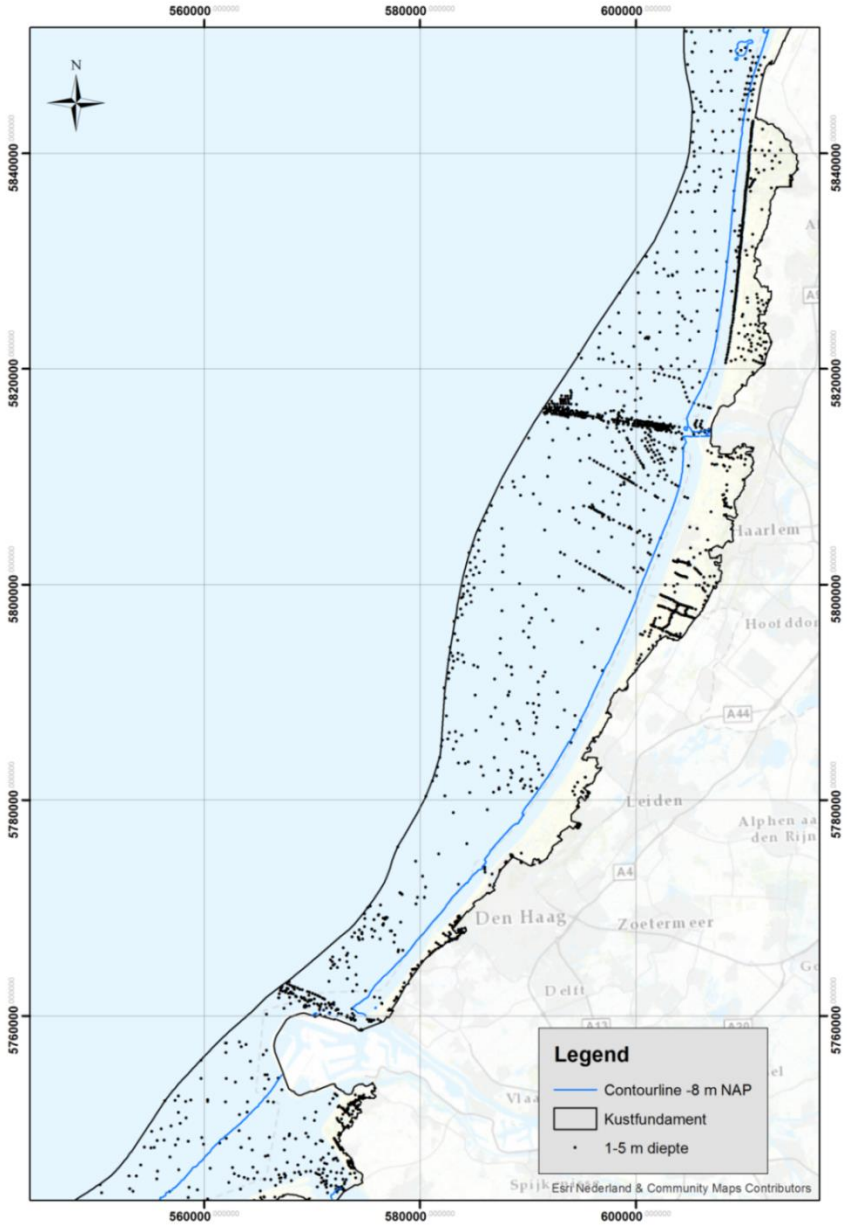

Figure 4.15 Available boreholes within the coastal foundation at the Holland coast with a depth of 1 to 5 m.

4.6 Overview

Figure 4.16 presents an overview of the process measurements at deep water along the Dutch coast, including the campaigns of Passchier & Kleinhans (2005) and Van Dijk & Kleinhans (2005). The deep water measurements were mainly carried out along the Holland coast; data for the Delta and Wadden Coast are lacking. The larger number of data sets focused on hydrodynamics and fine sediment dynamics; sand transport processes were measured during the SANDPIT, STRAINS and MegaPex campaigns and by Van de Meene & Van Rijn (2000). There is a relatively large amount of morphological and subsurface shoreface data of different types available. However, the quality (e.g. resolution) varies greatly. It is recommended to assess the quality of existing data for the selected areas of interest, given the intended application.

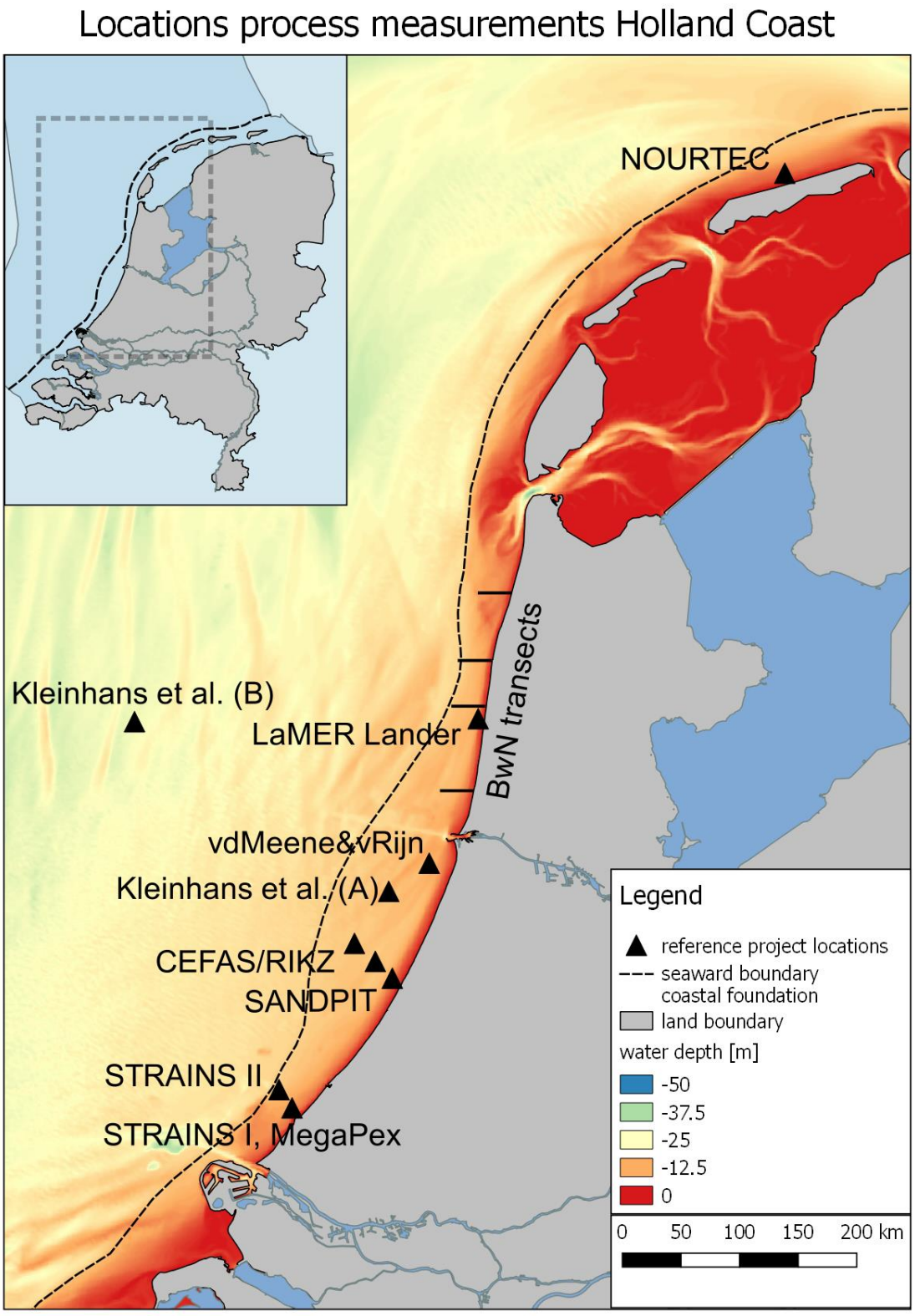

Figure 4.16 Location of the process measurements at deep water along the Dutch coast. Kleinhans et al. (A) and Kleinhans et al. (B) refer to the local morphological and subsurface measurements of Passchier & Kleinhans (2005) and Van Dijk & Kleinhans (2005), respectively.

5 Numerical modelling

5.1 Introduction

Computer modelling of hydrodynamics, sediment transport and morphology of the Dutch shoreface basically started with the development of the personal computer in the 1980s. Here we will discuss the approach and results of a number of large-scale Dutch shoreface sand transport modelling studies since these years. We will then discuss available hydrodynamic mode to provide boundary conditions for nesting local models or to develop further into sediment transport models.

5.2 Dutch shoreface sand transport modelling studies

5.2.1 Sand transport on the shoreface of the Holland coast (Roelvink & Stive, 1990)

5.2.1.1 Introduction

In the framework of the first Coastal Genesis research program of Rijkswaterstaat, Roelvink & Stive (1990) computed the yearly-averaged transport along a number of transects perpendicular to the coast on the shoreface of the Holland coast. The study by Roelvink & Stive (1990) provided an estimate of the large-scale net sand transport pattern on the shoreface, and identified the relative importance of the mechanism contributing to this pattern. It contributed to conceptual large scale evolution models of the Dutch coast, developed in the framework of the Coastal Genesis program (Stive *et al.*, 1990).

5.2.1.2 Approach

Roelvink & Stive (1990) applied a one-dimensional, depth-averaged, cross-shore (1D) model (precursor of the 2DV Unibest-TC model) to compute the depth-mean wave and current parameters and the resulting sediment transport components. The model was forced with schematised offshore tidal motion based on (interpolated) observation data from nearby measuring stations. The tide was schematised into 12 steps within a representative tidal cycle. The variation in offshore wave conditions was schematised by a climate of 80 combinations of wave heights and directions, each combination with its representative wave period and offshore water level set-up.

From the depth-mean wave and current parameters along the cross-shore transects, Roelvink & Stive (1990) computed the transport vectors and integrated these over all conditions; taking into account the frequency of occurrence of each condition. This then yielded the yearly-averaged transport vector for the cross-shore transect.

The model was calibrated against transport rates inferred from the long-term flattening of the middle shoreface over 90 years, the order of magnitude of the net longshore transport in the surfzone based on the study by Dijkman *et al.* (1990), and transport rates inferred from the observed northward migration of the navigation channel off IJmuiden Harbour. These observations led to an adjustment of the transport rates; cross-shore transports were reduced by a factor 2 and longshore transport multiplied by a factor of 2.

5.2.1.3 Results

Model computations were carried out for four transects along the Holland coast. The plot by Roelvink & Stive (1990) showing the resulting net transport vectors is presented in Figure 5.1. The arrows indicate the magnitude and direction of the yearly-averaged transport at NAP-20

m, NAP-15 m, NAP-10 m and NAP-8 m. The figure shows a transition from the tide-dominated transport (mainly alongshore-directed) to wave-dominated transport (in the direction of wave advance; also a cross-shore component). Towards the NAP-8 m depth contours, the onshore-directed cross-shore transport increases as a result of the increased importance of wave-induced streaming and wave asymmetry effects; the longshore transport also becomes more wave-dominated and shows a clear dependence on the coastal orientation with larger alongshore transports as the waves approach the coast more obliquely (transects at Scheveningen and north of Petten). The net onshore-directed cross-shore transport at NAP-20 m was 20 m^3/m/year and at NAP-8 m 2 m^3/m/year.

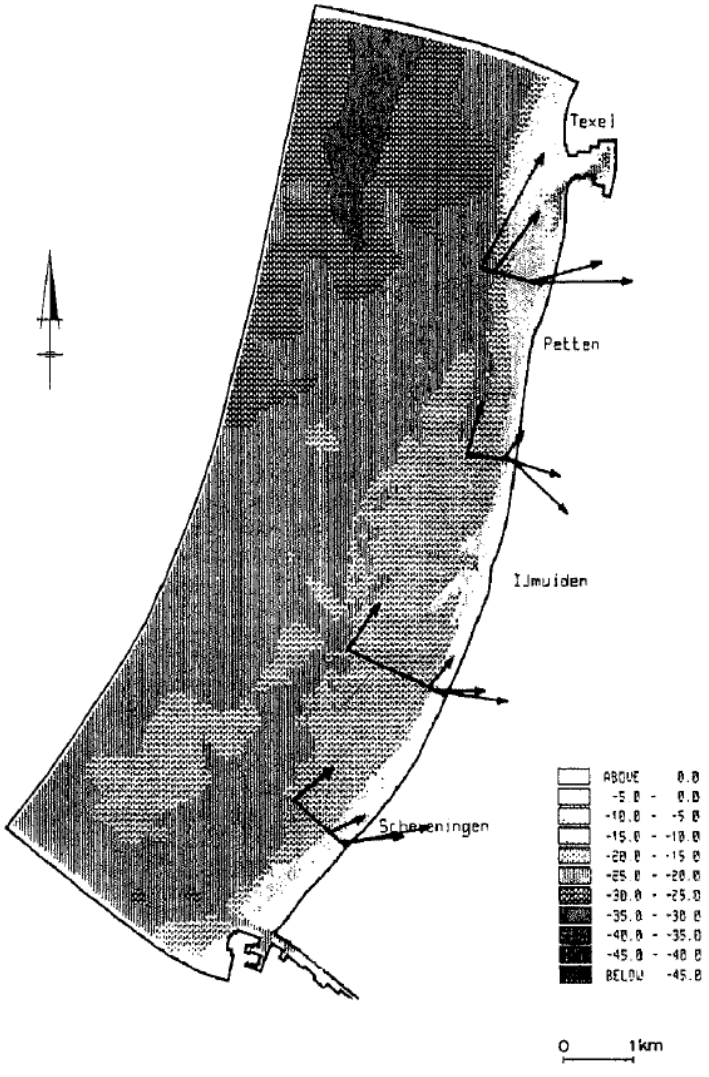

Figure 5.1 Computed net transport vectors (calibrated) at the 20, 15, 10 and 8 m depth contour. Figure taken from Roelvink & Stive (1990).

Roelvink & Stive (1990) analysed the computed transports as a function of tidal phase in more detail for the most northern transect at a depth of NAP-18 m and NAP-10 m. This clearly showed the dominance of tidal transport in deep water (NAP -18 m) as the transport direction closely followed the tidal velocity direction and the transport increased non-linearly with increasing tidal velocity. The picture was quite different at a water depth of 10 m. The

computed transports had a significant onshore component at this depth and the dependence of the transport on the tidal velocity was almost linear, indicating that the waves do most of the stirring at this depth and the tidal velocity merely advects the sediment.

Roelvink & Stive (1990) illustrated the variation of the cross-shore transport with water depth and showed a sharp increase of the onshore transport towards the NAP -8 m line. They describe a transition zone between approx. NAP -6 m and NAP -10 m from the highly dynamic “active zone” to the morphologically rather inactive part of the shoreface and conclude that the shoreface acts as a significant source of sand to the “active zone”.

Roelvink & Stive (1990) also computed the cross-shore transport gradients at different depths. The computed transport gradient at the 10 m depth contour agreed with observed shoreward migration of about 2 m/year.

5.2.2 Sediment transport and budget of the central Holland coast (Van Rijn, 1997)

5.2.2.1 Introduction

Van Rijn (1997) developed a sand budget model describing the sand volume change in three alongshore and three cross-shore compartments of the central coastal zone of Holland from Den Helder to Hoek van Holland. Figure 5.2 shows the compartments and schematised bed profile. The yearly average transport at the boundary of each compartment was computed with a Unibest-TC model using schematised wave and current conditions.

.

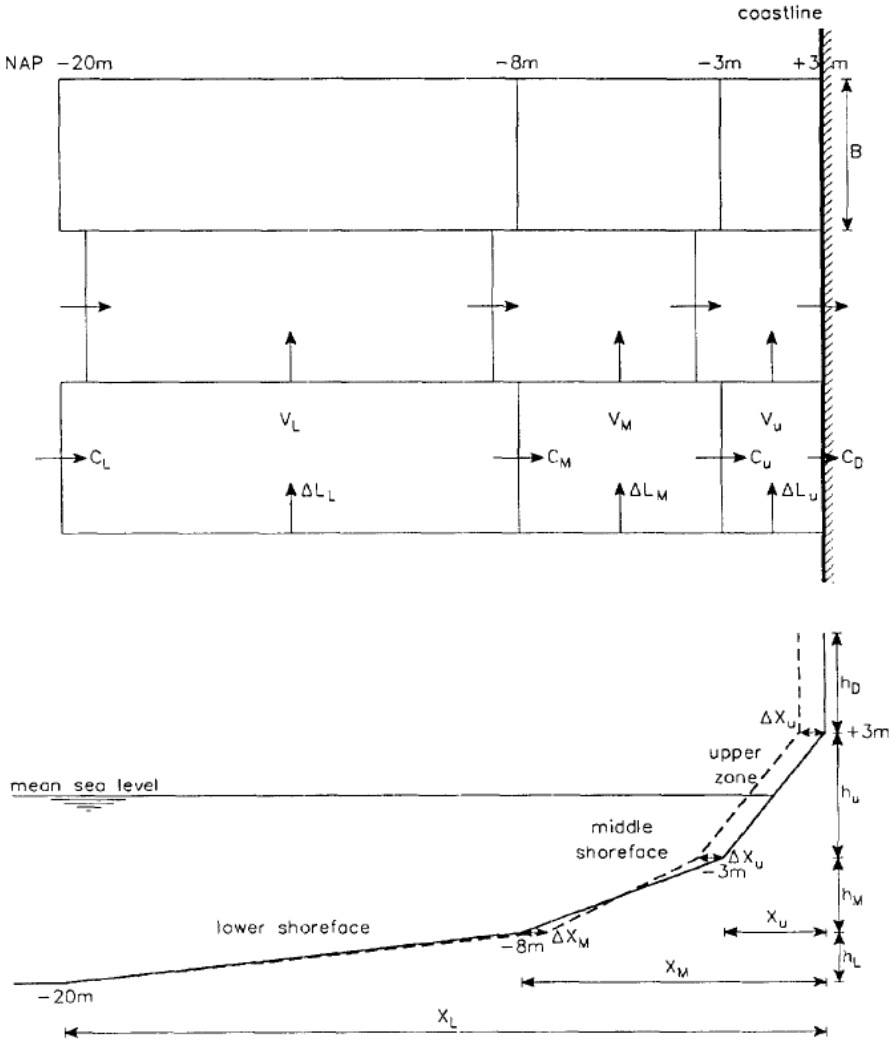

Figure 5.2 Compartments and schematized bed profile of the sand budget model of Van Rijn (1997).

Unibest-TC (TC: Time-dependent Cross-shore) is the cross-shore sediment transport module of the Unibest Coastal Software Package. It is designed to compute cross-shore and alongshore sediment transports and the resulting cross-shore profile changes along any coastal profile of arbitrary shape under the combined action of waves, longshore tidal currents and wind. The model allows for constant, periodic and time series of the hydrodynamic boundary conditions to be prescribed. It assumes that the modelled coastal section is longshore uniform.

5.2.2.2 *Approach*

Van Rijn (1997) computed the yearly average transport rates for four cross-shore profiles, i.e. at 14, 40, 76 and 103 km from Den Helder, which is at the boundary of each alongshore compartment. He computed the yearly-averaged sand transport rates based on a one-dimensional approach in a direction normal to the shore. The model consisted of a wave propagation model, a vertical flow structure model and a sand transport model. Wind growth was not included.

The wave propagation model computes the wave energy decay along a wave ray based on shoaling, refraction and energy dissipation by bottom friction and wave breaking (wave growth due to wind was not accounted for). The near-bed instantaneous velocities are computed as time series representing irregular wave groups (including wave asymmetry and bound long wave effects).

The vertical flow structure model computes the vertical distribution of horizontal flow velocity for a given depth-averaged velocity vector (input), wave height and wave period, fluid density gradient and wind shear stresses (surface). The Longuet-Higgins streaming in the wave boundary layer due to transfer of momentum by viscous and turbulent diffusion is taken into account. The expressions by Longuet-Higgins (1953), which are valid for laminar flow in the boundary layer, were applied. These expressions appeared to give quite reasonable results for the turbulent case as well, based on comparison of measured and computed near-bed velocities (Van Rijn *et al.*, 1994). The effect of wave breaking resulting in a longshore current and a cross-shore return current (undertow) and the Coriolis effect was taken into account. The model was improved by including the roller effect and a better vertical eddy viscosity coefficient (constant) with respect to the modelling of the longshore current in the surf zone.

The sand transport model computing the bed load and the suspended load was also updated. The formulations by Ribberink (1998) were applied to compute the net bed-load transport rates. The Van Rijn (1993) formulations were applied to compute the suspended load transports. The transport model of Bailard-Bagnold (see Roelvink & Stive, 1990) was used in the sensitivity computations.

Sediment transport rates were computed for schematised wave and corresponding current conditions. Tidal averaging was applied to obtain the tide-averaged transport rate for each wave direction and wave height class. The tide-averaged transport rate was multiplied by the percentage of occurrence of each specific wave condition, resulting in a weighted transport rate. Adding all individual weighted values, yielded the yearly-averaged sediment transport rate.

The boundary conditions required to compute the yearly-averaged sand transport rates were: cross-shore bottom profiles, yearly-averaged wave climate, tide- and wind-induced water levels and velocities, fluid density gradients, sediment composition and effective roughness.

The tidal water levels and depth-averaged flow velocities (including wind effects) in the stations of interest were derived from computations made by the RIKZ Department of Rijkswaterstaat using a 2DH flow model.

Van Rijn (1997) schematised the waves into 25 different classes, corresponding to 8 different wind directions and 3 different wind speeds and one condition with no wind (3x8+1=25). The tide was schematised as one representative so-called morphological tide, which was 10% larger than the mean tidal range.

Van Rijn (1997) applied characteristic sand grain sizes of D_{50} = 250 µm and D_{90} = 2xD_{50}, and made sensitivity computations with D_{50} = 200 µm and 300 µm. Current- and wave-related bed roughness values (k_c and k_w) between 0.01 and 0.1 m were applied.

The spatial distribution of the cross-shore density gradients along the coast were based on field measurements. The results are presented in Table 5.1 showing the strongest gradients

at a depth of 8 m near Scheveningen and the smallest values at a depth of 20 m near Scheveningen.

Table 5.1 Density gradients (x0.001 in kg/m^3/m) for various wind directions in profiles 14, 40, 76 and 103

Wind dir	Profile 14 Callantsoog		Profile 40 Egmond		Profile 76 Noordwijk		Profile 193 Scheveningen	
	Depth 8 m	Depth 20 m	Depth 8 m	Depth 20 m	Depth 8 m	Depth 20 m	Depth 8 m	Depth 20 m
Average	0.84	1.05	0.97	0.64	1.63	0.84	3.00	0.67
SW	0.50	1.50	1.50	1.00	2.75	1.00	3.50	0.50
E	1.00	0.50	0.50	0.25	1.00	0.75	1.75	0.50
NW	1.00	1.25	1.00	0.75	1.25	0.80	3.50	0.75

Based on a hindcast of observed morphological changes, Van Rijn (1997) estimated a net onshore transport of about 4 m^3/m/year over the NAP-8 m contour. This agrees reasonably with the computed net cross-shore transport at the NAP -8m depth contour of 0±10 m^3/m/year.

5.2.2.3 Results

Transports at NAP-20 m

Van Rijn (1997) determined the relative contribution of wave velocity asymmetry, bound long waves, Longuet-Higgins streaming, return current and fluid density gradient. Only the fluid density gradient effect played a role at the NAP-20 m contour line. The magnitude of this effect depends on the location along the coast.

Van Rijn (1997) made sensitivity computations for profile 76 near Noordwijk. The computed yearly-averaged cross-shore transport component at the NAP-20 m contour line was found to be onshore directed here and varied between 0 and 15 m^3/m/year. The cross-shore transport component was dominated by tide-induced, wind-induced and density-induced currents in combination with the wave motion acting as a stirring mechanism. The upper limit was mainly related to influence of the density gradient favouring onshore-directed near-bed velocities and hence transport rates. The fluid density decreases in landward direction due to the presence of less saline water in the nearshore zone caused by the fresh water discharge of the Rhine river at the southern boundary of the coast of Holland.

The year-averaged longshore transport for profile 76 near Noordwijk was northward directed and varied between 15 and 60 m^3/m/year. Van Rijn (1997) found the lower limit for reduced tidal current velocities and the upper limit for a relatively small particle diameter.

Van Rijn (1997) compared the contributions of the various hydrodynamic processes to the cross-shore transport rate at all profiles (Table 5.2). He found a negligible contribution of the wave asymmetry, the bound long wave effect and the return current to the cross-shore transport at NAP-20 m. In contrast, Van Rijn (1997) found a contribution of 10 to 25 m^3/m/year of the fluid density gradient dependent on the location along the coast.

Van Rijn (1997) found the computed net bedload transport at the NAP-20 m contour to be generally onshore directed and the net suspended load to be generally offshore directed. Dominance of the computed bed-load transport resulted in the net total load to be generally onshore directed. The alongshore net bedload and net suspended load transport components were northward directed and equally important for the total load transport rate at NAP-20 m.

Table 5.2 Computed contribution of different processes to total cross-shore transport rate at 20 m and 8 m depth (+ is onshore, - is offshore).

Process	Contribution to cross-shore transport rate (m^3/m/year)	
	NAP-20 m	NAP-8 m
Wave velocity asymmetry	0	15
Bound long wave effect	0	-15
Longuet-Higgins streaming effect	0	15
Reduced return current effect	0	25
Fluid density gradient effect	10-25	10

Transports at NAP-8 m

Wave velocity asymmetry, bound long waves, Longuet-Higgins streaming, return current and fluid density gradient effects all play an important role for the total cross-shore transport rate at NAP-8 m (Table 5.2). The best estimates showed a zero net cross-shore transports at NAP-8 m, but the sensitivity runs showed net offshore as well as net onshore transport rates with values varying between -15 and 15 m^3/m/year. Relatively fine sand generally results in offshore transport and coarser material in onshore transport, likely related to the dominance of suspended load and bedload, respectively. Van Rijn (1997) found large differences for different transport formulations. The net cross-shore transport at NAP-8 m reflects the equal importance of onshore-directed bedload transport and offshore-directed suspended load.

The computed year-averaged alongshore transport was directed northward and varied between 35 and 150 m^3/m/year with sensitivity runs showing variations of about 50 m^3/m/year. Smallest values were found for computations with small mean flow and no wind and largest for computations with relatively fine sand. The alongshore net suspended load component dominated over the bedload component at NAP-8 m.

Best estimates of net transport rates at 20 and 8 m water depths

Based on the results of all computations Van Rijn (1997) made best estimates and uncertainty bandwidths of the year-averaged transport rate at a depth of 20 m and 8 m (Table 5.3). It should be noted that the net values in Table 5.3 are small relative to the large gross bidirectional components.

Table 5.3 Computed yearly averaged total transport rates at a depth of 20 m and 8 m for four different profiles by Van Rijn (1997).

Cross-shore profile	Yearly averaged transport (m^3/m/year)			
	Cross-shore NAP-20 m	Cross-shore NAP-8 m	Alongshore NAP-20 m	Alongshore NAP-8 m
14 Callantsoog	5±10	0±10	75±30	150±60
40 Egmond	15±10	0±10	60±25	135±50
76 Noordwijk	10±10	0±10	35±15	85±45
103 Scheveningen	0±10	0±10	25±15	65±40

Transport in the surf zone

Van Rijn computed a net alongshore transport in the surf zone of 400,000 m^3/year. About 60-70% of this occurred in the inner surf zone of 200 m width. Suspended load was dominant over bedload.

The computed net alongshore transport was strongly affected by the wave-induced longshore current. A 50% reduction of the wave-induced alongshore current resulted in a reduction of the net alongshore transport rate by a factor 5 to 10.

Van Rijn (1997) found an alongshore varying contribution of tidal currents on the alongshore net transport rate. Near Noordwijk the tidal contribution to the total net alongshore transport rate was only 20% but this contribution increased to 40% further north near Egmond due to the larger tidal asymmetry here.

The presence of nearshore sandbars has a significant effect on the alongshore transport rate in the surf zone. Representation of the bars resulted in a 50% increase of the overall yearly-averaged longshore transport rate due to large transport peaks at the bar crests. This effect was less pronounced in profiles where small bars were present.

Van Rijn (1997) tested the influence of the wave climate on the longshore transport processes in the surf zone. This effect was simulated by assuming a 5° change of the local coastline orientation. This effect was small for profiles where the coastline orientation is relatively large (>15°) but larger for the profile near Egmond where the coastline orientation is about 8°. Changing the coastline orientation here by 5° (more waves from NW and less from SW) resulted in a 50% decrease of the net longshore transport rate from 600,000 to 300,000 m^3/year.

Van Rijn (1997) also tested the effect of wave climates of different years on the longshore transport rates in the surf zone. This effect was found to be profound, particularly in sections where the coastline orientation is relatively small (small angle to the north), such as near Egmond. Applying a wave climate from 1989 instead of that from 1994 resulted in a factor 20 difference in the net alongshore transport in the surfzone.

Comparison between Van Rijn (1997) and Roelvink & Stive (1990)
Van Rijn (1997) compared his sensitivity computations at profile 76 (Noordwijk) with those from Roelvink & Stive (1990). The CN-18 computation by Van Rijn (1997) is based on the Bailard-Bagnold transport formulations and is more or less comparable to the computation by Roelvink & Stive (1990).

The Van Rijn (1997) cross-shore transport component at NAP-20 m was 0 m^3/m/year, which is somewhat smaller than the value of 3 m^3/m/year reported by Roelvink & Stive (1990). The longshore component of the Van Rijn (1997) computation at NAP-20 m using the Bailard-Bagnold formulations is 32 m^3/m/year, which is much larger (factor 8) than the value of 4 m^3/m/year reported by Roelvink & Stive (1990). This latter discrepancy is likely related to the use of a more symmetrical tidal cycle by Roelvink & Stive (1990).

The Van Rijn (1997) cross-shore transport component at NAP-8 m was 30 m^3/m/year (computed using the Bailard-Bagnold transport model, unlike the values reported in Table 3.2 en Table 3.3), which is somewhat larger than the value of 20 m^3/m/year reported by Roelvink & Stive (1990). The longshore component of the Van Rijn (1997) computation at NAP-8 m using the Bailard-Bagnold formulations is about 5 m^3/m/year, which is somewhat larger (factor 2) than the value of 2 m^3/m/year reported by Roelvink & Stive (1990). As for the NAP-20 m transports, this latter discrepancy is likely also related to the use of a more symmetrical tidal cycle by Roelvink & Stive (1990).

The comparison between results from run CN-18 by Van Rijn (1997) and results from Roelvink & Stive (1990) is summarized in Table 5.4.

Table 5.4 Comparison of yearly-averaged total transport rates computed by Van Rijn (1997) run CN-18 and results from Roelvink & Stive (1990) for the Noordwijk transect.

	Yearly averaged transport based on Bailard Bagnold (m^3/m/year)			
	Cross-shore NAP-20 m	Cross-shore NAP-8 m	Alongshore NAP-20 m	Alongshore NAP-8 m
Van Rijn (1997) CN-18	0	30	32	5
Roelvink & Stive (1997)	3	20	4	2

5.2.3 Hydrodynamics, sediment transport and morphodynamics along the Dutch coast (Van der Werf & Giardino, 2009)

5.2.3.1 Introduction

Van der Werf & Giardino (2009) studied the effect of large scale sand extraction on the hydrodynamics, sediment transport and morphology along the Dutch coast. They validated their model based on yearly averaged alongshore transports between NAP -8 m and NAP +3 m similarly to Van Rijn (1997). The model showed good agreement with the earlier studies.

5.2.3.2 Approach

Van der Werf & Giardino (2009) set up a process-based 2D morphological model of the Dutch coast. The model is based on the Netherlands Coastal Model (see Section 5.3.7) and extended with a wave model and a sediment transport module. Van der Werf & Giardino (2009) forced their model with a so-called morphological tide that was derived based on the transport rates at ten transects along the Dutch coast (see also Tonnon *et al.*, 2009).

The flow grid resolution varies from about 75 m near the coast to 1500 m at deep water and varies in alongshore direction from 200 m to 1500 m. The wave model covers the same area as the Netherlands Coastal Model but has a coarser resolution (a cross-shore resolution between 150 and 4000 m and alongshore resolution between 300 and 6500 m). Boundary conditions were obtained from station Europlatform (EUR) located at xRD = 9963 m en yRD = 447601 m in a water depth of 32 m (see Figure 4.1). The wave data consisted of significant wave height $H_{1/3}$, significant wave period $T_{1/3}$, wave direction θ_{wave}, wind speed V_{wind}, wind direction θ_{wind} and storm surge every 3 hours for the period 1979-2001.

Wave data were clustered into 10 wave height classes from 0 to 5 m with 0.5 m intervals and 6 wave direction classes from 180° to 360° with 30° intervals. Wave input was reduced to 6 representative classes using the OPTI method (Van Duin *et al.*, 2004; Mol, 2007). The purpose of the OPTI method is to determine a smaller set wave conditions with which the tide- averaged sand transport based on all 60 conditions is well reproduced.

Van der Werf & Giardino (2009) applied a characteristic sand grain sizes of D_{50} = 215 µm with the Van Rijn (2007a,b) transport formulations and a bedload transport factor of 0.7, a suspended load transport factor of 0.7, a wave-related bedload transport factor of 1.0 and a wave-related suspended load transport factor of 0.3. The model did not include 3D effects or effects of salinity.

5.2.3.3 *Results*

Van der Werf & Giardino (2009) validated their model based on yearly averaged alongshore transports between NAP -8 m and NAP +3 m, similarly to Van Rijn (1997). Figure 5.3 shows the computed year-averaged alongshore transport rates between the NAP-8 and NAP+3 m depth contours from Hoek van Holland (118 km from Den Helder) to Den Helder. Positive longshore transport is directed towards Den Helder. This figure also contains the longshore transports in this zone from a number of other studies (see Van de Rest, 2004). The Van der Werf & Giardino longshore transports are in good agreement with earlier studies.

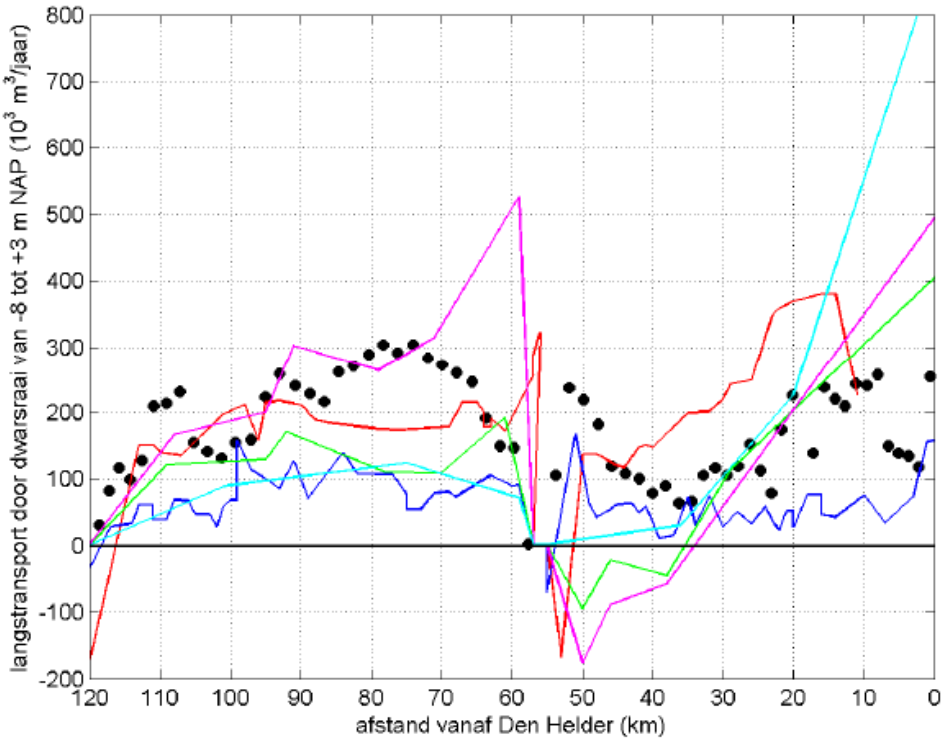

Figure 5.3 Yearly-averaged alongshore transport rates in the surfzone computed with the Van der Werf & Giardino (2009) model (black circles), and earlier studies. Red line: Steetzel & De Vroeg (1999), blue line: Roelvink (2001), magenta line: Van Rijn (1995), green line: Van Rijn (1995) adapted by Van de Rest (2004), cyan line: Stive & Eysink (1989). See also Van de Rest (2004). Figure taken from Van der Werf & Giardino (2009).

Van der Werf & Giardino (2009) illustrated the model results and the effects of large scale sand extraction based on effects on waves, tidal currents and sand transports. We will summarise the results here.

The wave height and, to a lesser extent, wave direction vary with the tidal phase. At low water, for example, the waves are generally somewhat lower because the water depths are lower and therefore the energy loss due to bed friction and wave breaking is larger. The tidal phase is of course not the same along the Dutch coast. Figure 5.4 Example of computed wave height and direction for the reference scenario 1. Figure taken from Van der Werf & Giardino (2009).
shows the computed significant wave height and average wave direction for the reference scenario. The moment shown is the situation near high water on the southwestern model boundary, low water at Noord Holland and near high water on the northeastern model

boundary. All of the following figures showing (differences in) wave heights are model results for the same tidal phase.

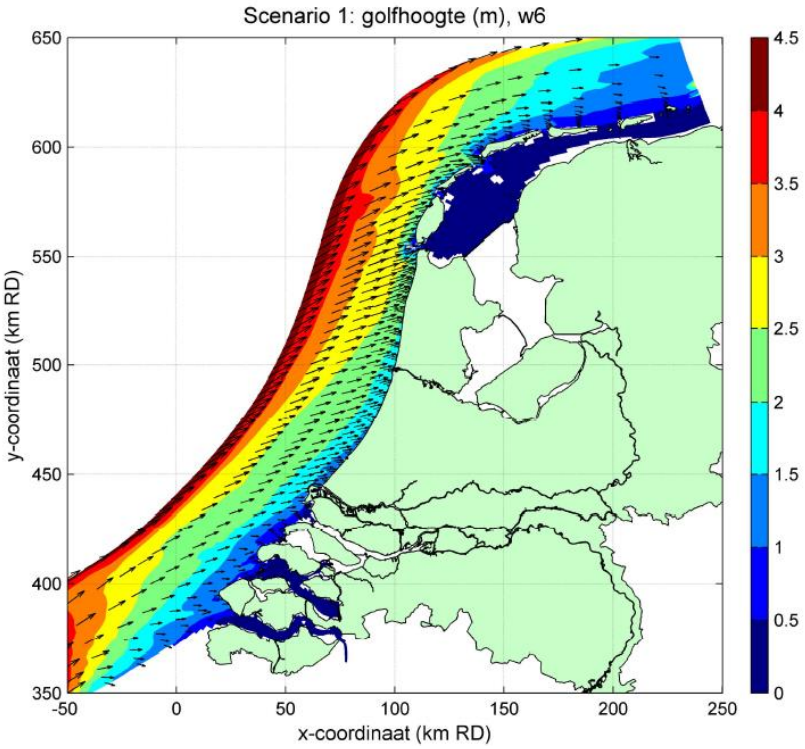

Figure 5.4 Example of computed wave height and direction for the reference scenario 1. Figure taken from Van der Werf & Giardino (2009).

Figure 5.4 shows how the wave height decreases by bed friction (dominant in deep water) and refraction (dominant in shallow water). It is also visible how wave refraction changes the propagation direction of the waves from deep to shallow water. The waves rotate towards the coast normal. Furthermore, it can be seen that the waves can hardly penetrate the Westerschelde, Oosterschelde and Wadden Sea, resulting in relatively low waves here (0-0.5 m).

Figure 5.5 shows the difference between the significant wave height computed for scenario 2 (sand extraction pit of 2 m) and scenario 1 (reference scenario). Red indicates an increase in wave height, blue a decrease. The black line indicates the sandpit boundary.

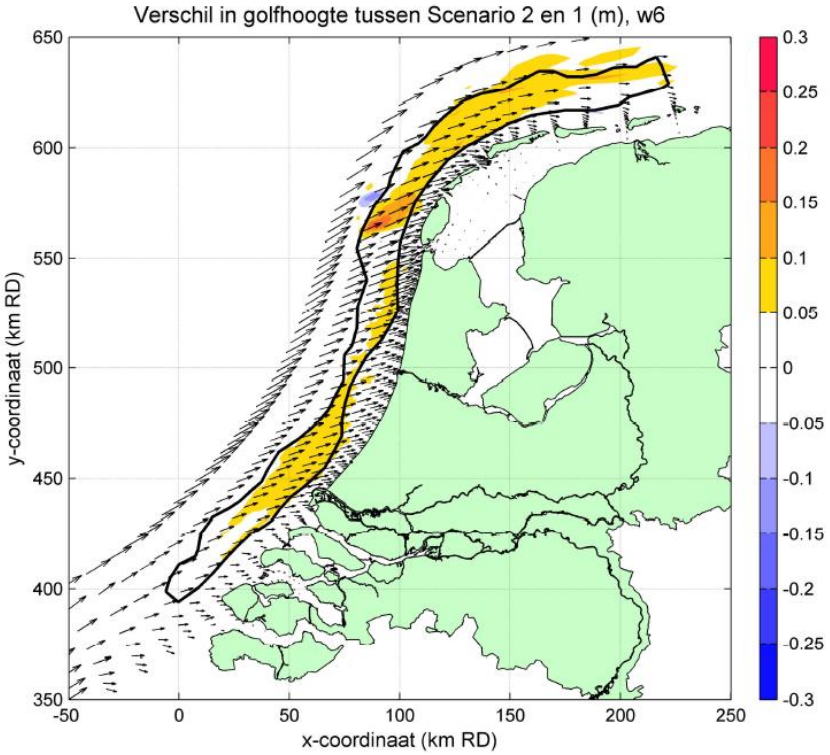

Figure 5.5 Difference in wave height between scenario 2 (sand extraction along the coast) and the reference scenario. Vectors show the wave direction for scenario 2. Figure taken from Van der Werf & Giardino (2009).

Figure 5.5 shows that large sandpit along the Dutch coast leads to an increase in wave height. This is because relatively less wave energy is dissipated by bed friction due to the increased water depth. This effect is the strongest at the sandpit and less important in the coastal area where wave breaking is the most important process for wave height reduction instead of bed friction. Seaward of the sandpit its effect is negligibly small, except for the area north of the Wadden Sea where the wave height increases. This is caused by wave refraction. In the deeper sandpit, waves can propagate faster, due to which the waves bend northward. This focuses the wave energy in these areas. This process depends on the wave direction.

The computations showed the following effect on the current velocities:

1 The flow accelerates just before the beginning of the sandpit due to flow contraction. The streamlines converge from the outside to the inside as the water in the sandpit can flow more quickly due to the smaller bed friction.
2 When the flow enters the sandpit, the flow rate decreases suddenly to compensate for the increased water depth (mass conservation).
3 Then the flow rate gradually increases in the sandpit given the decreased bed friction.
4 Then the flow rate decreases gradually towards the end of the sandpit. Mass conservation causes a sudden increase at the end of the sandpit, after which the flow rate gradually decreases to the undisturbed value.

Van der Werf & Giardino (2009) also studied how the balance of the coastal foundation of the entire Dutch coast was affected by the construction of a sandpit, see Figure 5.6. The sand balance is largely determined by the changes of cross-shore transport components.

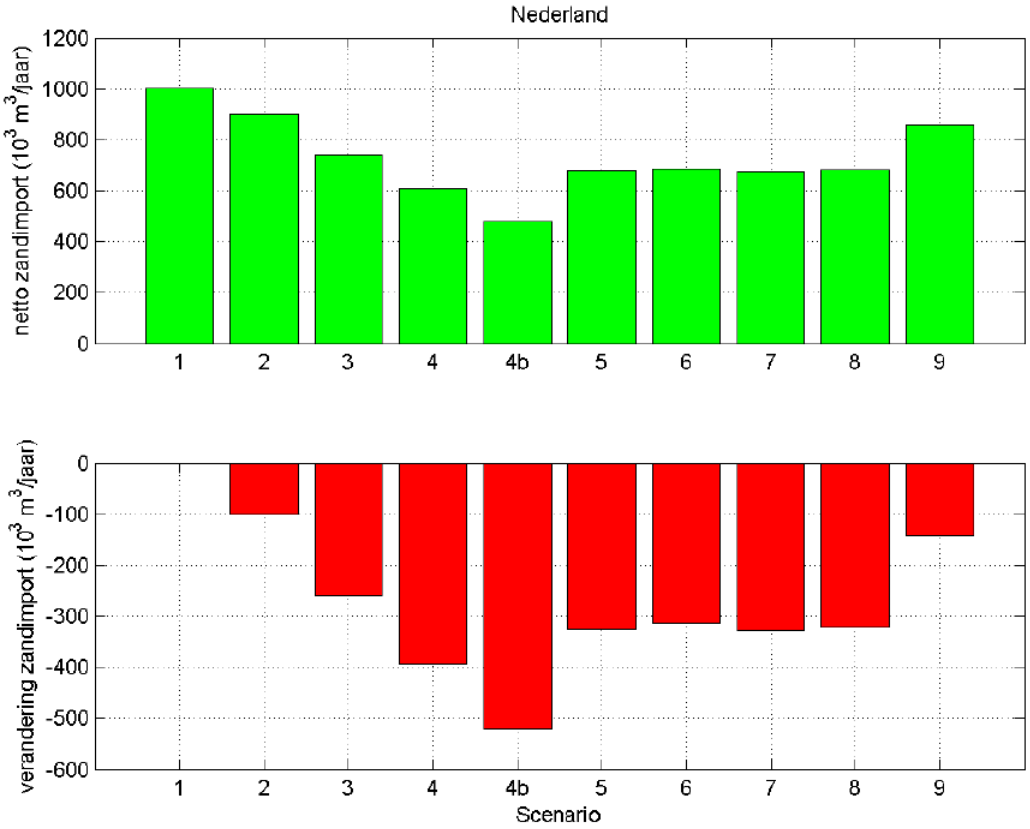

Figure 5.6 Net sand import and effect of sandpit scenario on Dutch coastal foundation. Figure taken from Van der Werf & Giardino (2009).

The sandpit initially resulted in a maximum decrease of the sand imports of 1.0 x 10^6 m^3 / year (Scenario 1, reference situation) to 0.6 x 10^6 m^3 / year (Scenario 4, 12 m deep sandpit), or approximately 40%. Initially, sand will be trapped in the sandpit. This effect increases with the depth of the sandpit. The most realistic sandpit scenarios (2 and 9) result in an approximately 10% decrease in sand imports. Furthermore, the computations show a non-negligible effect of the flow boundary conditions (Scenarios 4 and 4b). The one scenario used flow boundary conditions from the ZUNO-fijn model with and the other without a 12 m deep sandpit along the Dutch coast.

5.2.3.4 *Large-scale morphological model of the Holland coast and Western Wadden Sea (Van der Hout et al., 2009)*

5.2.3.5 *Introduction*

Van der Hout *et al.* (2009) developed a large-scale 2DH morphological model for the Holland coast and the Western Wadden Sea. The model was developed with the Roelvink *et al.* (2001a,b) model as a starting point. Differences are the Delft3D version, the hydrodynamic boundary conditions, the morphological updating scheme, the sediment transport formula and some parameter settings.

5.2.3.6 *Approach*

The model developed by Van der Hout *et al.* (2009) is about 60 km wide and about 220 km long. It comprises of 200x233 grid cells in Cartesian Rijksdriehoek coordinates (Figure 5.7). The cross-shore grid size in the surf zone varies from 100 m to 22 m. This is accurate enough

to represent the wave driven sediment transport. The average number of grid cells in the surf zone varies between 15 at the South-Holland coast and 8 at the North-Holland coast. The alongshore grid size in the surf zone varies between 260 m and 1000 m. The grid is relatively coarse in the Marsdiep Inlet varying in size between 800 m and 1200 m.

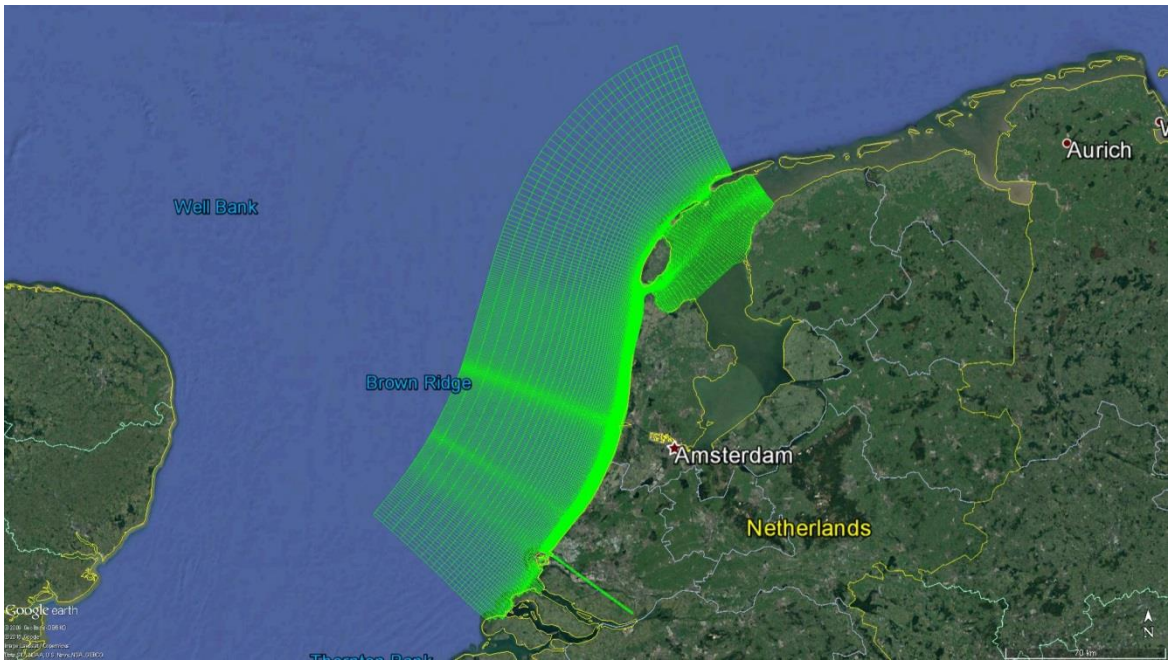

Figure 5.7 Model grid of the large-scale morphological of the Holland coast and Western Wadden Sea.

The model was forced by current velocities along the southern boundary and tidal water levels along the three other open boundaries. The tidal boundary conditions comprise of a 30 days spring-neap cycle defined by 39 astronomical components.

The boundary conditions include the long term averaged discharge volumes in m^3/s through the two sluices at both ends of the Afsluitdijk and through the Rotterdam Waterway. The large size of the model did not allow including secondary effects such as salinity and 3D circulation, to have a relatively fast model at the same time.

Van der Hout *et al.* (2009) selected morphologically representative wave conditions by schematising the wave climate of the YM6 station (IJmuiden Munitiestortplaats, see Figure 4.1) in directional sectors of 30º and determining low (H_s < 2 m) and high (H_s > 2 m) morphologically representative wave conditions by weighing the wave heights to the power 2.5 by their probability of occurrence. The wave period, wind speed and direction corresponding with the morphological wave conditions were selected from time series of measured data by computing the average wave period, wind speed and direction for each wave height and direction class.

Van der Hout *et al.* (2009) applied the Van Rijn (2007a,b) sediment transport formulations in Delft3D, a median grain diameter for sand of 250 µm and uniform bed roughness with a Chézy value of 65 $m^{1/2}/s$. For morphological updating, Van der Hout *et al.* (2009) apply the advanced parallel online method also referred to as MorMerge (Roelvink, 2006). Van der Hout *et al.* (2009) applied a simulation period of 10 years without dredging or nourishments. The morphological acceleration factor was set to 120, with values ranging between 1 and 25 for the different wave conditions because of the individual weight factors.

5.2.3.7 Results

The predicted hydrodynamics and sediment transport along the Holland Coast and the Texel Inlet compared quite well with reference studies (Van de Rest, 2004; Elias, 2006). The morphological development is somewhat overestimated, but the general pattern around the Texel Inlet compared well with the Vaklodingen bathymetry measurements.

The model was applied to study the morphological effects of mega nourishments. Four locations on the North Holland coast and the Texel Inlet were examined with mega nourishments of 5 million m^3/year for 10 years and two locations were examined for 10 years after a nourishment of 50 million m^3. Van der Hout *et al.* (2009) computed the effects of these nourishments and found them to not disappear but diffuse in 10 years up to two kilometres due to their influence on the local hydrodynamics. They conclude that a mega nourishment does no trigger the system to change the import of sediment into the Marsdiep tidal basin but that nourishment of the Noorderhaaks shoal or the Texelstroom tidal channel do have advantages on future development of the Marsdiep Delta. Van der Hout et al. (2009) note that a 2D model setting underestimates the cross-shore transports.

5.2.3.8 Recommendations

Van der Hout *et al.* (2009) recommended applying Neumann boundaries on the southern and eastern open boundaries with multiple sections when applying varying wave and wind conditions to limit the effect of inconsistent combination of prescribed water levels with different wind and wave fields. In addition, they recommended deriving a morphological time span, representative for the sediment transport in both shallow and deep water for the entire Dutch coastline (previously done only for deep water).

5.2.4 Sediment transport along the Holland shoreface (Knook, 2013)

5.2.4.1 Introduction

Knook (2013) analysed cross-shore sediment transport rates at various depths on the lower shoreface of the Central Holland coast to investigate the influence of bed profile perturbations shoreward of NAP-20m and to validate the scientific foundation of the NAP-20m depth contour. The analysis was based on computations with the Unibest-TC model, applying the Van Rijn (1993) sediment transport formulations.

5.2.4.2 Approach

Knook (2013) set up Unibest-TC models to compute the cross-shore transport at various depths on the shoreface. Dominant processes were identified by making sensitivity runs varying wave heights, wave periods, grain sizes, shoreface slopes and Longuet-Higgins streaming. Knook (2013) did not include density effects.

To assess the relative contribution of different transport modes (bedload and suspended load) and the contribution of different wave classes, Knook (2013) schematised the wave and tidal conditions into discrete classes with accompanying frequency of occurrence.

Knook (2013) applied a D50 of 200 µm and made transport computations for the coastal profile of Noordwijk for conditions with waves only and conditions with waves and tidal currents. The wave climate in front of the coast of Noordwijk was used. The tidal elevation and the gradient of the horizontal tide were derived from tidal stations at Scheveningen and IJmuiden.

5.2.4.3 *Results*

Knook (2013) showed histograms of transport rates per wave class multiplied with the frequency of occurrence per wave class for the depth contours NAP -25 m, NAP -20 m, NAP -15 m, NAP -10 m and NAP -5 m.

For waves only, the computations by Knook (2013) show net cross-shore transports rates that are nearly always onshore directed and dominated by relatively calm conditions as these occur relatively frequently. Knook (2013) attribute this to Longuet-Higgins streaming and wave related suspended load transport. However, density effects were not taken into account.

For conditions with waves and tidal currents the computations show net cross-shore transport rates that are nearly always offshore directed between NAP -25 m and NAP -10 m and onshore directed at NAP -5 m. Knook (2013) finds tide at relatively large water depths to produce an offshore transport, which to some extent is a surprising result and might be related to the schematization and forcing method.

Knook (2013) concluded that an onshore transport on the upper shoreface and offshore transport on the lower shoreface induce a lower shoreface flattening and an upper shoreface steepening.

5.3 Available numerical models

5.3.1 Introduction

Here we discuss recently developed state-of-the-art models (since 1995) available at Deltares to simulate hydrodynamic processes on the Dutch lower shoreface. These models can either be applied to generate boundary conditions for more detailed models or developed further into sediment transport models.

5.3.2 Dutch Continental Shelf Model (DCSMv5)

The 2DH Dutch Continental Shelf Model (DCSM) comprises the continental shelf from 48° North to 62.25° North and 12° West to 13° East. The southern boundary is located near Brest in France and the northern boundary near Ålesund in Norway. The eastern boundary lies near Copenhagen in Denmark and Malmö in Sweden. The seaward boundary follows the edge of the continental slope. Figure 5.8 shows the model grid. The present version is Simona-DCSM-v5 (Gerritsen *et al.*, 1995). The effects on water levels of time-dependent baroclinic pressure gradients (e.g. due to the Rhine Region of Freshwater Influence (ROFI) and salinity intrusion in rivers and estuaries) are essentially much smaller than the dominating tide and surge signals in coastal regions and were therefore not included in the DCSMv5 model.

The grid is defined in spherical coordinates and consists of 201x171 grid cells. The resolution is 1.8° in longitudinal (west-east) direction and 12.1° in lateral (south-north) direction. From south to north this corresponds to 9.3 to 6.5 km in the west-east direction and 9.25 km in the south-north direction.

The model is forced with 11 tidal constituents at the boundaries and spatially and temporally varying wind en pressure fields. The model has been applied for storm surge forecasting in the Netherlands. DCSM was originally developed in the 1980s and has been through numerous improvements since then. Besides works on improving the wind input (e.g. from a 55- to 11-km-resolution HIRLAM model), a series of studies focused on model sensitivity analysis, parameter estimation and model calibration (Ten Brummelhuis *et al.*, 1993;

Mouthaan *et al.*, 1994; Heemink *et al.*, 2002). The last calibration was performed in 1998 using an adjoint method (Philippart *et al.*, 1998). It was concluded that, with the model resolution of approximately 8–9 km and the quality of the bathymetry information available at the time, further improvement should not be attempted (Verlaan *et al.*, 2005). For the development of DCSMv5, see (Verboom *et al.*, 1992; Philippart *et al.*, 1998; Flather, 2000; Verlaan *et al.*. 2005).

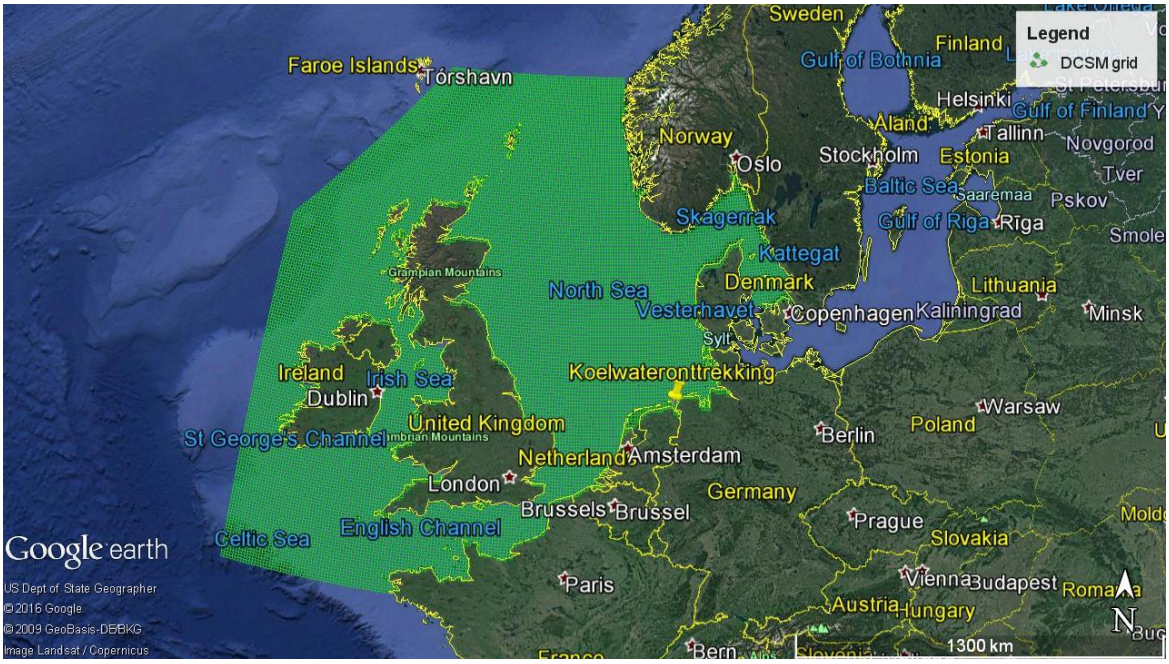

Figure 5.8 Dutch Continental Shelf Model grid

5.3.3 Southern North Sea Model (SNSM; ZUNOv3)

The 2DH Southern North Sea Model (in Dutch: Zuidelijke Noordzeemodel) covers the southern North Sea and the English Channel from Aberdeen (Great Britain) - Hanstholm (Denmark) in the north and Bournemouth (UK) - Cherbourg (France) in the south-west. The present version is Simona-ZUNO-1999-v3.

The grid is defined in Cartesian Rijksdriehoek coordinates and consists of 485x169 grid cells. The grid resolution varies between 4.5 and 6 km along the English and Scottish coast, 2.5 to 4 km in the English Channel and German Bight and 1 to 2 km along the Dutch coast (Figure 5.9).

The model is forced by water levels along the sea boundary derived from the Dutch Continental Shelf (DCSM) model. In addition, the model is also driven with spatially and temporally varying wind and pressure fields. River and sluice discharges are imposed as point discharges. Salinity effects were neglected.

The model average standard deviation of water levels has been determined for a 24-hour forecast for the period 22 June 2008 to 22 September 2008. These data have been obtained from MATROOS, a database containing, among other things, calculated water levels and flow velocities of the operational predictive model train (Nautboom). The average RMSE value, derived from 20 main stations for the above-mentioned period, in the ZUNO model is 0.099 meters.

The model has often been applied for water quality computations and suspended particle matter (SPM) predictions in the Dutch coastal zone (e.g. Blaas et al. 2012) and to create the so-called ZUNO StroomAtlas (Dutch) to have accurate flow information for efficient and safe shipping in the Southern North Sea.

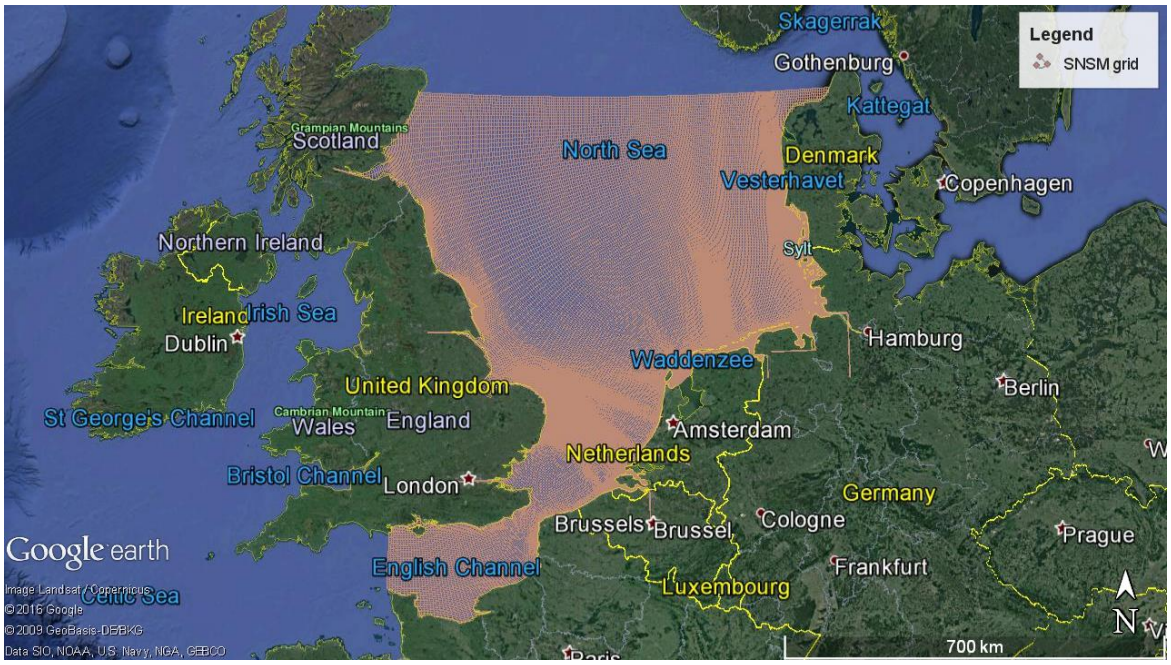

Figure 5.9 Southern North Sea Model grid

5.3.4 Improved Dutch Continental Shelf Model (DCSMv6)

Zijl *et al.* (2013, 2015) constructed a new generation 2DH tide–surge model for the northwest European Shelf with improved tide and surge representation using satellite altimeter data and data assimilation techniques to reduce parameter uncertainty. Salinity effects were not included.

The grid is specified in geographical coordinates (WGS84) and covers the area between 15° W and 13° E and 43° N and 64° N. The spherical grid has a uniform cell size of 1.5′ (1/40°) in east–west direction and 1.0′ (1/60°) in north–south direction, which corresponds to a grid cell size of about 1.8×1.8 km, yielding approximately 10^6 computational cells. The grid resolution is a factor five finer than the existing, currently operational DCSMv5 model grid.

At the northern, western and southern sides of the model domain, open water-level boundaries are defined. The imposed water levels at the open boundaries can be split into a tidal and non-tidal part. The tidal water levels at the open boundaries are specified in the frequency domain, i.e. the amplitudes and phases of 22 harmonic constituents are specified.

For meteorological surface forcing the model uses time- and space varying wind speed (at 10 m height) and air pressure (at MSL) provided by the Numerical Weather Prediction high-resolution limited area model (HiRLAM). These data are provided (operationally) by the KNMI (Royal Dutch Meteorological Institute).

5.3.5 Improved Dutch Continental Shelf Model and Southern North Sea (DCSMv6-ZUNOv4)

Zijl (2013) constructed the 2DH DCSMv6-ZUNOv4 model to replace the existing operational model train for water level predictions in Dutch coastal waters. DCSMv6-ZUNOv4 is based on DCSMv6, but with a refinement in de southern North Sea and Dutch coastal waters. Salinity effects were not accounted for.

The main reason for the development of DCSMv6-ZUNOv4 alongside DCSMv6 is that in DCSMv6 resolution is lacking in the inland areas of Dutch coastal waters (e.g. Wadden Sea, Eastern Scheldt, Western Scheldt and Ems-Dollard Estuary). The increased resolution of DCSMv6-ZUNOv4 in these areas offers the prospect of improved water level representation there.

The DCSMv6-ZUNOv4 model consists of two separate grids, coupled by means of horizontal domain decomposition. The outer part of the model is covered by the DCSMv6 model grid, with the part covering the Southern North Sea and English Channel cut out (the blue part in Figure 5.10 Overview of the DCSMv6-ZUNOv4 hydrodynamic model grids, with the DCSMv6 domain in green and the ZUNOv4 domain in blue. The red, dashed lines represent the internal coupling boundaries.). This cut-out part, i.e., the inner domain, is covered by the ZUNOv4 model grid (the red part in Figure 5.10). At the internal coupling boundaries a variable factor (1:1 to 1:4) of refinement between the two adjacent grids is applied.

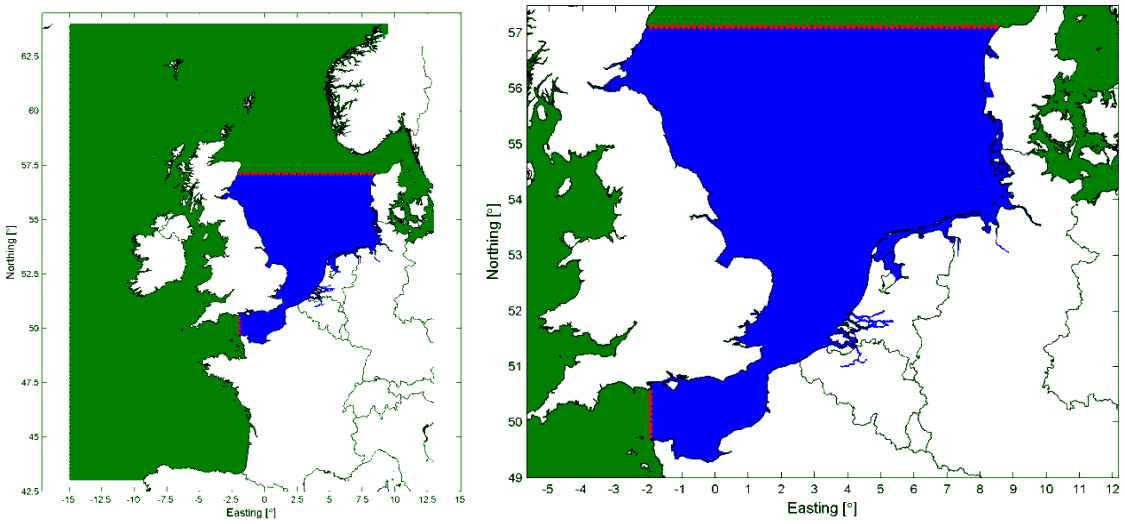

Figure 5.10 Overview of the DCSMv6-ZUNOv4 hydrodynamic model grids, with the DCSMv6 domain in green and the ZUNOv4 domain in blue. The red, dashed lines represent the internal coupling boundaries.

The ZUNOv4 model grid is based on the ZUNOv3 grid, converted to WGS84 geographical coordinates. The northern extent was moved southward to more shallow water, to ensure a more robust domain decomposition coupling. Furthermore, at the northern and English Channel boundary, the grid lines have been adjusted to ensure a proper coupling to the DCSMv6 model grid.

The grid resolution of the ZUNOv4 model varies between 4.5 and 6 km along the English and Scottish coast, 2.5 to 4 km in the English Channel and German Bight and 1 to 2 km along the Dutch coast.

The DCSMv6-ZUNOv4 model contains four movable barriers and four sluice complexes. The four barriers (Maeslant Barrier, Hartel Barrier, Eastern Scheldt Barrier and Ems Barrier) are open under normal conditions. Closure only takes place when extreme water levels are expected. The closure procedure depends on local circumstances and is different for each barrier. In DCSMv6-ZUNOv4 closures can be prescribed by specifying time series of gate levels. The closure of the Maeslant Barrier, Hartel Barrier and Eastern Scheldt Barrier on 8-9 November 2007 is taken into account in the calibration and validation computations of DCSMv6-ZUNOv4.

The four sluices are used to periodically discharge fresh water into the North Sea and Wadden Sea. Three of the four sluices complexes in the model are assumed to be permanently closed. The operations of the fourth sluice complex, the Haringvliet Sluices, are modelled according to the LPH'84 table, which implies that the openings depend on the instantaneous water level difference over the sluices as well as the upstream discharge rate of the River Waal.

Discharges are prescribed at eight locations in DCSMv6-ZUNOv4 to represent rivers or sluice complex. Most discharges consist of daily values from the MATROOS database. Only at Hagestijn (river Lek) and Tiel (river Waal) hourly values are used. At location Eems and location Schelde constant values of 80 m^3/s and 300 m^3/s are prescribed.

Computing one year with DCSMv6-ZUNOv4 takes about 4 days on 24 parallel 3.6 MHz CPUs. Computing one day takes approximately 16 minutes.

Zijl (2013) compared the DCSMv6-ZUNOv4 and DCSMv6 models, and showed that on average the quality of the water level representation increased with respect to all of the above Goodness-of-Fit criteria. The quality improvement was especially apparent in the Dutch estuaries (Western Scheldt, Eastern Scheldt and Ems-Dollard) and Wadden Sea.

5.3.6 Delft3D-FM North Sea model

Zijl (2017) constructed an improved 3D Delft3D-FM North Sea model to make water level and also water quality predictions in Dutch coastal waters. The model is based on DCSMv6, but with an upgraded flexible resolution grid making it 3-4 times faster. Figure 5.11 shows the model grid. The horizontal grid resolution is about 1.8 km along the Dutch coast. The 3D model consists of 25 equidistant σ-layers in the vertical with a k-ε turbulence model; the model includes effects of salinity and temperature.

Figure 5.11 Delft3D-FM North Sea model grid.

Figure 5.12 shows examples of the computed salinity (left) and temperature (right). The model accurately represents the observed salinities distributions. Figure 5.13 shows the comparison for a transect offshore off Noordwijk. Figure 5.14 shows the root-mean-square error between computed and observed high waters along the Dutch coast. The model accurately represents the water levels along the Dutch coast.

There is model output available for more than 20 years of hindcast. The computational time for 1 year is about 1 day on 10 nodes with 40 cores in total.

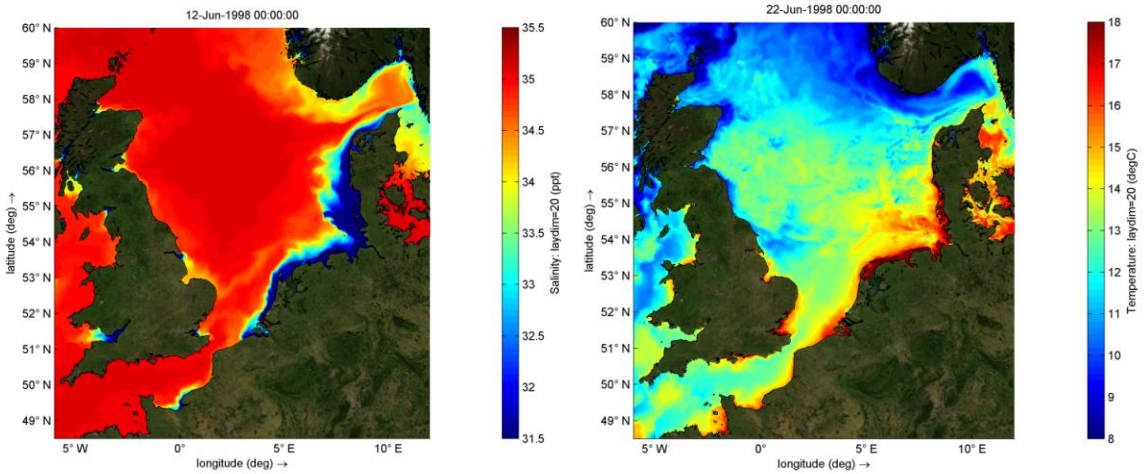

Figure 5.12 Examples of salinity (left) and temperature (right) computed with the Delft3D-FM North Sea model.

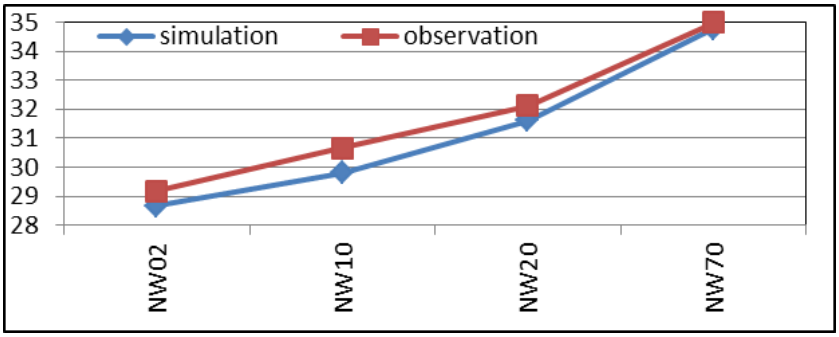

Figure 5.13 Computed and observed salinities (PPT) along a transect offshore off Noordwijk.

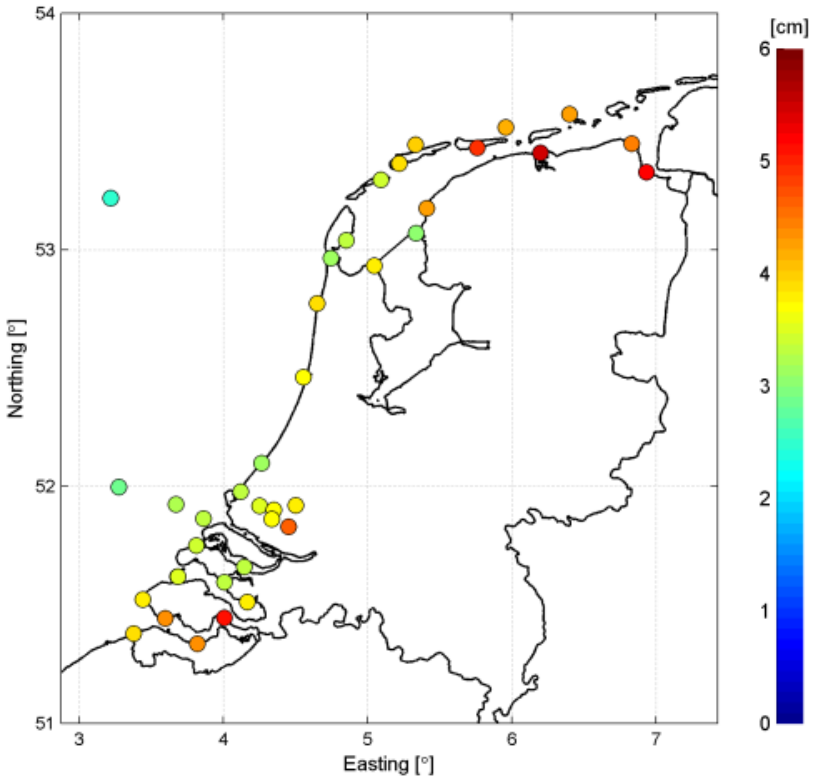

Figure 5.14 Root-mean-square-error between observed and computed high waters.

5.3.7 Netherlands Coastal Model (NCM)

The Netherlands Coastal Model (in Dutch: Nederlands Kuststrookmodel) covers the entire Dutch coast from the Belgian-French border in the east up to 50 km east of the Dutch-German border, near the German island Norderney. It is a 2DH model; salinity effects are not included. The grid extends seaward to about 60 to 70 km offshore. Figure 5.15 shows the Netherlands Coastal Model grid. The present version is Simona-Kuststrook-fijn-1999-v4.

The grid is defined in Cartesian Rijksdriehoek coordinates and consists of 941x401 grid cells. The resolution varies strongly. It is about 300-800 m alongshore and 1.5-2.5 km cross-shore along the western boundary. Towards the coast the grid cells are squarer with a resolution of 300 to 400 m, which is finer than in the DCSMv6-ZUNOv4 model.

In the Wadden Sea, the IJsselmeer and in the Ems-Dollard estuary the resolution of the NCM is about 300 m. In the Rotterdam Waterway it is about 250 m. In the Oosterschelde and Westerschelde the resolution is around 200 m. The rivers are captured with two to four grid points across the width of the main channel and while the grid size in the flow direction is 200 to 300 m.

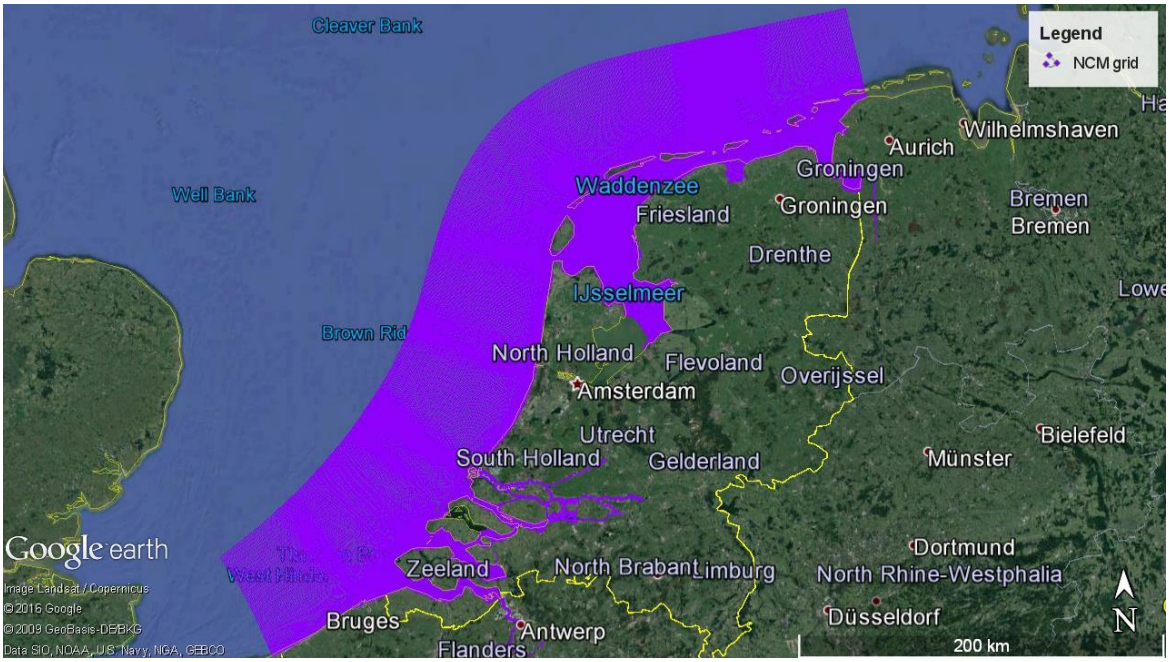

Figure 5.15 Netherlands Coastal Model grid.

The model is forced with water levels or Riemann invariants along the sea boundary and discharge for the river Lek, Waal and Maas boundaries. The sea boundary conditions are derived from the Southern North Sea Model. Sluice discharges can be controlled by water levels or by imposing time series in discharge points.

The model average standard deviation of the water levels has been determined for a 24-hour forecast for the period from 22 June 2008 to 22 September 2008. These data are obtained from MATROOS, a database which includes calculated water levels and flow rates of the operational predictive model train (Nautboom). The average RMSE value, derived from 13 main stations for the coastal strip-fine model is 0.095 m.

5.3.8 PACE model

In the framework of the PACE project, Duran-Matute *et al.* (2014) constructed a Wadden Sea 3D numerical model system carefully calibrated to observational data sets of sediment concentrations and other key parameters. The system consists of various models (e.g. GETM, Delft3D) which interact on a modular basis, coupling abiotic processes to biotic processes.

A rectangular domain rotated in the anticlockwise direction with respect to the east–west axis was defined with its corners located at (4.4693E, 52.4975N); (4.0260E, 53.3269N); (6.3871E, 53.7607N); (6.7896E, 52.9232N), see Figure 5.16 Numerical model domain and bathymetry of the PACE model. Figure taken from Duran-Matute et al. (2014).. Within this domain, an equidistant grid with a 200m resolution using the Rijksdriehoek projection was defined. The Delft3D model has 10 vertical computational sigma-layers, 10% of the water depth each.

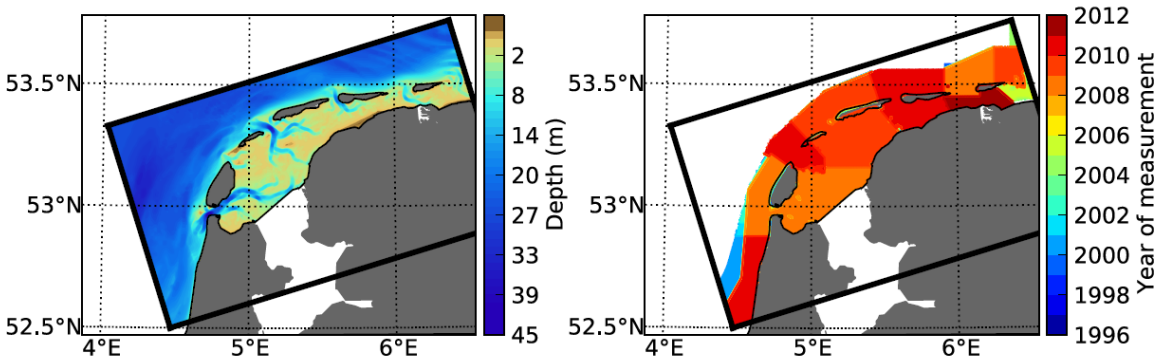

Figure 5.16 Numerical model domain and bathymetry of the PACE model. Figure taken from Duran-Matute et al. (2014).

The depths were determined from the netCDF-CF-OPeNDAP version of the 20m RWS vaklodingen provided by OpenEarth, interpolated in space-time with OpenEarthTools. For the GETM stability some smoothing was required, which has been kept for Delft3D-FLOW (even though not needed).

The model input was configured to produce a hydrodynamic database for Delft3D-WAQ. The model was set-up in the German GETM model system comparable to Delft3D-FLOW, and was automatically converted to Delft3D-FLOW input.

At the open boundaries of the numerical domain, boundary conditions for the sea surface height (SSH), vertically integrated velocities, and vertical profiles of salinity and temperature were applied. On the watershed at the eastern boundary (south of Rotummerplaat), a wall was placed since it is difficult to match the position of the channels in this region with the boundary conditions. The vertically integrated velocities and sea surface elevation at the boundaries were taken from results of a two-dimensional model with data assimilation ran by Rijkswaterstaat to predict the SSH along the Dutch coast (Plieger, 1999; Verlaan and Heemink, 1998). Salinity and temperature at the boundaries were obtained from simulations with a set of nested setups. The simulations for these setups were performed with GETM. The usage of boundary conditions from two different models might cause slight inconsistencies. However, due to data assimilation, the Rijkswater tide/surge model shows a superior accuracy in the tidal and intra-tidal variability. For the 2 Afsluitdijk sluices high-frequency (10m) discharge data have been generated using data from sluice openings. Lake Lauwersmeer has been added and from waterboards small sluices were gathered.

The rise or decline of the Wadden Sea floor was inferred from the sedimentation and erosion fluxes computed by the sediment model and compared to the existing direct observations of bed level change. The overall model system was analysed for sensitivity on climate parameters such as net precipitation, storm patterns and temperature rise to project the present-day situation into the next century. Maps of net erosion and net accumulation were drawn for the various different present and future situations, to show the intertidal areas with increased risk for drowning.

Results of the simulations were compared with several observational data sets namely: (1) sea surface height (SSH) measurements at 14 tidal stations, (2) time series of salinity and temperature at one station with 30 min temporal resolution, and (3) gross transport through the Texel Inlet as measured by the ferry across the Texel Inlet. In all cases, the accuracy

of the simulations are quantified using the coefficient of determination R^2 and the root-mean-square (rms) error ϵ_{rms} obtained by comparing the measured data and the simulated data.

Figure 5.17 shows the position of the tidal stations, and the amplitude and phase lag (in minutes with respect to Greenwich) for the M2 tidal constituent, which is the dominant tidal constituent in the region. Station numbers from 1 to 4 correspond to stations in the North Sea; station numbers from 5 to 11 correspond to stations inside the WDWS; and numbers from 12 to 14 correspond to stations in the eastern Dutch Wadden Sea (EDWS). The tidal wave travels along the Dutch coast from Southwest to Northeast with a (measured) phase lag of 262 min in station 1 to 475 min at station 4. In other words, it takes about 3.5 h to travel from station 1 to station 4. In general, a good agreement is found between the measured and the simulated characteristics of the M2 component. All stations had an error in the M2 amplitude between 2% to 12% and an error in phase between −1 min and −20 min (0.2–3% of the tidal period). More details can be found in the paper by Duran-Matute *et al.* (2014).

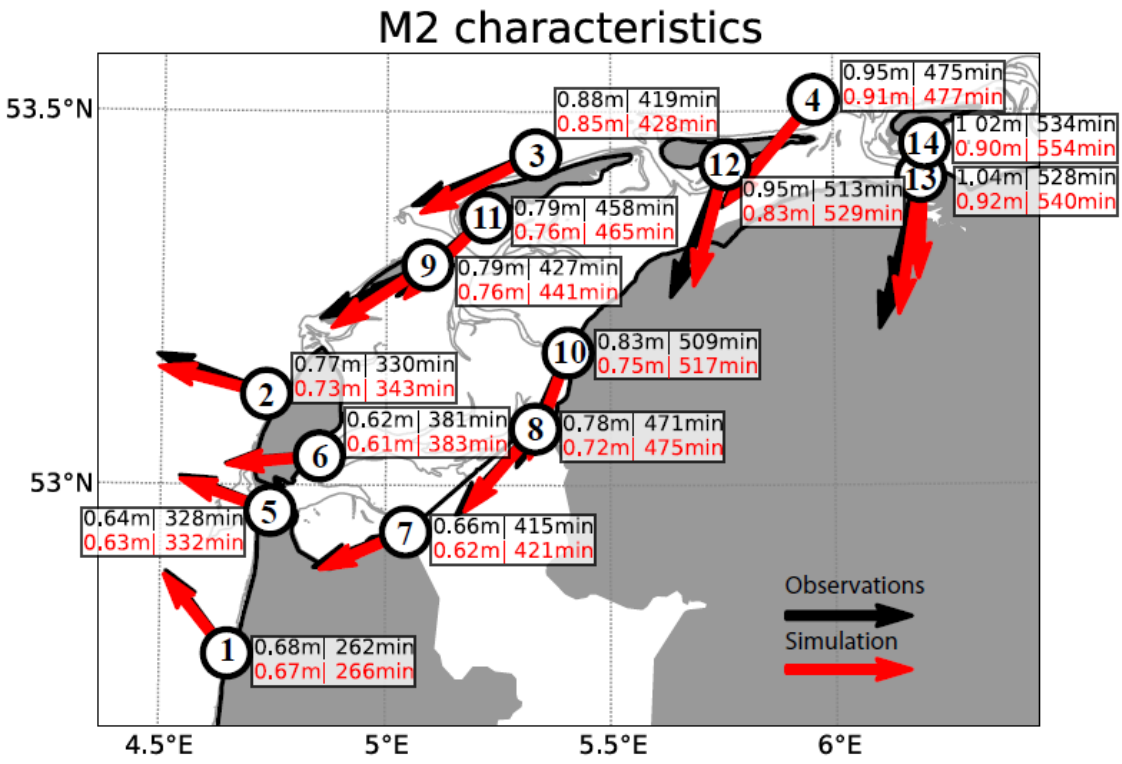

Figure 5.17 Comparison between the simulated and observed characteristics of the M2 tidal constituent at the 14 tidal stations in the domain. The position of each station is represented by a black circle, and the number inside the circle serves to identify the station. The length of the arrow represents the amplitude of the M2 tidal constituent, and the angle of the arrow represents its phase lag in degrees. The numerical values for the amplitude and the phase lag (in minutes with respect to Greenwich) are presented next to every station both for the observations and the simulation. Figure taken from Duran-Matute et al. (2014).

5.3.9 Submodels to study changes in sediment transport patterns (Van der Spek *et al.*, 2015)

Van der Spek et al. (2015) applied existing 2D flow and sediment transport models in Delft3D to study changes in the sediment transport patterns caused by bed level changes and sea level rise. Van der Spek et al. (2015) worked with existing submodels for the Wadden Sea, the central Dutch coast, the northern delta area and the southern delta area, to address the relevant morphological development per area. This was done by simulating (1) the present situation, (2) the expected situation over 20 years (bottom 2035) and (3) expected situation after 100 years (bottom 2100).

Based on these different bathymetries, computations were made of the water motion and sediment transports along the coast. By comparing the sediment transport patterns for the current situation, the extrapolated situation in 2035 and the scenarios for 2100, the effects of the expected morphological development on the sediment transport patterns were derived. Figure 5.18 Computed transport vectors in the Wadden Sea and the tidal deltas in the present situation. Figure taken from Van der Spek et al. (2015).
shows an example of computed transport vectors in the Wadden Sea and the tidal deltas in the present situation. Figure 5.19 shows the computed transport vectors in de Amelander Inlet for the present situation, 2035 and 2100.

Comparison of the sediment transport patterns gave an indication of the expected changes in both location and size of sedimentation and erosion along the coast. No detailed computations of bed level changes were made. No model calibration was performed as the interest was primarily focusses on the differences between the morphological situations of the coast to be simulated.

The conclusions of the study were that the effects of the expected morphological changes between now and 2035 are relatively small, that there is no reason to expect a distinctly different erosion pattern or volume and that the expected morphological changes do not give rise to adaptation of the current annual nourishment volume. Computations with a higher sea level showed major seabed changes in the Wadden area.

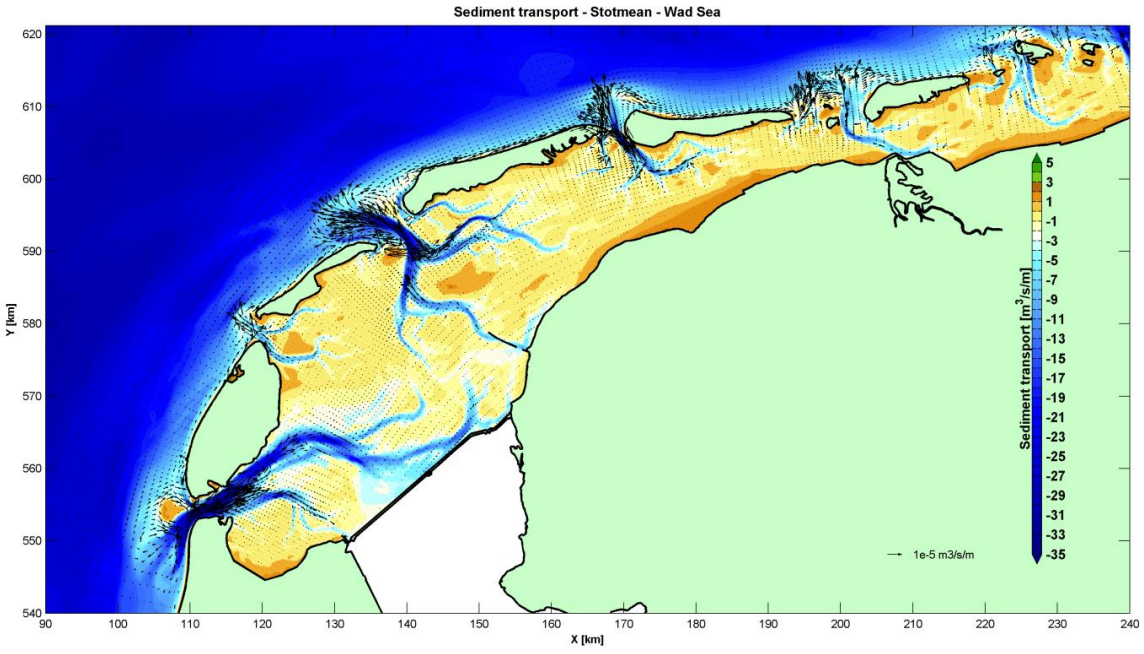

Figure 5.18 Computed transport vectors in the Wadden Sea and the tidal deltas in the present situation. Figure taken from Van der Spek et al. (2015).

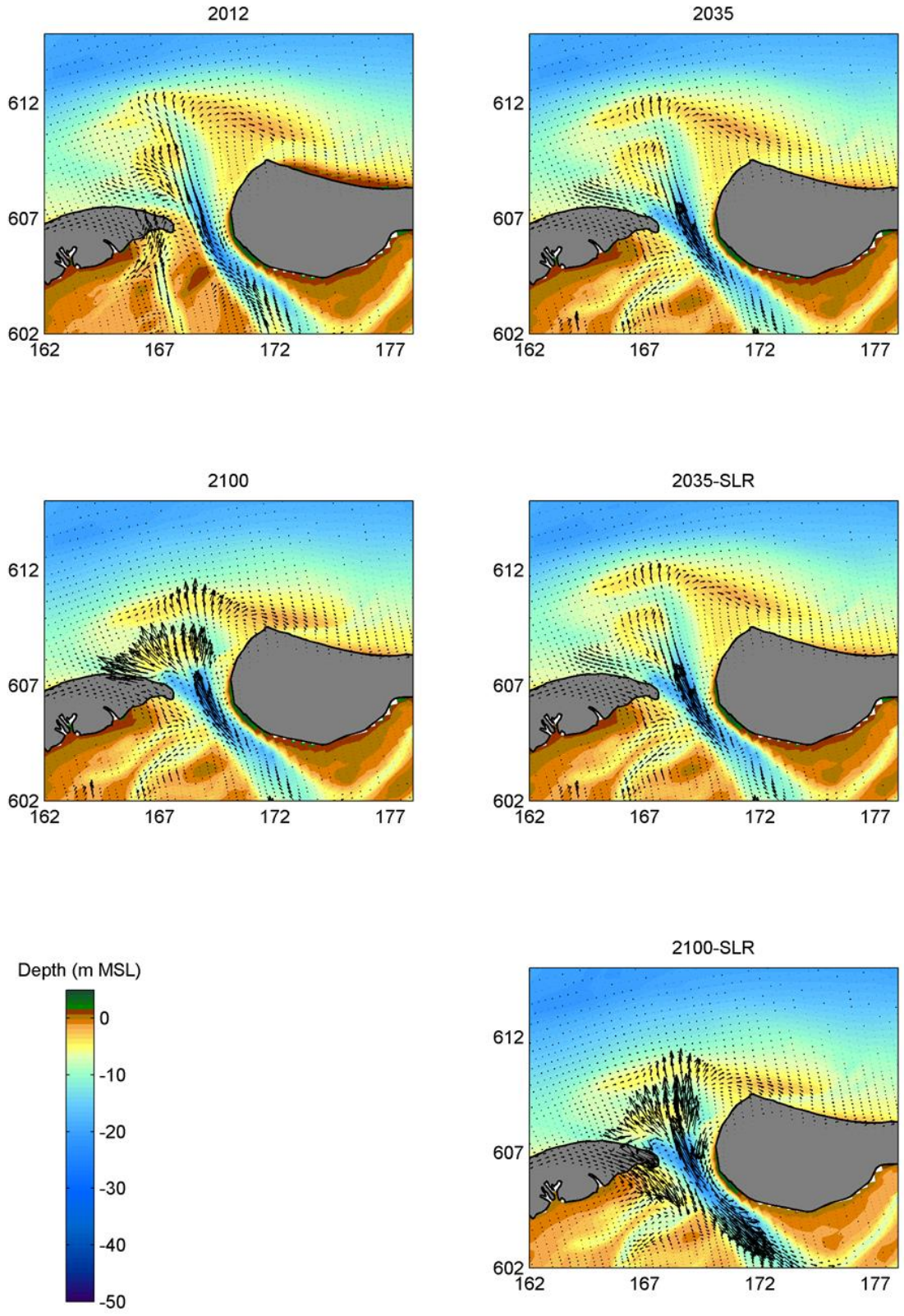

Figure 5.19 Computed transport vectors in the Amelander Inlet for the present situation, 2035 and 2100

5.3.10 Operational wave model Dutch North Sea

An operational SWAN wave model of the North Sea has been set-up by Gautier (2012) to provide wave forecasts focusing on the Dutch coast. The model consists of two grids (Figure 5.20). The first grid (G1) is regular and covers a large domain based on the Dutch Continental Shelf Model (DCSMv6) but somewhat smaller and with four times less resolution (cell size about 3.6 km x 3.6 km). The second grid (G2) is curvilinear and covers almost the Southern North Sea model (ZUNOv4) grid, except for the rivers, the Wadden Sea and the northern 200 km. Grid G2 is nested in the G1 grid, i.e. it gets the wave boundary conditions from the G1 SWAN grid. The G1 grid gets the wave boundary conditions from the operational European Centre for Medium-range Weather Forecast (ECMWF) WAM wave model. The wind forecasts come from the HIRLAM model, run by the Royal Netherlands Meteorological Institute (KNMI). SWAN is run in non-stationary mode.

Since July 1st 2011 the G1 grid runs automatically and the results are stored in the MATROOS database. Grid G2 is pre-operational from August 17th and its results are also stored in MATROOS. The model runs in a FEWS-like environment, starting with a 6 hour hindcast providing a restart-file, followed by a 48 hours forecast. As with other operational forecasts, this is repeated every 6 hours, when new wind forecast and wave boundary conditions become available.

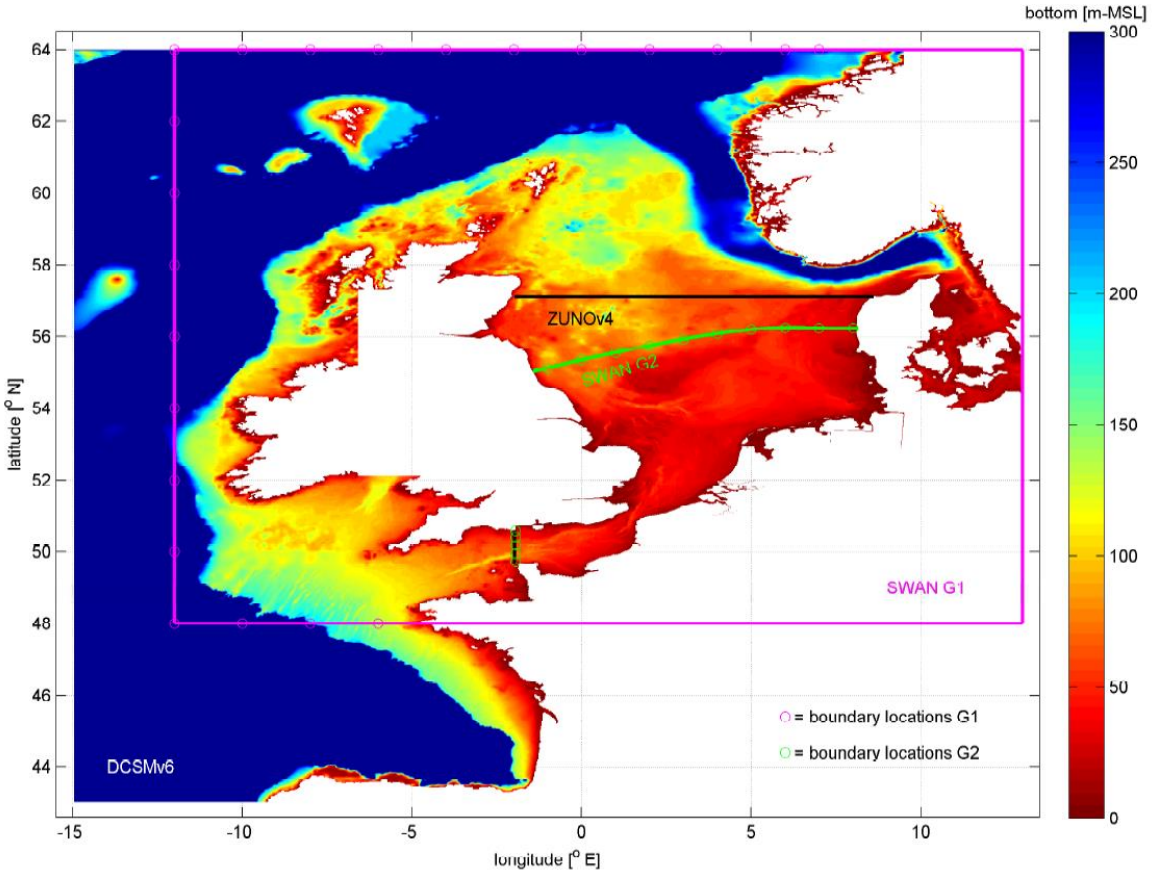

Figure 5.20 Operational wave grids Dutch Continental Shelf Model (DCSMv6) en Southern North Sea (ZUNOv4). Figure taken from Gautier (2012).

5.4 Synthesis

5.4.1 Existing studies

Important modelling research has been done in 1990's in the framework of the first Coastal Genesis research program of Rijkswaterstaat. Roelvink & Stive (1990) and Van Rijn (1997) published research on the sediment transport of Holland coast. In both studies, the yearly averaged transport was computed along a number of coast-normal transects. Important finding in these earlier studies is that the net sand transport on the Holland shoreface is determined by various subtle effects such as a density-gradient driven current but also that storm events play an important role and that a changing wave climate has a relatively big effect on the net transports.

Improved computer techniques facilitated the development of large scale 2D models of the Dutch coast. Van der Werf & Giardino (2009), Van der Hout *et al.* (2009) and Van der Spek *et al.* (2015) computed the hydrodynamics, sediment transport and morphodynamics (only Van der Hout *et al.*) along the Dutch coast with a Delft3D model. The predicted hydrodynamics and sediment transport along the Holland Coast and the Texel Inlet compared quite well with reference studies. A recent study of the large scale sediment transport along the Dutch coast is from Knook (2013). He analysed cross-shore sediment transport rates at various depths on the lower shoreface of the Central Holland coast. This analysis was based on computations with the Unibest-TC model, which makes the approach similar to the one by Roelvink and Stive in 1990 and Van Rijn in 1997, although density-gradient effects were not accounted for. Probably, related to this he found offshore cross-shore transport on the lower shoreface (due to tidal currents) and onshore transport at the upper shoreface (due to waves). This induced a lower shoreface flattening and an upper shoreface steepening.

The earlier work has mainly focussed on the central Dutch coast between Hoek van Holland and Den Helder without the effects of tidal inlets or estuaries. The computations were based on cross-shore profile models (2DV) or horizontal depth-averaged models (2DH). This required schematising wave and current conditions based on results from large scale models or excluding effects such as salinity and 3D circulation in order to keep the computation time limited. However, 3D circulation patterns by e.g. fluid density gradients play an important role for the total cross-shore transport rate at water depths deeper than about 8 m. Process-based 3D modelling to study the transport processes along the entire Dutch coast has not been done before.

5.4.2 Recommended future modelling approach

In light of this, we would like to suggest a two-sided modelling approach. The first is by setting up detailed models of the measurement areas near Ameland (in close co-op with the *Zeegaten* KG-2 project as well as the SEAWAD research project), Terschelling and Noordwijk. These models require boundary conditions from wave buoy data and/or models that cover the complete North Sea, e.g. the existing 3D Delft3D-FM North Sea model and operational wave model of the Dutch North Sea.

These models will be calibrated and validated using the Coastal Genesis measurements in 2017 and 2018. These models will use to make sensitivity computations to investigate lower shoreface sand transport processes for different scenario's (varying input parameters and boundary conditions). This is a so-called online sand transport model approach, including wave-current interaction.

The second approach is by applying the existing 3D hydrodynamic Delft3D-FM model of the complete Dutch coast. This model includes effects of tide, wind and river discharge (density-driven currents, in particular). The necessary wave parameters to compute the sand transports can either be taken from wave observation data in combination with a wave transformation matrix to assess the wave conditions anywhere along the Dutch coast or by applying the operational wave model of the Dutch North Sea. The current and wave parameters will feed into a local 1DV sand transport model. This is the offline approach, in which wave-driven current effects are excluded or accounted for in a simplified way.

This more schematised model approach will be validated using new and existing field data, and the local Terschelling, Ameland and Terschelling models. It enables computing net transport rates along the complete Dutch shoreface and allows for investigating effects of climate change (sea level rise and consequences for wind and wave climate and tidal motion) and effects of policy decisions (boundary of coastal foundation, effects of changes coastal foundation and maintenance requirements thereof).

These models are aimed to predict lower shoreface transport, with water depths between NAP-20 and -8 m. Important processes to consider are (either directly or in a parameterised way):

- Effects of tide, wind and waves.
- Density gradient effects, especially for the Holland Coast, which is affected by the Rhine ROFI.
- The vertical flow structure, especially density gradient driven currents, wave breaking induced undertow, Longuet-Higgins and other boundary layer streaming, up- and downwelling during storms.
- Alongshore effects, especially at outer deltas of the Delta and Wadden Coast.
- Wave effects: velocity skewness, (bound) long waves.

6 Synthesis

6.1 Conclusions

This report describes an inventory of existing knowledge, field data and models of the Dutch lower shoreface. The Dutch lower shoreface is defined as the area between the upper shoreface (with regular and dominant wave action) and the continental shelf (wave action limited to storms). This is roughly the zone between the outer breaker bar (around NAP -8 m) and the NAP -20 m depth contour. This literature review is the first phase of the Coastal Genesis 2.0, Lower Shoreface project in support of Dutch coastal policy, in which the definition of the offshore boundary of the coastal foundation plays an important role.

6.1.1 Large-scale morphology, sedimentology and geology

The shoreface of the Dutch coast is a complex area. It is partly determined by its evolution in the past, whereas present-day processes are influencing or even changing it. The present situation and large-scale artificial supply of sediment will determine its future development.

The shoreface morphology varies along the Dutch coast, depending on the coastal slope and superposition of ridges (central Holland coast) and ebb-tidal deltas (Delta area, Wadden Sea). The architecture of the shoreface-connected ridges off the central Holland coast indicates that they are still active today. The ridges are outbuilding to the northwest at their seaward sides, although they turn out to be erosive features at their southern edge. The development of most ebb-tidal deltas along the Dutch coast is largely influenced by interventions in the tidal inlets and tidal basins.

The lower part of the shoreface is formed by tidal-basin and river deposits stemming from the transgressive phase before 5000 BP. These deposits are overlain by an active sand layer that responds to variations in tidal, wave and wind conditions.

Shoreface deposits of the prograding beach barriers of the Holland coast indicate dominance of wave processes that decrease with depth at the upper shoreface. Moreover, they indicate that resuspension by storm waves impacted the middle and lower shoreface, with a frequency decreasing with depth. The validity of this conceptual model of shoreface processes and evolution for the present-day situation needs to be tested.

Analysis of profile changes at the middle and lower shoreface of the Holland coast did not show an offshore-directed translation of sediment volumes, despite the addition of large volumes of sand to the upper shoreface in many locations.

6.1.2 Sand transport processes

The lower shoreface sand transport is episodic with annual transport determined by high-wave events, and typically bedload-dominated. Except for storm events, current- (mainly tide) and wave-induced small-scale bedforms with typical heights of 0.02-0.04 m and lengths of 0.4-0.6 m were frequently observed on the lower shoreface. Also the observed variation in grain-size distributions with time at the lower shoreface reflects the impact of varying wind and wave conditions.

Potential cross-shore transport mechanisms are:

- Onshore: density gradient driven near-bed current, velocity skewness, Longuet-Higgins boundary layer streaming and upwelling.

- Offshore: undertow, (bound) long wave effects (both more important at shallow water), offshore turbulence asymmetry streaming and downwelling.
- On- or offshore: cross-shore tidal current component.

The importance of offshore turbulence asymmetry streaming and up- and downwelling on cross-shore sand transport has not yet been quantified. Furthermore, it is unclear how cross-shore tidal current components contribute to on- and offshore sand transport. This could especially be important for the Delta and Wadden Coast. The density-driven current seems to be very important for the net cross-shore transport at the 20 m water depth, but might not be so at the Delta and Wadden Coast since these are relatively far away from Rhine river mouth.

A first conceptual model of Dutch lower shoreface sand transport is presented in Appendix E. It shows the (relations between) external factors, input parameters and indicators contributing to the key indicator of the KG-2 lower shoreface project: cross-shore sand transport at the Dutch lower shoreface.

Typical estimates of the annual net cross-shore transport rates are 0-20 m^3/m/year (including pores) in the onshore direction, which amount to 0-2 million m^3/year into the Holland Coast area. At the 8 m depth contour on- and offshore contributions seem to cancel each other out, leading to a nearly zero net cross-shore transport along the Holland Coast. It is unclear what typical net transport rates are in between the 20 and 8 m water depth. Furthermore, we could not find estimates of lower shoreface transport rates along the Delta and Wadden Coast.

The episodic nature, relatively low values and the important bedload contribution make it very difficult to accurately measure and predict lower shoreface sand transport processes.

6.1.3 Field measurements

Existing lower shoreface measurements were mainly carried out along the Holland coast; data for the Delta and Wadden Coast are lacking. The larger number of data sets focused on hydrodynamics and fine sediment dynamics; sand transport processes were only measured during three measurement campaigns (SANDPIT, STRAINS/MegaPex, Kustgenese). There is a relatively large amount of morphological and subsurface shoreface data available, of which the quality varies greatly.

6.1.4 Numerical modelling

The first serious numerical modelling work on Dutch shoreface morphodynamics has been done in the 1980s and 1990s in the framework of the Kustgenese project. Roelvink & Stive (1990) and Van Rijn (1997) computed annual cross-shore and alongshore transport rates for a number of cross-shore transects along the Holland coast using the relatively simple 1DH/2DV Unibest-TC model, assuming alongshore uniformity and accounting for density gradient effects in a relatively simple way. Later on, improved computer techniques facilitated the development of large-scale, depth-averaged 2DH morphological models of the Dutch shoreface (e.g. Van der Werf & Giardino (2009); Van der Hout *et al.*, 2009; Van der Spek *et al.*, 2015). These models typically reproduced hydrodynamics and surfzone-integrated transport reasonably well. The model performance was not explicitly assessed for the lower shoreface, given the different focus of the modelling study and a lack of validation data. A well-validated Dutch lower shoreface sand transport model, accounting for the vertical flow structure and alongshore effects, is lacking.

6.1.5 Offshore boundary coastal foundation

The nourishment volume for the coastal foundation to grow with sea-level rise is directly related to the area of the coastal foundation. In this computation it is currently assumed that there is no net sand transport at a decadal time scale across the seaward boundary, which is defined at the NAP-20m depth contour. This boundary is strongly linked to the onshore extent of the sand extraction zone to ensure there is a limited effect on the nearshore zone. The offshore boundary of the coastal foundation is not very well substantiated. Mainly the bed slope transition from ~1:100 to ~1:1000 was used as indicator. At the Delta and Wadden Coast, this slope transition occurs close to the NAP -20 m depth contour. In front of the central Holland Coast this transition is at round the NAP -16 m depth contour. The NAP -20 m depth contour is taken as seaward boundary here as well, because of the supposed positive effect of shoreface connected ridges at 16-20 m water depths between Katwijk and Petten on coastal stability. Different ways of determining the depth of closure (based on wave action, morphological envelope, lag deposits of heavy minerals) indicate that current 20 m water depth is a safe choice as the offshore boundary of the coastal foundation. However, direct monitoring of dredge disposals along the Holland coast over 1-2 decades showed that the transition of morphological active to inactive seabed occurs at a water depth of about 19 m.

6.2 Further research

The generally and internationally accepted conceptual model for cross-shore sediment transport on the shoreface comprises a short-term circulation of sand, including bar morphodynamics, on the upper shoreface that is driven by daily wave processes and a long-term circulation that consists of offshore sand transport by downwelling currents during storms that brings the sediment out of reach of the daily wave processes, and a slow return of this sand volume driven by more energetic wave conditions. Aigner (1985) described specific storm beds that are deposited on the North Sea floor north of the East Frisian islands that are supposed to be formed by storm-driven downwelling currents. This kind of deposit has up to the present day not been found offshore the Dutch coast. An explanation might be found in the fact that the above-mentioned conceptual model has been derived for exposed, open-ocean shorelines. The Dutch coast seems to be comparatively sheltered from frequent extreme storms. Moreover, the direction of wave incidence during storms in combination with the upper shoreface bar systems might prevent the development of large-scale offshore-directed sediment transport. In conclusion, the validity of the above-mentioned conceptual model for the Dutch coast is unclear. However, it is important to understand the net sediment transport directions on the shoreface in order to predict the redistribution of nourished sand over the shoreface.

Agaard (2011) determined the sediment budget for part of the Danish North Sea coast on the basis of a combination of cross-shore profile analysis, numerical modelling and field measurements of cross- and longshore sediment transport at the boundary between upper and lower shoreface. He concluded that a substantial part of the longshore sediment supply by wave-driven currents is transferred seaward across the shoreface by systematically offshore-migrating nearshore bars that deliver sediment to the lower shoreface. In a later paper, Agaard (2014) used measurements of suspended sediment load and cross-shore transport on the lower shoreface at five different field sites that exhibit a wide range of wave conditions and sediment characteristics, to put together a model for sediment supply from the lower to the upper shoreface at large spatial and temporal scales. The applicability of both the concept of seaward sediment transport by offshore migrating bars and the long-term cross-shore sediment exchange model for the Dutch coast needs to be assessed. A first investigation will be based on the results of the field campaigns and modelling study. A more in-depth investigation could be part of an extended study in another framework.

Our knowledge of the Dutch lower shoreface sediment dynamics is limited, which makes it difficult to advice on the offshore boundary of the Dutch coastal foundation and the associated nourishment volume. This limited knowledge is mainly related to a lack of high-quality field data, and detailed numerical modelling. In the following two paragraphs three new measurement areas are recommended, and first ideas for the numerical modelling study are outlined.

6.2.1 Field measurements

The Dutch coast has a total length of 350 km and can be divided in three main areas: the south-western Delta coast, the Holland coast and the Wadden Sea coast. Between and within these areas there are large differences in the dominant hydrodynamic processes, morphodynamics and human interventions, as described in Section 6.1. The selection of the three new KG-2 lower shoreface measurement areas is based on the following considerations.

The new measurements will have to be used to gain more insight in especially the contribution of waves to (cross-shore) sediment transport and to improve numerical models. To learn most from the measurements it is important to be able to make a good interpretation. For this, locations which are relatively undisturbed, for which more (older) measurements are available and where tidal influence is relatively small were selected.

No location was chosen in the south-western Delta. This area has a deviating morphology and geology compared to the rest of the coast: older (resistant) deposits lie (almost) at the surface and the area is dominated by tidal channels close to the coast, lacking a typical profile with breaker bars. This area is largely affected by human interventions. Also, no prior lower shoreface measurements are available and in this area tide is a dominant factor in shoreface morphodynamics.

The following locations meet the above mentioned criteria and are chosen for field measurements: Noordwijk, Terschelling and Ameland. Table 6.1 gives the main arguments for choosing these field sites; below a short description of these three areas is presented.

Table 6.1 Main arguments for choosing the Noordwijk, Terschelling and Ameland shoreface field sites.

Field site	Main arguments
Noordwijk	- wave-dominated - existence of earlier field work (CEFAS/RIKZ measurements, SANDPIT) - well-studied
Terschelling	- wave-dominated - different coastal orientation and profile than Noordwijk - relatively undisturbed (no nourishments) - existence of earlier field work (Nourtec campaign) - adjacent to Ameland field site
Ameland	- link with KG-2 tidal inlet subproject and the SEAWAD research project - offshore from an outer delta

6.2.1.1 Noordwijk

The Noordwijk location is located at the uniform, straight, Holland coast, located about 35 km north of Rotterdam. The coastline has an orientation of approximately 28 degrees clockwise to the North (Figure 6.1). At the upper shoreface breaker bars are present, at deeper water

sandwaves occur, expected to be superpositioned by megaripples (based on higher resolution data in similar areas, not visible on presented bathymetry due to resolution). The profile is relatively steep to a depth of ca. NAP -15 m, down below the slope is very small (Figure 6.2).

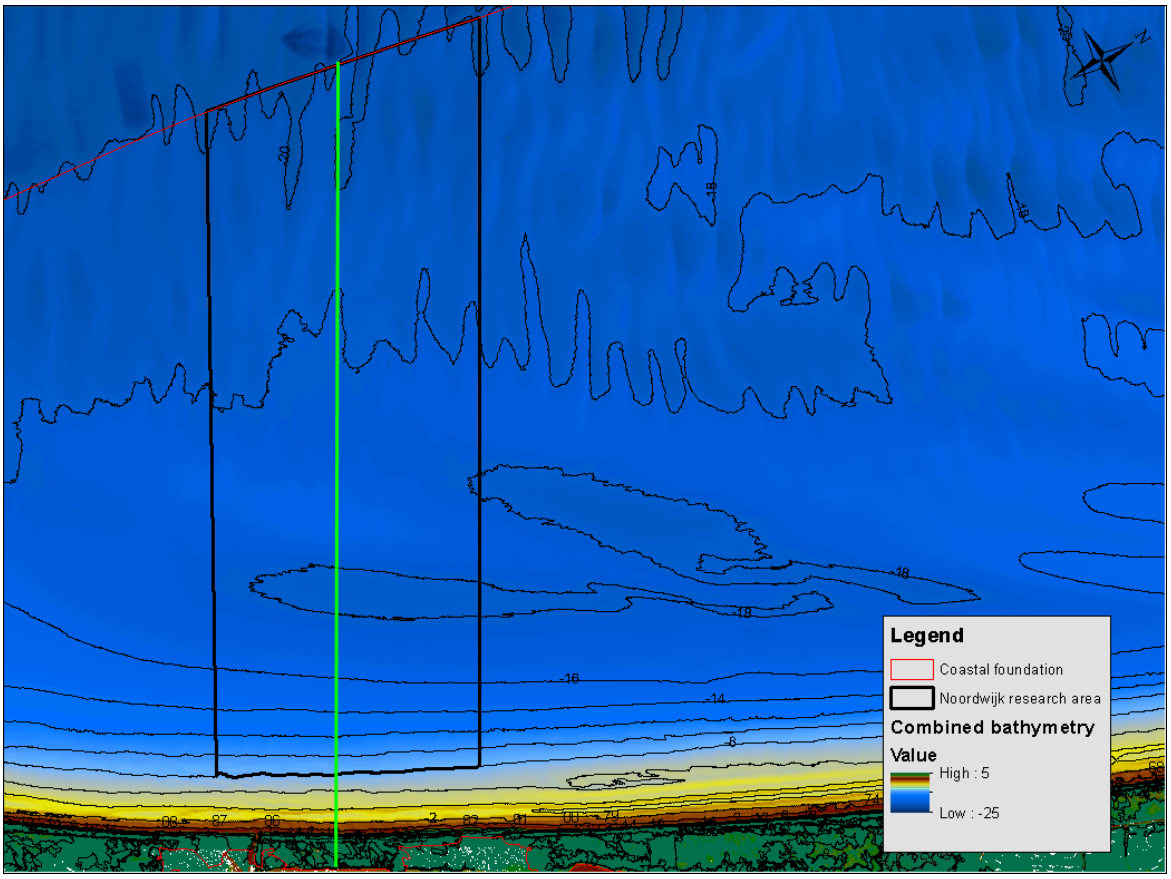

Figure 6.1 Study area at Noordwijk, the green line indicates location of cross-section shown in Figure 6.2 (map is rotated, see north arrow).

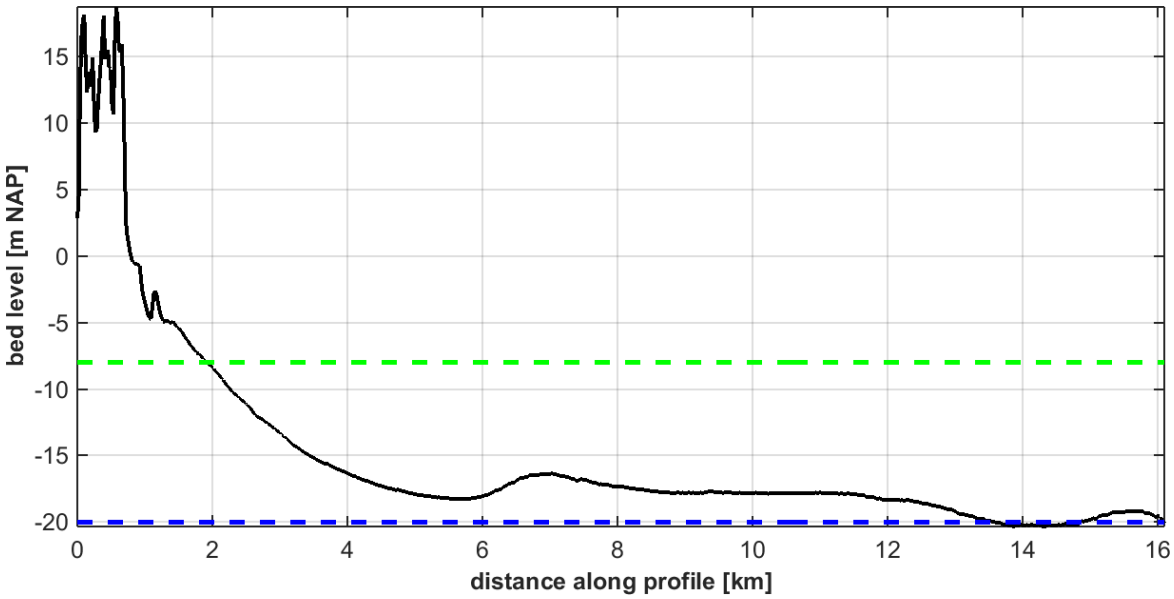

Figure 6.2 Cross-section at study area Noordwijk, green dashed line is NAP -8 m and blue dashed line is NAP -20 m, see Figure 6.1 for location.

6.2.1.2 *Terschelling*

Like Noordwijk, the central part of Terschelling is a uniform, straight coast. It is also wave-dominated, but has a different orientation and cross-shore profile compared to Noordwijk. The study area at Terschelling is located at the middle of the island. This part of the coast is outside the direct influence of the tidal inlets (Vlie Inlet in the west, Ameland Inlet in the east) and is a straight, closed coast (Figure 6.3). The orientation of the coastline is about 75 degrees to the North (clockwise). At the upper shoreface breaker bars are present, at deeper water no larger bedforms like sandwaves are present, but here megaripples are expected to be present. The absence of sandwaves is probably related to the grain-size of the sediment. The slope of the profile does not decrease around NAP -15 m, but remains almost constant until the NAP -20 m, where is becomes more gradual (Figure 6.4).

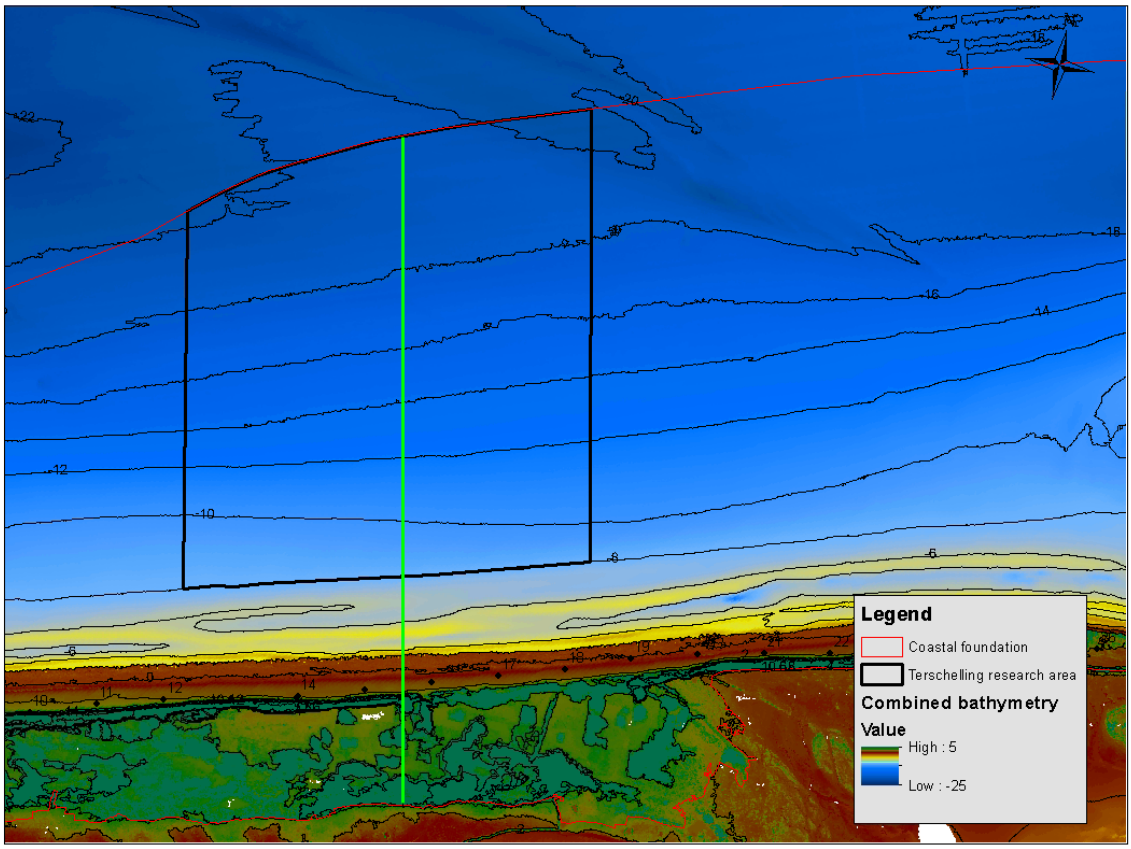

Figure 6.3 Study area at Terschelling, green line indicates location of cross-section shown in Figure 6.4 (map is rotated, see north arrow).

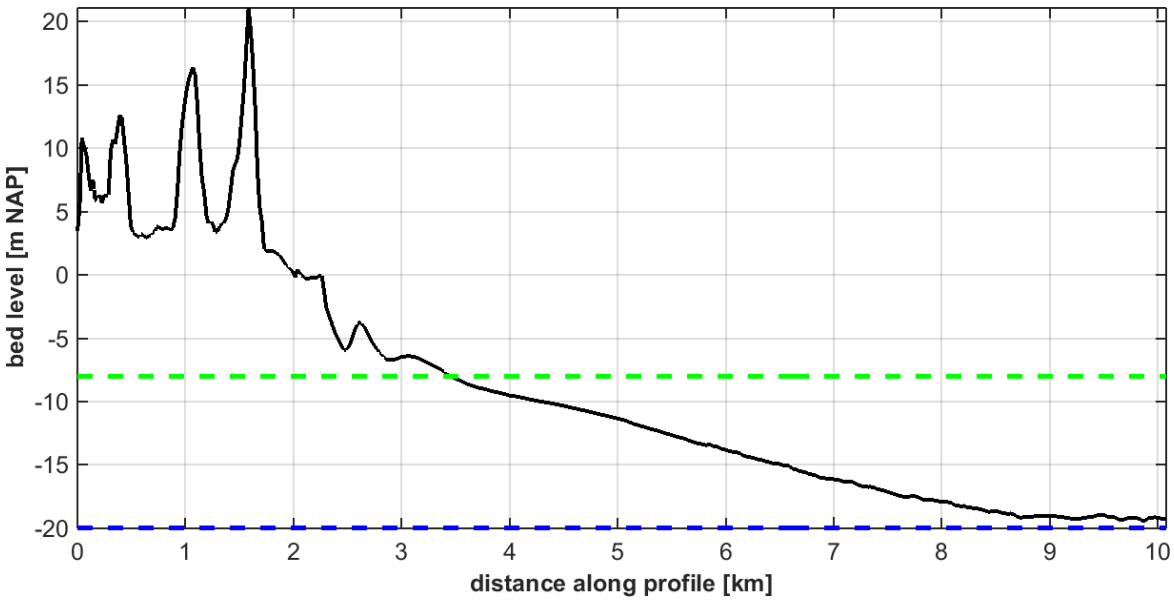

Figure 6.4 Cross-section at study area Terschelling, the green dashed line is NAP -8 m and blue dashed line is NAP -20 m, see Figure 6.3 for location.

6.2.1.3 *Ameland*

Although the lower shoreface of this location is in the very close proximity of the tidal channels, connection with the other subproject of Coastal Genesis 2 (*Zeegaten*, tidal inlets) and the SEAWAD research project is anticipated to be very valuable. The Amelander Inlet is located between the islands Terschelling and Ameland. It is one of the most intensively studied inlets and will be monitored and measured in the KG-2 tidal inlets subproject. To connect with the measurements and knowledge of the inlet, the study area is located on the outer part of the ebb-shield (the shallow area at the end of the channel) of the Akkepollegat channel (Figure 6.5). Like the study area at Terschelling, megaripples are expected to be present at the lower shoreface and no sandwaves are expected to be present. The ebb-shield has a much steeper slope than the main coast of the other measurement areas, decreasing from NAP -8 m to NAP -19 m in a bit more than 1 km (Figure 6.6). The slope of the last part of the profile is much smaller.

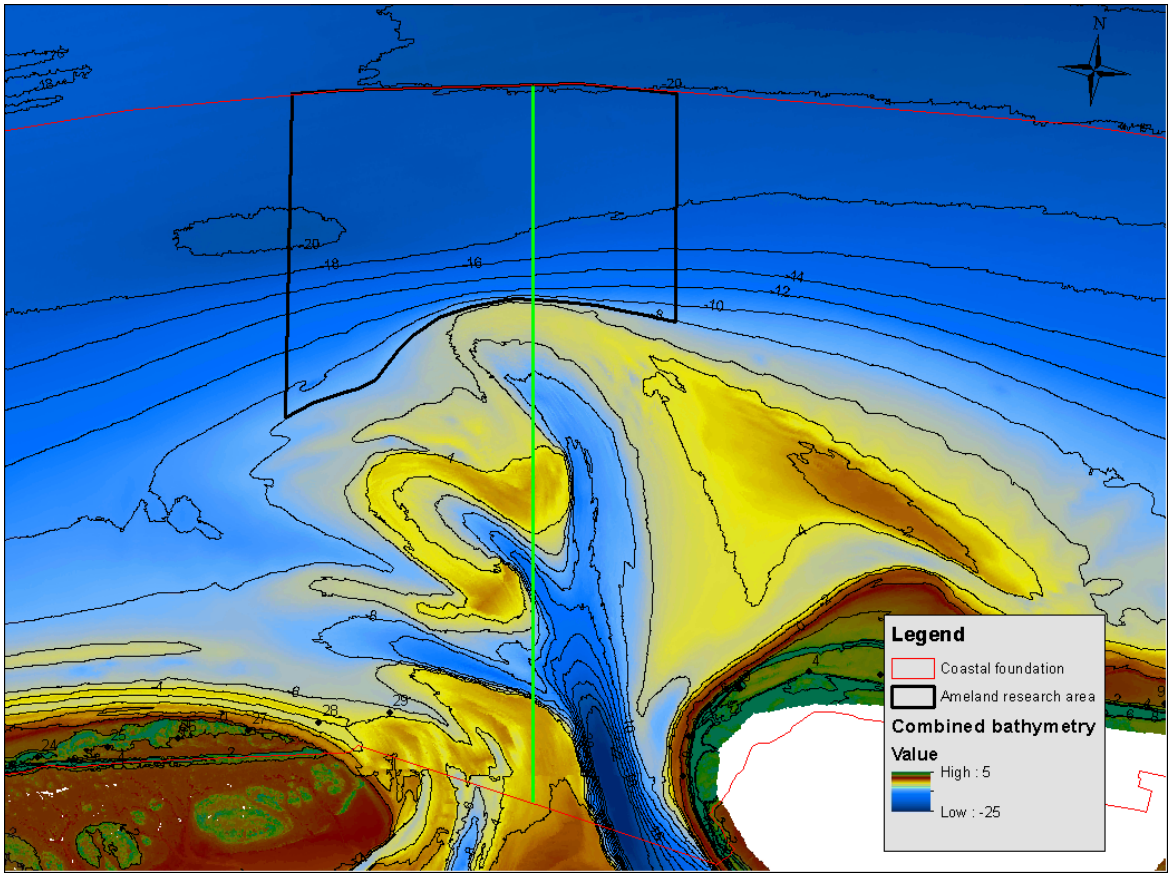

Figure 6.5 Study area at Ameland Inlet, green line indicates location of cross-section shown in Figure 6.6 (map is rotated, see north arrow).

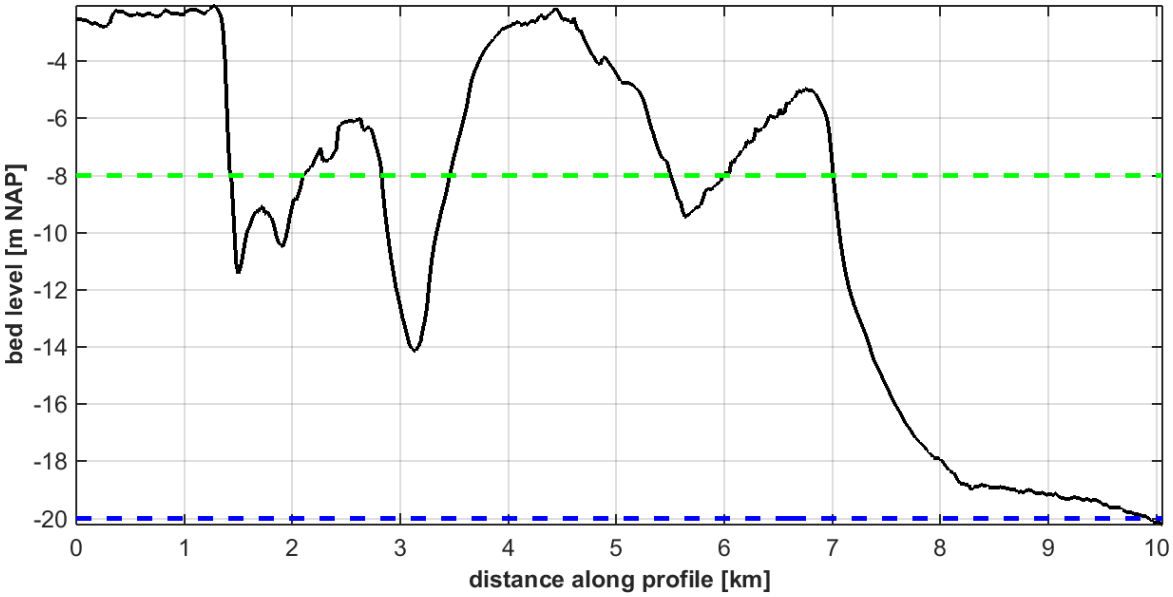

Figure 6.6 Cross-section at study area Ameland Inlet, green dashed line is NAP -8 m and blue dashed line is NAP -20 m, see Figure 6.5 for location.

6.2.2 Numerical modelling

The numerical modeling will be complementary to the field measurements, which are limited in time and space. Furthermore, the models can be used for scenario testing, e.g. investigating the importance of storm waves vs. regular wave conditions and the wind and wave climate (which might change due to climate change). This will add greatly to our understanding of the lower shoreface sand dynamics.

The models should be able to predict lower shoreface sand transport on the Dutch surface due to the combined tide, wind and wave influence. In particular the following processes should be considered, either directly or in a parameterised way:

- Density gradient effects, especially for the Holland Coast, affected by the Rhine ROFI.
- The vertical flow structure, especially density gradient driven currents, wave breaking induced undertow, Longuet-Higgins and other boundary layer streaming, up- and downwelling during storms.
- Alongshore effects, especially at outer deltas of the Delta and Wadden Coast.
- Wave effects: velocity skewness, (bound) long waves.

We recommend a two-folded modelling approach:

1 Detailed, local 2DH/3D wave-current-sand transport models for the measurement sites Terschelling, Ameland and Noordwijk. These models will be directly validated using the new field measurements, and using existing data (Nourtec, SANDPIT). The Amelander shoreface model should be developed in close co-operation with the model being developed for the Amelander Zeegat in the framework of the KG-2 sister project *Zeegaten* (tidal inlets) and the SEAWAD research project.

2 An offline 1DV sand transport model approach, fed with vertical flow profiles computed with a 3D flow model and modelled/measured wave parameters. This schematised approach will exclude wave-driven current effects or account for it in a simplified way. However, it enables relatively fast computing of the net transport rates along the complete Dutch shoreface. This approach will be validated using new and existing field data, and the local models developed mentioned under #1.

7 References

Agaard, T. (2011). Sediment transfer from beach to shoreface: The sediment budget of an accreting beach on the Danish North Sea Coast. Geomorphology, 135, 143-157.

Agaard, T. (2014). Sediment supply to beaches: Cross-shore sand transport on the lower shoreface. Journal of Geophysical Research: Earth Surface, 119, 913-926. doi:10.1002/2013JF003041.

Aigner, T. (1985). Storm Depositional Systems. Dynamic Stratigraphy in Modern and Ancient Shallow-Marine Sequences. Lecture Notes in Earth Sciences, Nr. 3, Springer-Verlag, Berlin, 174 pp.

Beets, D.J., Cleveringa, P., Laban, C., Battegazore, P. (1995). Evolution of the lower shoreface of the coast of Holland between Monster and Noordwijk. Mededelingen Rijks Geologische Dienst, 52, 235-247.

Beets, D.J., Van der Spek, A.J.F. (2000). The Holocene evolution of the barrier and the back-barrier basins of Belgium and the Netherlands as a function of late Weichselian morphology, relative sea-level rise and sediment supply. Geologie en Mijnbouw / Netherlands Journal of Geosciences, 79 (1), 3-16.

Beets, D.J., Van der Spek, A.J.F., Van der Valk, L. (1994). Holocene ontwikkeling van de Nederlandse kust. Report 40.016, Geological Survey of The Netherlands, Haarlem, 53 pp. (in Dutch)

Bagnold, R.A. (1963). Mechanics of marine sedimentation, The Sea (ed. by M. N. Hili), 3, Interscience, New York, 507-528

Bruun, P. (1954). Coast erosion and the developmentof beach profiles. Tech. Memo. NQ. 44, Beach Erosion Board, U.S. Army Engr. Waterways Expt. Stn., Vicksburg, MS.

CEFAS (2003). RIKZ/CEFAS Minipod deployments At Noordwijk 2 and 5. Final Report.

Cleveringa, J. (2000). Reconstruction and modelling of Holocene coastal evolution of the Netherlands. Geologica Ultraectina, 200. PhD thesis, University of Utrecht, The Netherlands.

Cleveringa, J. (2016). Kennisvraagspecificatie zeewaartse grens Kustfundament, Kustgenese 2 Ministerie van Infrastructuur en Milieu. Rapport, Arcadis, Nederland.

Davies, A.G., Villaret, C. (1999), Eulerian drift induced by progressive waves above rippled and very rough beds, J. Geophys. Res., 104(C1), 1465–1488, doi:10.1029/1998JC900016.

Dean, R.G. (1977). Equilibrium beach profiles - U.S. Atlantic and Gulf Coasts, Ocean Eng. Rep., 12, Univ. Delaware, 1-45.

De Boer, G.J. (2009). On the interaction between tides and stratification in the Rhine Region of Freshwater Influence. PhD thesis, Technical University of Delft, The Netherlands.

De Boer, G.J., Pietrzak, J.D., Winterwerp, J.C. (2006). On the vertical structure of the Rhine region of freshwater influence. Ocean Dynamics 56, 198–216. doi:10.1007/s10236-005-0042-1

De Boer, G.J. (2009). On the interaction between tides and stratification in the Rhine Region of Freshwater Influence. Technische Universiteit Delft, Delft.

De Leeuw, C.J. (2005). Model predictions of wave-induced sediment transport on the shoreface. MSc thesis, University of Twente, The Netherlands.

Deltaprogramma (2015). Werk aan de delta. De beslissingen om Nederland veilig en leefbaar te maken.

De Mulder, E.F.J. (1984). Geologische geschiedenis van de Hondsbossche Zeewering. Grondboor en Hamer, 1984-1, 15-31. (in Dutch)

De Ronde, J.G. (2008). Toekomstige langjarige suppletiebehoefte. Rapport Z4582.24, Deltares, Nederland.

De Ruiter, W.P.M., Van der Giessen, A., Groenendijk, F.C. (1992). Current and density structure in the Netherlands coastal zone. In: Dynamics and exchanges in estuaries and

in coastal zone, edited by D. Prandle, American Geophysical Union.

Dijkman, M.J., Bakker, W.T., De Vroeg, J.H. (1990). Prediction of coastline evolution for the Holland coast. In: Proceedings of the 22nd International Conference on Coastal Engineering, Delft, The Netherlands, July 2-6, 1990, Vol. 2 ; p. 1935-1947

Dolphin, T.J., Grasmeijer, B.T., Vincent, C.E. (2005). Sand suspension due to waves and tidal flow over short and long wave ripples, and flat beds on the Dutch shoreface. Paper T, SANDPIT endbook, edited by Van Rijn *et al* (2005).

Dorst, L.L. (2009). Estimating Sea Floor Dynamics in the Southern North Sea to Improve Bathymetric Survey Planning. doi:10.3990/1.9789036528788.

Duran-Mutate et al. (2014). Residual circulation and freshwater transport in the Dutch Wadden Sea: a numerical modelling study. Ocean Science, 10, 611–632, 2014.

Ebbing, J.H.J., Laban, C. (1996). Geological history of the area off Walcheren and Zeeuwsch-Vlaanderen (southwestern Netherlands), since the start of the Eemian. Mededelingen Rijks Geologische Dienst, 57, 251-267.

Ebbing, J.H.J., Laban, C., Frantsen, P.J., Nederlof, H.P. (1993). Geologische kaart Rapsbank, 51°20'N-3°00'E, Schaal 1:100 000. Rijks Geologische Dienst, Haarlem.

Elias, E.P.L., Van der Spek, A.J.F. (2006). Long-term morphodynamic evolution of Texel Inlet and its ebb-tidal delta (The Netherlands). Marine Geology, 225, 5-21.

Elias, E.P.L., Van der Spek, A.J.F., Lazar, M. (2016). The 'Voordelta', the contiguous ebb-tidal deltas in the SW Netherlands; Large-scale morphological changes and sediment budget 1965-2013; Impacts of large-scale engineering. Netherlands Journal of Geoscience. Online doi:10.1017/njg.2016.37

ENW (2017). Advies rekenregel suppletievolume. Brief ENW-17-14 aan het Ministerie van Infrastuctuur en Milieu, Directeur-Generaal Ruimte en Water, Expertisenetwerk waterveiligheid.

Flather, R.A. (2000). Existing operational oceanography. Coast Engineering 41:13–40.

Gautier, C. (2012). Pre-Operational Wave Forecasting for the North Sea, SWAN model for the Dutch North Sea. Report 120457-004-HYE-0003, Deltares, The Netherlands.

Grasmeijer, B.T., Kleinhans, M.G. (2005a). Net transport at the Dutch Noordwijk field site based on measurements. Paper B, SANDPIT endbook, edited by Van Rijn *et al*.

Grasmeijer, B.T., Dolphin, T.J., Vincent, C.E., Kleinhans, M.G. (2005b). Suspended sand concentrations and transport in tidal flow with and without waves. Paper U, SANDPIT endbook, edited by Van Rijn *et al* (2005).

Guillén, J., Hoekstra, P. (1996). The "equilibrium" distribution of grain size fractions and its implications for cross-shore sediment transport: a conceptual model. Marine Geology, 135, 15-33.

Hallermeier, R.J. (1981). A Profile Zonation for Seasonal Sand Beaches from Wave Climate. Coastal Engineering, Vol. 4, 253-277.

Heemink A.W., Mouthaan E.E.A., Roest, M.R.T. *et al* (2002). Inverse 3D shallow water flow modeling of the continental shelf. Cont Shelf Res 22:465–484

Henriquez, M., Meirelles, S., Horner-devine, A.R., Souza, A.J., Pietrzak, J.D., Stive, M.J.F. (2013). Near-bottom currents on the middle shoreface in the presence of the rhine river plume, in: Coastal Engineering Proceedings. pp. 1–4.

Hijma, M.P. (2017). Geology of the Dutch coast. The effect of lithological variation on coastal morphodynamics. Report 1220040-007-ZKS-0003, Deltares, Nederland.

Hijma, M.P., Van der Spek, A.J.F., Van Heteren, S. (2010). Development of a mid-Holocene estuarine basin, Rhine-Meuse mouth area, offshore The Netherlands. Marine Geology, 271, 198-211.

Hinton, C.L. (2000). Decadal morphodynamic behaviour of the Holland shoreface. PhD thesis, Middlesex University, UK.

Houwman, K.T., Hoekstra, P. (1994). Shoreface hydrodynamics; Report part 1, field measurements near Egmond aan Zee. IMAU report R94-2, University of Utrecht, The Netherlands.

Kleinhans, M.G., Grasmeijer, B.G. (2006). Bed load transport on the shoreface by currents

and waves. Coastal Engineering 53, 983-996.

Knook, P.P. (2013). Sediment transport on various depth contours of the 'Holland Coast' shoreface. MSc. thesis, 82 pages, Delft University of Technology, Delft, The Netherlands.

Koomans, R.L. (2000). Sand in motion: effects of density and grain size. PhD thesis, University of Groningen, The Netherlands.

Kranenburg, W.M., Ribberink, J.S., Uittenbogaard, R.E., Hulscher, and S.J.M.H. (2012), Net currents in the wave bottom boundary layer: On waveshape streaming and progressive wave streaming, J. Geophys. Res., 117, F03005, doi:10.1029/2011JF002070.

Lodder, Q. (2016). Rekenregel suppletievolume. Rijkswaterstaat Memo.

Longuet-Higgins, M.S. (1953), Mass transport in water waves, Philos. Trans. R. Soc. London, Ser. A, 245(903), 535–581, doi:10.1098/rsta.1953.0006.

Marsh, S.W., Nicholls, R.J., Kroon, A., Hoekstra, P. (1998) Assessment of depth of closure on a nourished beach: Terschelling, The Netherlands. In: International Conference on Coastal Engineering (Ed. by B. L. Edge), pp. 3110-3124. ASCE, Copenhagen.

Meirelles, S., Horner-devine, A.R., Henriquez, M., Stive, M., Pietrzak, J., Souza, A.J. (2014). Middle shoreface sand transport under the influence of a river plume. J. Coast. Res. 70, 182–186. doi:10.2112/SI65-xxx.1

Meirelles, S., Henriquez, M., Souza, A.J., Horner-Devine, A.R., Pietrzak, J.D., Rijnsburg, S., Stive, M.J.F. (2016). Small scale bedform types off the South Holland coast. In: Vila-Concejo, A.; Bruce, E.; Kennedy, D.M., and McCarroll, R.J. (eds.), Proceedings of the 14th International Coastal Symposium (Sydney, Australia). Journal of Coastal Research, Special Issue, No. 75, pp. XX-XX. Coconut Creek (Florida), ISSN 0749-0208.

Ministerie van Verkeer en Waterstaat (1991). Regionaal Ontgrondingenplan Noordzee, Deel A beleidsnota, Deel B Nota van toelichting (milieu-effect-rapport) en Deel C Appendices, Rijkswaterstaat Directie Noordzee.

Ministerie van Verkeer en Waterstaat (1998). Vierde nota waterhuishouding.

Ministerie van Volkshuisvesting, Ruimtelijke Ordening en Milieu (2004). Nota Ruimte.

Mol, A.C.S. (2007). R&D Kustwaterbouw Reductie Golfrandvoorwaarden, OPTI Manual. Rapport H4959.10, WL|Delft Hydraulics, Nederland.

Mouthaan E.E.A., Heemink A.W., Robaczewska K.B. (1994) Assimilation of ERS-1 altimeter data in a tidal model of the continental shelf. Deutsche Hydrographische Zeitschrift 36(4):285–319

Mulder, J.P.M. (2000) Zandverliezen in het Nedrlandse kustsysteem; Advies voor Dynamisch Handhaven in de 21e eeuw. Rijkswaterstaat RIKZ rapport RIKZ/2000.36.

Nederbragt, G.J. (2005). Zandvoorraden van het kustsysteem: onderbouwing van een conceptueel model met behulp van trends van de winst- en verliesposten over de periode 1973-1997. Ministerie van Verkeer en Waterstaat, Rijkswaterstaat, Rijksinstituut voor Kust en Zee, RIKZ, 09-2006

Niessen, A.C.H.M. (1989). Project Kustgenese. Geologisch onderzoek van het kustgebied van de Zeeuwse en Zuidhollandse eilanden en de ‘gesloten’ Hollandse kust. Report Geological Survey of The Netherlands, Haarlem (24 mei 1989). (in Dutch)

Niessen, A.C.H.M. (1990). Project Kustgenese. Geologisch onderzoek van het kustgebied van de Waddeneilanden. Report Geological Survey of The Netherlands, Haarlem (21 februari 1990). (in Dutch)

Niessen, A.C.H.M., Laban, C. (1987). Project Kustgenese, Taakgroep 100. Voortgangsrapportage van het door de Rijks Geologische Dienst uitgevoerde onderzoek 1986/1987 in het kustgebied tussen Castricum en Camperduin. Report Geological Survey of The Netherlands, Haarlem (30 oktober 1987). (in Dutch)

Oost, A.P. (1995). Dynamics ans sedimentary development of the Dutch Wadden Sea with emphasis on the Frisian Inlet. Geologica Ultraiectina, 126. (PhD thesis Utrecht University)

Passchier, S. (2003). Bedform development and sediment composition on a shoreface-to-shelf transition, North Sea. In: van Heteren, S (ed.), Delft Cluster - Ecomorphodynamics

of the seafloor; final report, p. 20-24.

Passchier, S., Kleinhans, M.G. (2005). Observations of sand waves, megaripples, and hummocks in the Dutch coastal area and their relation to currents and combined flow conditions. J. Geophys. Res. Earth Surf. 110, 1–15. doi:10.1029/2004JF000215.

Philippart M.E., Gebraad A.W., Scharroo R, Roest M.R.T., Vollebregt E.A.H., Jacobs A., Van den Boogaard H.F.P., Peters H.C. (1998). DATUM2: data assimilation with altimetry techniques used in a tidal model, 2nd program. Tech. rep., Netherlands Remote Sensing Board

Ribberink, J.S. (1998). Bed-load transport for steady flows and unsteady oscillatory flows. Coastal Engineering, 34, 59–82.

Ribberink, J.S., Van der Werf, J.J., O'Donoghue, T., Hassan, W.N.M. (2008). Sand motion induced by oscillatory flows: Sheet flow and vortex ripples. Journal of Turbulence, 9, N20.

Rieu, R., Van Heteren, S., Van der Spek, A.J.F., De Boer, P.L. (2005). Development and preservation of a mid-Holocene tidal-channel network offshore the western Netherlands. Journal of Sedimentary Research, 75 (3), 409-419

Roelvink, J.A., Stive, M.J.F. (1990). Sand transport on the shoreface of the Holland coast, in: Proceedings of the 22nd International Conference on Coastal Engineering. Delft, The Netherlands, pp. 1909–1922.

Roelvink, J.A., van der Kaaij, T., and Ruessink, B.G. (2001a). Calibration and verification of large-scale 2D/3D flow models, MARE consortium report no. Z3029.11, ONL Coast and Sea studies, June 2001 (final)

Roelvink, J.A., van der Kaaij, T., Ruessink, B.G., Bos, K.J. (2001b) Reference scenarios and design alternatives, MARE consortium report no. Z3029.12, ONL Coast and Sea studies.

Roelvink, J.A. (2006). Coastal morphodynamic evolution techniques. Coastal Engineering 53 (2006) 277-287.

Ruessink, B.G. (1998). Infragravity waves in a dissipative multiple bar system. PhD thesis, University of Utrecht, The Netherlands.

Ruessink, B.G., Houwman, K.T., Grasmeijer, B.T. (2006). Modeling the nonlinear effect of wind on rectilinear tidal flow. J. Geophys. Res. Oceans 111, 1–11. doi:10.1029/2006JC003570

Sha, L.P. (1989a). Holocene-Pleistocene interface and three-dimensional geometry of the ebb-delta complex, Texel Inlet, The Netherlands. Marine Geology, 89, 207-228

Sha, L.P. (1989b). Geology of the Dutch shoreface along the wadden islands: application of shallow seismic methods. Report NZ-N-89.21, Rijkswaterstaat, North Sea Directorate, Rijswijk.

Sha, L.P. (1992). Geological research in the ebb-tidal delta of 'Het Friesche Zeegat'. Report 40010 project Kustgenese, Geological Survey of The Netherlands, Haarlem.

Sha, L.P., Laban, C., Zonneveld, P.C. (1996). Influence of the Pleistocene topography on the Holocene coastal development off Texel. Mededelingen Rijks Geologische Dienst, 57, 79-95

Sha, L.P., De Boer, P.L. (1991). Ebb-tidal delta deposits along the west Frisian Islands (The Netherlands): processes, facies architecture and preservation. In: Smith, DG, Reinson, GE, Zaitlin, BA, Rahmani, RA (red.), Clastic Tidal Sedimentology. Canadian Society of Petroleum Geologists, Memoir 16, p. 199-218

Steetzel, H.J., De Vroeg, J.H. (1999). Update and validation of the PonTos-model. Report A244/Z2259, Alkyon Hydraulic Consultancy & Research en WL|Delft Hydraulics, The Netherlands.

Stive, M.J.F., Roelvink, J.A., De Vriend, H.J. (1990). Large-scale coastal evolution concept, in: Proceedings of the 22nd International Conference on Coastal Engineering. Presented at the Coastal Engineering, Delft, The Netherlands, pp. 1962–1975.

Stive, M.J.F., De Vriend, H.J. (1995). Modelling shoreface profile evolution. Marine Geology, 126, 235–248. doi:10.1016/0025-3227(95)00080-I

Stive, M.J.F., Eysink, W.D. (1989). Voorspelling ontwikkeling kustlijn 1990-2090, fase 3 (deelrapport 3.1): dynamisch model van het Nederlandse kustsysteem deelrapport. Rapport H0825, WL|Delft Hydraulics, Nederland.

Ten Brummelhuis P.G.J., Heemink A.W., Van den Boogard H.F.P. (1993). Identification of shallow sea models. Int J Numer Meth Fluid 17:637–665

Tonnon, P.K., Van der Werf, J.J., Mulder, J.P.M. (2009). Morfologische berekeningen MER zandmotor. Rapport 1201001-001, Deltares, Nederland.

Van Alphen, J.S.L.J., Damoiseaux, M.A. (1987). A morphological map of the Dutch shoreface and adjacent part of the continental shelf (1 :250.000). Report Rijkswaterstaat Directie Noordzee NZ-N-87.21 / Meetkundige Dienst MDLK-R-87.18 (december 1987)

Van de Meene, J.W.H. (1994). The shoreface connected ridges along the central Dutch coast. Netherlands Geographical Studies 174, 222 pp. (PhD thesis Utrecht University)

Van de Meene, J.W.H., Van Rijn, L.C. (2000). The shoreface-connected ridges along the central Dutch coast - Part 1: Field observations. Cont. Shelf Res. 20, 2295–2323. doi:10.1016/S0278-4343(00)00048-0

Van de Rest, P. (2004). Morfodynamica en hydrodynamica van de Hollandse kust. Afstudeerrapport, Technische Universiteit Delft, Nederland (in Dutch).

Van der Giessen, A., De Ruijter, W.P.M., Borst, J.C. (1990). Three-dimensional current structure in the Dutch coastal zone. Netherlands Journal of Sea Research 25, 45–55. doi:10.1016/0077-7579(90)90007-4

Van der Hout, C.M., Tonnon, P.K., De Ronde, J.G., 2009. Morphological effects of mega nourishment (No. 1200659-000). Deltares, Delft, The Netherlands.

Van der Hout, C.M., Gerkema, T., Nauw, J.J., Ridderinkhof, H., 2015. Observations of a narrow zone of high suspended particulate matter (SPM) concentrations along the Dutch coast. Cont. Shelf Res. 95, 27–38. doi:10.1016/j.csr.2015.01.002Van Dijk, T.A.G.P., Kleinhans, M.G. (2005). Processes controlling the dynamics of compound sand waves in the North Sea, Netherlands. J. Geophys. Res. Earth Surf. 110, 1–15. doi:10.1029/2004JF000173Van Duin, M.J.P., Wiersma, N.R., Walstra, D.J.R., Van Rijn, L.C., Stive, M.J.F. (2004). Nourishing the shoreface: observations and hindcasting of the Egmond case, The Netherlands. Coastal Engineering 51: 813-837.

Van der Spek, A.J.F. (1997). De geologische opbouw van de ondergrond van het mondingsgebied van de Westerschelde en de rol hiervan in de morfologische ontwikkeling. TNO report NITG 97-284-B, Netherlands Institute of Applied Geosciences TNO - National Geological Survey, Utrecht. (in Dutch)

Van der Spek, A.J.F. (1999). Reconstructie van de ontwikkeling van de Hollandse kust in de laatste 2500 jaar. TNO report NITG-99-143-A, Netherlands Institute of Applied Geosciences TNO - National Geological Survey, Utrecht. (in Dutch)

Van der Spek, A., Elias, E., Lodder, Q., Hoogland, R. (2015). Toekomstige suppletievolumes - Eindrapport. Rapport 1208140-005-ZKS-000 1. Deltares, Nederland. (in Dutch)

Van der Valk, L., (1996). Coastal barrier deposits in the central Dutch coastal plain. Mededelingen Rijks Geologische Dienst, 57, 133-199.

Van der Werf, J.J., Giardino, A. (2009). Effect van zeer grootschalige zandwinning langs de Nederlandse kust op de waterbeweging, zandtransporten en morfologie (No. 1200996-000-NaN-0010). Deltares, Delft, The Netherlands.

Van der Werf, J., Hendriks, E., Vermaas, T. (2017) Inventory field measurements Dutch shoreface. Memo 1230658-000-ZKS-0014, Deltares, The Netherlands.

Van Duin, M.J.P., Wiersma, N.R., Walstra, D.J.R., Van Rijn, L.C., Stive, M.J.F. (2004). Nourishing the shoreface: observations and hindcasting of the Egmond case, The Netherlands. Coastal Engineering 51: 813-837.

Van Heteren, S., Baptist, M.J., Van Bergen Henegouw, C.N., Van Dalfsen, J.A., Can Dijk, T.A.G.P. and 11 others (2003). Delft Cluster - Ecomorphodynamics of the seafloor; final report. 52 pp.

Van Heteren, S., Van der Spek, A.J.F. (2003). Long-term evolution of a small estuary: the Lauwerszee (northern Netherlands). TNO report NITG 03-108-A, Netherlands Institute of

Applied Geosciences TNO - National Geological Survey, Utrecht. (april 2003)
Van Heteren, S, Van der Spek, A.J.F. (2008). Waar is de delta van de Oude Rijn? Grondboor & Hamer, 62 (3/4), 72-76. (in Dutch)
Van Heteren, S, Van der Spek, A.J.F., De Groot, T.A.M. (2002). Architecture of a preserved Holocene tidal complex offshore the Rhine-Meuse river mouth, The Netherlands. TNO report NITG 01-027-A, Netherlands Institute of Applied Geosciences TNO - National Geological Survey, Utrecht. (oktober 2002)
Van Heteren, S., Van der Spek, A, Van der Valk, B. (2011). Evidence and implications of middle- to late-Holocene shoreface steepening offshore the western Netherlands. Proceedings Coastal Sediments 2011, 188-201.
Van Rijn, L.C. (1993). Principles of sediment transport in rivers, estuaries, and coastal seas. Aqua Publications, The Netherlands.
Van Rijn, L.C. (1997). Sediment transport and budget on the central coastal zone of Holland. Coastal Engineering, 32, 61–90.
Van Rijn, L.C. (1998). Principles of coastal morphology. Aqua Publications, The Netherlands
Van Rijn, L.C. (2007a). Unified view of sediment transport by currents and waves, I: Initiation of motion, bed roughness, and bed-load transport. Journal of Hydraulic Engineering 133: 649-667.
Van Rijn, L.C. (2007b). Unified view of sediment transport by currents and waves, II: Suspended transport. Journal of Hydraulic Engineering 133: 668-689.
Van Rijn, L.C. (2013). Principles of fluid flow and surface waves in rivers, estuaries, seas and oceans. Aqua Publications, The Netherlands.
Van Rijn, L.C., Soulsby, R.L., Hoekstra, P., Davies, A.G. (2005a). SANDPIT Sand Transport and Morphology of Offshore Mining Pits.
Van Rijn, L.C., Walstra, D.J.R., Van Kessel, T. (2005b). Net transport at the Dutch Noordwijk site, North Sea. Paper A, SANDPIT endbook, edited by Van Rijn *et al* (2005).
Van Rijn, L.C. (2007b). Unified view of sediment transport by currents and waves, II: Suspended transport. Journal of Hydraulic Engineering 133: 668-689.
Van Straaten, L.M.J.U. (1965). Coastal barrier deposits in South- and North-Holland, in particular in the areas around Scheveningen and IJmuiden. Mededelingen van de Geologische Stichting, Nieuwe Serie, 17, 41-75.
Van Woudenberg, C.C. (1996). De onderwater zanddam bij Loswal Noord: Gedrag en zandtransport. Rapport NZ-96.03, Rijkswaterstaat Directie Noordzee, Rijswijk. (in Dutch)
Verboom G.K., De Ronde J.G., Van Dijk R.P. (1992) A fine grid tidal flow and stormsurgemodel of theNorth Sea. Cont Shelf Res 12:213–233.
Verhagen, W, Wiersma, J (1991). Evaluatie zandstort voor de kust van Wijk aan Zee. Conceptrapport NZ-N-91, Rijkswaterstaat Directie Noordzee, Rijswijk. (in Dutch)
Verlaan M., Zijderveld A., De Vries H., Kroos J. (2005). Operational storm surge forecasting in the Netherlands: developments in the last decade. Phil Trans R Soc A 363:1441–1453
Vermaas, T. (2010). Morphological behaviour of the deeper part of the Holland coast. Report Deltares / Physical Geography Department - Utrecht University (October 2010)
Vermaas, T., Van Dijk, T., Hijma, M. (2015). Bodemdynamiek van de diepe onderwateroever met oog op de -20 m NAP lijn. Rapport 1220034-003-ZKS-0002, Deltares, Nederlands.
Vermaas, T. Van der Spek, A. (2016). Profielen dynamiek kustfundament. Deltares presentatie als onderdeel van het project KPP B&O Kust, projectnummer 1230043.
Wiersma, J., Van Alphen, J.S.L.J. (1988). The morphology of the Dutch shoreface between Hook van Holland and Den Helder (The Netherlands). In: P.L. de Boer et al. (eds), Tide-influenced sedimentary envionments and facies, pp. 101-111.
Witbaard, R., Duineveld, G.C.A., Bergman, M.J.N., Witte, H.I.J., Groot, L., Rozemeijer, M.J.C. (2015). The growth and dynamics of Ensis directus in the near-shore Dutch coastal zone of the North Sea. J. Sea Res. 95, 95–105. doi:10.1016/j.seares.2014.09.008
Zijl, F., Verlaan, M., Gerritsen, H. (2013). Improved water-level forecasting for the Northwest European Shelf and North Sea through direct modelling of tide, surge and non-linear

interaction. Ocean Dyn. 63, 823–847. doi:10.1007/s10236-013-0624-2

Zijl, F., Sumihar, J., Verlaan, M. (2015). Application of data assimilation for improved operational water level forecasting on the northwest European shelf and North Sea. Ocean Dynamics 65, 1699–1716. doi:10.1007/s10236-015-0898-7.

Zijl, F. (2017). D-Flow FM for the North Sea, 3D model set up and results. Presentation, Deltares, The Netherlands.

A Vertical structure of the Rhine region of freshwater influence (De Boer, 2006, 2009)

A.1 Introduction

River plumes occur wherever significant amounts of buoyancy, due to freshwater from rivers, flow out into coastal seas and oceans. Under the influence of the Earth's rotation, the out-flowing estuarine waters tend to turn to the right on leaving the river mouth (in the Northern Hemisphere) forming narrow coastal currents. River plumes can maintain their cross-shelf structure for hundreds of kilometres. Consequently, they are important in determining the transfer of matter in coastal seas. To investigates this, De Boer (2006, 2009) set-up an idealised three-dimensional Delft3D numerical model of the Rhine region of fresh water influence (ROFI) to explore the effect of stratification on the vertical structure of the tidal currents.

A.2 Approach

De Boer (2006, 2009) used the flow module of Delft3D with a 20-m deep rectangular domain. Figure 7.1 shows a schematic overview of the model grid. The inner high-resolution part of the domain was 65 km in cross-shore width by 105 km in alongshore length. Here, the grid consisted of 130×210 cells with a grid size of 500 m. On the northern and western sides of the inner domain, an additional margin of 25 cells was added. The grid size of these cells increased with a factor of 1.2 per cell from the 130×210 inner domain towards the boundaries. In this way, the open boundaries could be located as far away as possible, while still satisfying the numerical constraint of a maximum 20% grid size variation.

A coastal wall was located on the eastern side of the domain with a river discharge located 30 km to the north of the southern boundary. The river had a constant discharge of 2,500 m^3/s located at the head of the estuary. The estuary consisted of a uniform 1-grid-cell wide, 45-km-long channel. The width of the river discharge at the mouth was 500 m. The depth decreased linearly from 20 m at the mouth to 5 m at the head, where a 0 psu fresh water source was located. This lay-out allowed for the development of a stable salt wedge.

The model was initialised with a salinity of 34.5 psu, which is the long term average for the North Sea, as found by Suijlen & Duin (2002). The model is located at the position of the Rhine outflow, at a latitude of 52° north. Coriolis was constant throughout the domain. The model had 16 equidistant sigma-layers in the vertical, which, combined with the depth of 20 m and a water level variation of less than 1.25 m, always gave a resolution better than 1.33 m in the vertical in the entire domain.

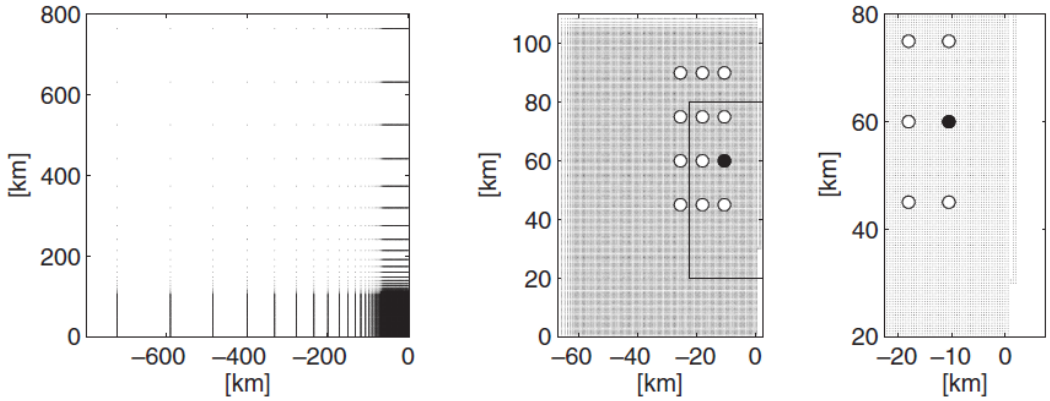

Figure 7.1 Schematic overview of the model grid by De Boer (2006, 2009). The middle panel shows the cell corners of the orthogonal equidistant 65×105 km grid covering the plume region of interest with a resolution of 500 m. The left panel shows a 25-cell grid margin added to both the west and north side, with cell sizes increasing with the maximum allowed 20% per cell towards the boundary. The right panel zooms closer into the 1-cell-wide river branch region, debouching into the sea at the coastal wall 30 km from the southern boundary. The river depth decreases from 20 m at the mouth to 5 m at the head, where a 0-psu discharge is located. Figure taken from De Boer (2006, 2009).

A.3 Results

Computations by De Boer (2006, 2009) showed a pattern of recurring stratification on neaps and de-stratification on springs, in accordance with observations collected from field campaigns in the 1990's.

The residual current profiles at a number of stations, compared to the analytical model of Heaps (1972), are shown in Figure 7.2 and Figure 7.3. It can be seen that in the bottom layer, frictional effects may cause residual onshore velocities of 0.02-0.05 m/s for large part of the time. This likely affects year-averaged sand transports on the Dutch shoreface.

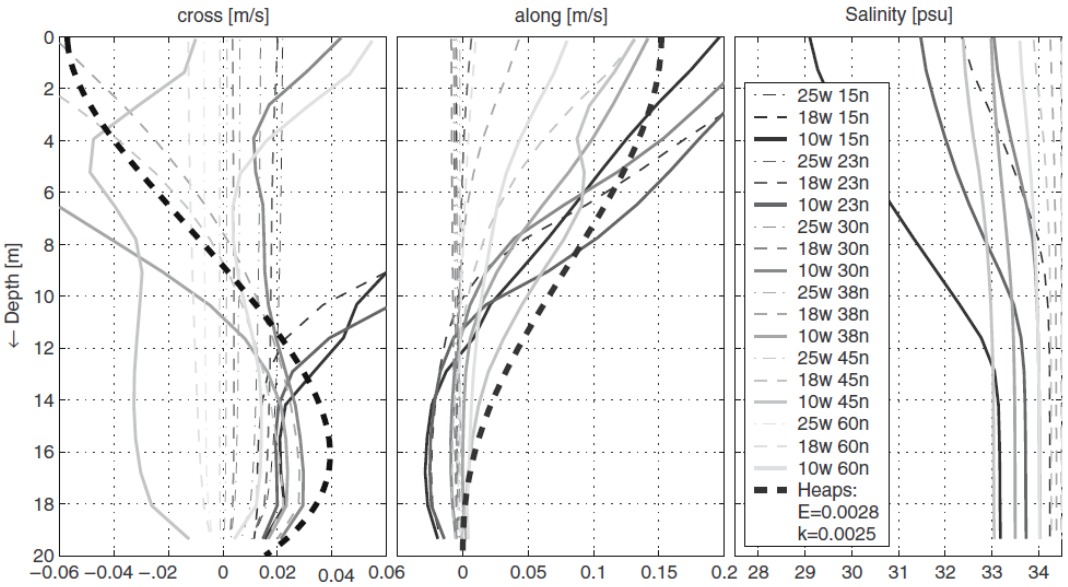

Figure 7.2 Vertical profiles of residual velocities and mean salinities during neap tide. The line types refer to cross-shore positions in the numerical model: 10 w, 17.5 w and 25 w refer to kilometres west (offshore) of the coastal wall, the grey tones refer to alongshore positions in the numerical model: 15 n, 23 n, 30 n, 38 n, 45 n and 60 n refer to kilometres north of the river mouth. Figure taken from De Boer (2006, 2009).

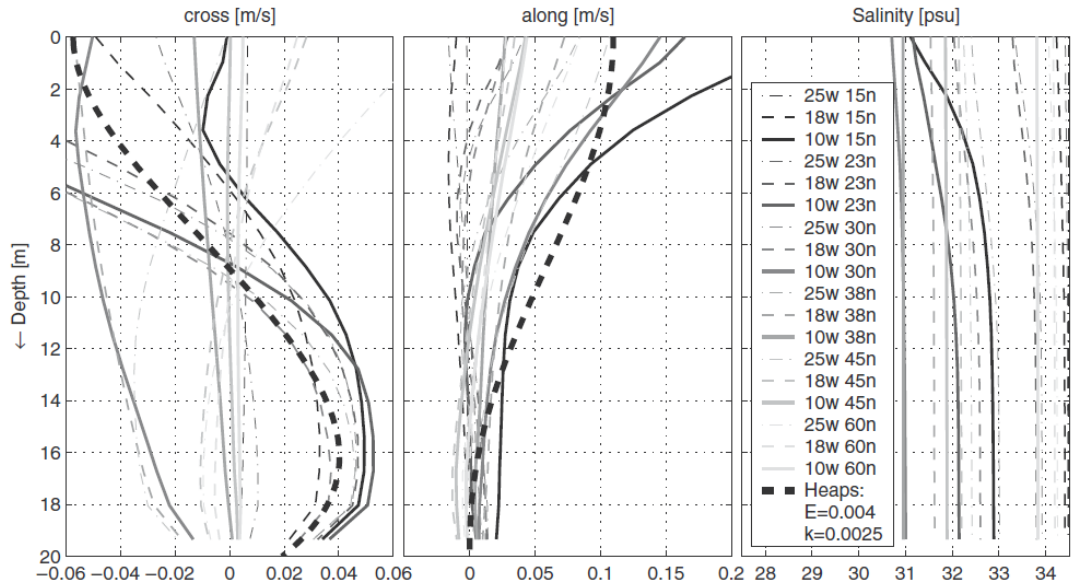

Figure 7.3 Vertical profiles of residual velocities and mean salinities during spring tide. The line types refer to cross-shore positions in the numerical model: 10 w, 17.5 w and 25 w refer to kilometres west (offshore) of the coastal wall, the grey tones refer to alongshore positions in the numerical model: 15 n, 23 n, 30 n, 38 n, 45 n and 60 n refer to kilometres north of the river mouth. Figure taken from De Boer (2006, 2009).

B Measuring instruments

Abbreviation	Name	Parameter
ABS	Acoustic Backscatter System	Suspended sediment concentration (profile; mainly used for sand)
ADCP	Acoustic Doppler Current Profiler	Flow velocity (profile)
ADV	Acoustic Doppler Velocimetry	Flow velocity (point)
ASTM	Acoustic Sand Transport Meter	Flow velocity and suspended sediment concentration (point; mainly used for sand)
Box corer		Sampling bed cores with typical diameters of 0.3 m and penetration depths of 0.3 m
CTD	Conductivity, Temperature, Depth	Water density, temperature and depth
EMF	Electro Magnetic Flow meter	Flow velocity (point)
LIDAR	Laser Imaging Detection And Ranging	Bed level
LISST	Laser In-Situ Scattering and Transmissometer	Suspended sediment size and concentration (point; mainly used for mud)
MALVERN		Grain-size (using laser diffraction technique)
Multibeam echosounder		Bedlevel (wide footprint compared to singlebeam)
Nile bedload sampler		Current-related bedload
OBS	Optical Backscatter System	Suspended sediment concentration (point; mainly used for mud)
Pressure sensors		Water levels, wave height and period
Ripple profiler		Bedlevel along longitudinal section (to measure small-scale, <~1 m, bedforms)
(Rotary) Side-scan sonar		Imaging of the seafloor (e.g. objects, bed structures)
Singlebeam echosounder		Bedlevel (narrow footprint compared to singlebeam)
(Directional) Waverider buoys		Wave height, period (and direction)

C Meta data field campaigns

NOURTEC	
Location	Terschelling (pilot shoreface nourishment)
Period	1993-1995
Principal investigators	Piet Hoekstra, Gerben Ruessink and others
References	Houwman (2000), Ruessink et al. (2006)
Conditions	
Water depths	3-10 m; 15 m (wave buoy)
Wave heights	N/A
Peak current velocity	~0.6 m/s
D50	N/A
Measurements	
Measurements frames (6)	
Velocities	EMFs
Fine sediment concentrations	OBS
Pressures (water levels, wave height, wave period)	Pressure transducer
Wave buoy	Wave height, period, direction

Van de Meene & Van Rijn (2000)	
Location	Shoreface-connected ridges near IJmuiden
Period	1989-1991 (6 periods)
Principal investigators	Jan van de Meene, Leo van Rijn
References	Houwman (2000), Ruessink et al. (2006)
Conditions	
Water depths	14-18 m
Wave heights	<4 m
Peak current velocity	0.2-0.5 m/s (1 m above the bed)
D50	0.25-0.30 mm
Measurements	
Measurements frames	
Velocity profile	ADCP
Velocities	NBA-2DNC current meters
Pressures (water levels, wave height, wave period)	Pressure sensors
Ship-based	
Density and temperature (cross-shore transect)	CTD
Current-related bedload and near-bed suspended load	Nile bedload sampler equipped with EMFs and suction samplers

Noordwijk CEFAS/RIKZ	
Location	Noordwijk 2, 5 and 10 km offshore
Period	2000-2002 – year round (Smartbuoy), winter (Minipod)
Principal investigators	David Mills, Jon Rees, Jo Suijlen
References	CEFAS/RIKZ (2003)
Conditions	
Water depths	10-16 m
Wave heights	<3.5 m
Peak current velocity	0.2-0.7 m/s (0.65 m above the bed)
D50	0.2-0.275 mm
Measurements	
Measurement frame (Minipod)	
near-bottom flow	Nortek ADV (Vector)
wave height and tidal elevations	2x pressure transducer (Digiquartz & Druck)
suspended sediment (fines)	OBS (Cambridge)
suspended sediment (sand)	ABS (CEFAS)
platform orientation	roll, pitch compass
chlorophyll-a	fluorometer (Seapoint)
light intensity	light sensor (LICOR)
oxygen	oxygen sensor (YSI)
sediment trap (fine sediment)	Booner tubes
Measurement buoy (Smartbuoy)	
chlorophyll-a	fluorometer (Seapoint)
fluorescence	N/A
suspended sediment (fines)	OBS
light intensity	light sensor (LICOR)
pressure	Pressure sensor
salinity	CTD

Building with Nature transects	
Locations	0.5-0.7 km offshore. Locations: Wijk aan Zee, Egmond, Camperduin, Callantsoog
Period	2003, 2010, 2011 - episodical
Principal investigators	Carola van der Hout (NIOZ), Theo Gerkema (NIOZ), Herman Ridderinkhof (UU)
Reference	van der Hout et al., 2015
Conditions	
Water depths	5-20 m
Wave heights	<1.5 m
Peak current velocity	0.5-0.8 m/s
D50	0.125-0.25 mm
Ship-based measurements	
currents	vessel-mounted ADCP
water samples	Niskin bottles
conductivity, temperature, depth	CTD (Seabird SBE)
suspended sediment (fines)	OBS (Seapoint)

SANDPIT	
Location	Noordwijk
Period	Spring and autumn 2003
Principal investigators	Leo van Rijn, Maarten Kleinhans and others
Reference	Van Rijn et al. (2005)
Conditions	
Water depths	12-16 m
Wave heights	< 5 m
Peak current velocity	0.5-0.7 m/s
D50	0.2 mm
Measurements	
Ship-based	
Velocity profile (cross-shore transect)	ADCP
Bedforms (cross-shore transect)	Echosounder
Sediment composition (along cross-shore transect)	Boxcore
Density and temperature (cross-shore transect)	CTD
Current-related bedload	Nile bedload sampler
Measurements frames (4)	
Velocity profiles	ADCP
Velocities	EMF
Fine sediment concentrations	OBS
Sand concentrations and fluxes	ASTM
Pressures (water levels, wave height and period)	Pressure transducer
Height of frame above the bed	Altimeter
Grain-size suspended sediment	Suspended sediment trap

Passchier & Kleinhans (2005)	
Locations	Area 1: SFCR ~10 km West of Zandvoort (1 x 2.5 km) Area 2: Landward SFCR ~5 km west of Noordwijk (1 x 2.5 km) Area 3: ~55 km west of Bergen aan Zee (1 x 5 km)
Period	2001, October 2002, February 2003 (5 measurements)
Principal investigators	S. Passchier, Maarten Kleinhans
Reference	(Passchier and Kleinhans, 2005)
Conditions	
Water depths	14-18 m (Areas 1 and 2); 25-30 m (Area 3)
D50	0.25-0.35 mm
Ship-based measurements	
Bed levels	Multibeam, sonar-imaging
Sediment composition	Boxcore

Van Dijk & Kleinhans (2005)	
Locations	Area 1: SFCR, 6-8 km west of Zandvoort (1.7 x 1.3 km) Area 2: sand wave field, 50 km west of Egmond (5.5 x 1.1 km)
Period	March, June/July and September/October 2001 and April 2002 (4 expedition)
Principal investigators	Thaiënne van Dijk, Maarten Kleinhans
Reference	Van Dijk & Kleinhans(2005)
Conditions	
Water depths	14-18 m (Area 1); 27-30 m (Area 2)
D50	0.25-0.35 mm
Ship-based measurements	
Bed levels	Multibeam, side-scan sonar
Sediment composition	Boxcore (Malvern 2000)

LaMER Egmond lander	
Location	Noordwijk 2, 5 and 10 km offshore
Period	Feb 2011 – Nov 2012 - continuous
Principal investigators	Rob Witbaard (NIOZ), Carola van der Hout (NIOZ), Marcel Rozemeijer (IMARES)
References	Witbaard et al., 2015
Conditions	
Water depths	11 m
Wave heights (H_S at Ijmuiden munitiestortplaats, 35 km offshore)	<5.5 m
Peak current velocity	0.7-1.2 m/s (1.4 m above the bed)
D50	0.125-0.25 mm
Measurements	
Measurement frame (Lander)	
near-bottom flow	Nortek ADV (Vector)
currents	Nortek Aquadopp
conductivity, temperature, depth	CTD (Seabird SBE)
turbidity and fluorescence	OBS (CLW ALEC-JFE)
Miscellaneous	
Sediment composition	boxcore
mud content	MEDUSA measurements

STRAINS I	
Location	1,5 km offshore from Sand Motor, Holland Coast
Period	Spring 2013 (3 weeks)
Principal investigators	Saulo Meirelles Nunes Da Rocha (TUD), Martijn Henriquez (TUD), Marcel Stive (TUD)
Reference	Henriquez et al., (2014), Meirelles et al.,(2014)
Conditions	

Water depth	12 m
Wave heights	<1.5 m
Peak current velocity	0.5 m/s (0.6 m above the bed)
D50	0.3 mm
Measurements from frame	
Velocity profile & waves	ADCP
Velocities	ADVs

STRAINS II	
Location	Sand Motor 1, 1.5 and 5.5 km offshore
Period	September-October 2014 – 6 weeks
Principal investigators	Julie Pietrzak (TUD), Alex Horner-Devine (UW), Alex Souza (NOC)
References	Rijnsburger (pers comm.)
Conditions	
Water depths	8, 12, 18 m
Wave heights	N/A
Peak current velocity	N/A
D50	0.2-0.3 mm
Measurements	
Measurement frames (4 frames)	
currents, waves	ADCP
conductivity, temperature, depth	CTD (FSI, AML)
suspended sediment (fines)	OBS (Seapoint, D&A)
currents, waves	Aquadopp (Nortek Pro & HR)
near-bottom flow	ADV (Nortek Vector)
currents, waves, turbulence	ADCP (Nortek Signature 1000)
suspended sediment (fines)	LISST (Holo and 100X)
suspended sediment (sand)	ABS
suspended sediment (sand)	Aquascat sediment profiler
Moorings (2 moorings)	
conductivity, temperature, depth	CTD (MC & SBEplus)
suspended sediment (fines)	OBS
chlorophyll and suspended sediment (fines)	C3
Ship-based	
floc size & population	2x floc camera (HR-Wallingford & TUD)
water samples	Niskin bottles
currents	vessel-mounted ADCP
conductivity, temperature, depth	CTD (Seabird SBE)
suspended sediment (fines)	OBS (Seapoint)
conductivity, temperature, depth	castaway CTD (NOC Liverpool)
Miscellaneous	
bottom samples	van Veen grab sampler

D Example borehole descriptions

D.1 Borehole B01D0287

Top [m NAP]	Bottom [m NAP]	Lithology	Color	Description
3	2.5	Z	grijs	[ZAND,***,****,*] grijs
2.5	2.3	Z	geel	[ZAND,***,155,*] geel, goed gesorteerd
2.3	2	Z	grijs	[ZAND,***,155,*] geelgrijs, goed gesorteerd
2	0.8	Z	grijs	[ZAND,***,155,*] grijs, goed gesorteerd
0.8	-0.4	Z	grijs	[ZAND,***,160,2] grijs, MET schelpgruis
-0.4	-1	Z	grijs	[ZAND,***,160,2] grijs, veel schelpgruis

D.2 Borehole B24H0136

Top	Bottom	Lithology	Color	2nd Color	Carbonate	Sand median Class	Sorting sand	Rounding sand	Fraction shells	Fraction shell remains	Description
4.8	-2.85	Z	grijs	bruin-	licht-	matig grof (O)	matig kleine spreiding	afgerond	veel schelpen	Veel schelpresten	[ZAND,***,*****,*] matig grof, helderlichtroestbruingrys, gelykkorrelig, MEEST afgerond, bont MET veel schelpgruis, ZELDEN GROTER DAN 2 MM.
-2.85	-15.05	Z	grijs	-	licht-	matig grof (O)	matig kleine spreiding	-	weinig schelpen	Weinig schelpresten	[ZAND,***,*****,*] matig grof, ietwat ongelykkorrelig, helderlichtgrys VAN KLEUR, enkele leembrokjes, weinig schelpgruis EN enkele schelpstukjes, ma
-15.05	-16	L	grijs	-	licht-	-	-	-	-	-	[LEEM,***,*****,*] fynzandig, IN GEDROOGDEN TOESTAND: FYN gelaagd, IETWAT SCHILFERIG, helderlichtgrys, kalkhoudend, VOCHTIG, VAALDONKERGRYS EN zwak plastisch.
-16	-21.7	Z	grijs	-	licht-	fijne categorie (O)	matig kleine spreiding	Matig afgerond	schelpen	schelpresten	[ZAND,***,*****,*] fyn, zwak slibhoudend, helderlichtgrys, glimmerhoudend, gelykkorrelig, MEEST weinig afgerond TOT HOEKIG, bont MET schelpgruis,
-21.7	-24.35	Z	grijs	-	licht-	grove categorie (O)	matige spreiding	afgerond	schelpen	Hele schelpen	[ZAND,***,*****,*] grof, helderlichtgrys, ongelykkorrelig, MEEST fraai afgerond, bont zand MET FYNE EN WEINIG GROVE grind, MET schelpstukjes EN schelpgruis
-24.35	-28.45	Z	grijs	-	licht-	matig grof (O)	-	afgerond	spoor schelpen	Spoor schelpresten	[ZAND,***,*****,*] matig grof, helderlichtgrys, MEEST fraai afgerond, bont, MET enkele glimmerblaadjes, MET sporen schelpgruis EN MET sporen grind. zuidelyk MATERIAA
-28.45	-31.6	Z	grijs	-	licht-	grove categorie (O)	matige spreiding	afgerond	-	-	[ZAND,***,*****,*] OF3680 grof, helderlichtgrys, ongelykkorrelig, MEEST fraai afgerond, bont, MET weinig grind BENEDEN 1 CH sporen glimmer. POLYGEEN, zuidelyk, MEEST fraai afge
-31.6	-35	Z	grijs	-	licht-	grove categorie (O)	matige spreiding	afgerond	-	-	[ZAND,***,*****,*] grof, helderlichtgrys, ongelykkorrelig, MEEST fraai afgerond, bont, DOCH WEL MATIG GROF VAN KORREL, sporen glimmer, MET weinig grind EN ENKELE ROLsteentjes EN
-35	-37.3	Z	grijs	-	licht-	grove categorie (O)	matige spreiding	afgerond	-	-	[ZAND,***,*****,*] grof, helderlichtgrys, ongelykkorrelig, MEEST fraai afgerond, bont, MINDER STERK, ongelykkorrelig, sporen glimmer, MET weinig grind EN EEN ENKEL ROLsteentje.
-37.3	-42.8	Z	grijs	-	licht-	grove categorie (O)	matige spreiding	afgerond	spoor schelpen	hele schelpen	[ZAND,***,*****,*] grof, helderlichtgrys, ongelykkorrelig, MEEST fraai afgerond, bont, DOCH MATIG GROF VAN KORREL, sporen glimmer, ENKELE afgerond
-42.8	-44.5	Z	grijs	-	licht-	matig grof (O)	matig kleine spreiding	afgerond	-	-	[ZAND,***,*****,*] matig grof, helderlichtgrys, TAMELYK gelykkorrelig, MEEST fraai afgerond, bont, glimmerarm

D.3 Borehole BQ140002

Top	Bottom	Lithology	Color	Secndary Color	Carbonate	Remark	Description
-15.6	-15.9	Z	grijs	geel-	kalkrijk	AAN DE TOP ENKELE BROKKEN STERK ZANDIGE KLEI	GRONDSOORT: Z; SCHELPNAAM: CERASTODERMA EDULE; SCHELPINH: EEN ENKEL SCHELPJE; FORM: BH; STRAT: HOL; KLEUR: GEELGRIJS; CA: CA4; SPREIDING: 73; LT_63UM: 7; INH: UITERST FIJN T/M MA
-15.9	-17.2	Z	grijs	-	kalkrijk	IETS SLIBHOUDEND	GRONDSOORT: Z; KLEUR: LICHT GRIJS; FORM: ELW; GELAAGDHEID: GELAAGD MET DUNNE LAAGJES KLEI ,ENKELE; SCHELPINH: ENKELE SCHELPFRAGMENTEN EN SCHELPEN; STRAT: HOL; CA: CA3; INH: MATIG FIJN
-17.2	-18	Z	grijs	-	kalkrijk	IETS SLIBHOUDEND	GRONDSOORT: Z; STRAT: HOL; SCHELPINH: SCHELPFRAGMENTEN; GELAAGDHEID: GELAAGD MET EEN ENKEL BANDJE KLEI; ORGANISCH_MAT: VEEN -DETRITUS ,ENKELE BANDJES- ENKELE BROKJES VEEN.; SCHELPNAAM: CERASTODERMA EDULE,ECHINI
-18	-18.1	K	grijs	-	kalkarm	-	GRONDSOORT: K; CA: CA2; STRAT: HOL; FORM: ELW; KLEUR: GRIJS; INH: ,VRIJ VET, GYTTJA-ACHTIG
-18.1	-18.18	Z	grijs	-	-	-	GRONDSOORT: Z; INH: MATIG GROF T/M ZEER GROF; STRAT: HOL; SCHELPINH: ZEER VEEL SCHELPEN ,CERAST. BROED; SCHELPNAAM: CERASTODERMA EDULE,SCROBICULARIA PLANA,HYDROBIA ULVAE; FORM: ELW; KLEUR: GRIJS
-18.18	-18.57	K	bruin	grijs-	kalkrijk	-	GRONDSOORT: K; CA: CA3; KLEUR: GRIJS BRUIN; FORM: ELW; SCHELPNAAM: HYDROBIA ULVAE; GELAAGDHEID: GELAAGD MET DUNNE LAAGJES ZAND ,AAN DE BASIS EEN ENKEL DIKKER ZANDBANDJE; SCHELPINH: SCHELPEN IN ZANDLAAGJES; STRAT: HOL; INH
-18.57	-18.6	K	bruin	grijs-	-	-	GRONDSOORT: K; STRAT: HOL; ORGANISCH_MAT: KLEI IS IETS VENIG; FORM: ELW; KLEUR: GRIJS BRUIN; INH: VRIJ VET, GYTTJA-ACHTIG

E Conceptual model lower shoreface sand transport

Conceptual model lower shoreface sand transport, KG-2

Orange boxes: external factors, green boxes: input parameters, transparent boxes: indicators, blue box: key indicator.
Spatial scale: Dutch lower shoreface, ~350 km alongshore, ~5-10 km cross-shore, water depths of ~10-20 m
Two time scales: process-scale of ~weeks-months (solid lines, focus of KG-2), engineering scale of ~10-50 years (dashed lines)
Grey arrows: relation unclear and/or not main focus KG-2